INVESTIGATION OF THE BOUNDARY LAYER ON A PLANE SURFACE.

Thesis
submitted by

John Gordon Burns.
B.Sc. (Edinburgh).

for the degree of
Doctor of Philosophy.

University of Edinburgh
October, 1958.

SYMBOLS

The following symbols are used to describe the quantities indicated in this list unless otherwise stated in the text.

x = distance from leading edge of flat plate

y = distance from surface of flat plate

z = distance in flat plate perpendicular to x

U_o = Free stream velocity

U = mean velocity at a point in boundary layer

u = instantaneous x component of fluctuation velocity

v = instantaneous y component of fluctuation velocity

w = instantaneous z component of fluctuation velocity

u', v', w' = root- mean - squares of u, v, and w.

c = wave velocity

β_r = $2\pi f = w$, where f = oscillation frequency

α = wavenumber

ρ = density of air

ν = kinematic viscosity

δ = boundary layer thickness

δ^* = boundary layer displacement thickness

$$\delta^* = 1.72\sqrt{\frac{\nu x}{U_o}}$$ for Blasius distribution.

R = $\frac{U_o \delta^*}{\nu}$ = Reynolds number

R_x = $\frac{U_o x}{\nu}$ = x - Reynolds number

TABLE OF CONTENTS.

CONTENTS (Contd.)

PREFACE.

The research in this thesis was carried out in the Heriot Watt College, Edinburgh, under the joint supervision of Professor W.H.J. Childs, Professor of Physics in the Heriot Watt College, and Dr. M.A.S. Ross of the Department of Natural Philosophy, University of Edinburgh. The major part of the work was carried out in conjunction with Mr. A.A. Nicol who was mainly responsible for the design and construction of the electronics.

Chapter I.

Introduction & Historical Review.

I. 1. Introduction

The present work has been undertaken in an attempt to gain further insight into the physical processes which govern fluid flow.

Since the equations of motion governing fluid flow are complex, even in the simplest cases, it was decided to confine the investigation to a well studied type of flow, namely, the boundary layer flow on a flat plate at zero pressure gradient.

It was hoped to develop a new instrumental technique which could first be used to verify the present knowledge regarding the stability of the laminar boundary layer and, having thus proved the technique, to use it to investigate further into the nature of the transition from laminar to turbulent flow.

I. 2. Historical Review

(a) General Survey

In order to understand fully the nature of the problem it is proper that we should consider the development of our understanding from its origins. The following precis of the literature is brief and, in its latter stages, refers only to the work which is directly related to flow on a smooth flat plate. A comprehensive review of the development of boundary layer theory was presented by H.L. Dryden (1955).

The recognition of two distinct regimes, namely laminar and turbulent, stems from the work of Osborne Reynolds (1883).

His classic experiments amply demonstrated that the classical theoretical hydrodynamics, which was highly developed mathematically, was totally inadequate when dealing with real flows. This theory ignored the existence of viscosity in fluid flows and had been developed largely because of its mathematical elegance and similarity to electrodynamics, although the complete equations of motion for flows with friction, the Navier-Stokes equations had been known since 1820. These equations are so intractable that only a few special cases have been solved, and these solutions were restricted to laminar flows.

The first step towards a reunification of theory and experiment was made by L. Prandtl (1904) when he proposed the boundary layer concept. It had puzzled workers that in cases where the viscosity is very small, particularly, water and air, the classical theory failed so completely to predict, for example, such a basic phenomenon as drag. Prandtl showed that it was possible to consider the flow as being divided into two distinct regions. Firstly a small region, the 'boundary layer,' near any boundaries, in which the effect of viscosity was important and secondly a region covering the rest of

the field in which viscosity effects are negligible and potential theory can be expected to predict the flow accurately. In physical terms this means that viscosity is important in a region in which considerable velocity gradients exist. Prandtl also showed how the Navier Stokes equations could be simplified and yet conform with the boundary layer conditions, these modified equations being known as Prandtl's boundary layer equations.

In the case of theflat plate with zero pressure gradient these equations become:-

$$U\frac{\partial U}{\partial x} + V\frac{\partial U}{\partial y} = \nu\frac{\partial^2 U}{\partial y^2}$$

$$\frac{\partial U}{\partial x} + \frac{\partial V}{\partial y} = 0$$

with $y = 0: \quad U = V = 0: \quad y = \infty: \quad U = U_\infty$

as boundary conditions.

H. Blasius (1908) solved these equations by means of a substitution which transformed both equations into an ordinary differential equation for the stream function. The resulting equation is nonlinear and of the third order, and can therefore be solved completely since we have three boundary conditions. The general solution, even in this simple case, cannot be given in a closed form and it is necessary to solve by purely numerical methods or by means of a series expansion. Blasius obtained the solution in the form of a power series. The solution was tabulated by L. Howarth (1938) and it is these

figures which have been used in this report.

The careful work of, for example, Nikuradse (1942) has verified Blasius' solution for the laminar flow. It was found however that the laminar flow underwent a transition to turbulent flow, the parameters governing this transition being numerous. So far as can be ascertained the following parameters may be regarded as distinct causes of transition.

(a) Free stream turbulence; that is, turbulence inherent in the main flow.

(b) Roughness of the flat plate.

(c) Plate Curvature.

(d) Pressure gradients along the plate.

(e) Temperature gradients.

(f) Noise, vibration.

Of these causes only the first has been considered in detail since the remaining causes, excepting the last, can be effectively removed. Noise and vibration are unavoidable to some extent and a compromise must be accepted in any experimental study.

At first boundary layer theory had been developed to deal with laminar flows, but it soon became imperative that a theory be developed for the practically more important case of the turbulent boundary layer. Prandtl (1925) by means of his mixing length theory, laid the basis of a group of more or less refined semi-empirical theories which

serve well in predicting practical solutions, which are for the most part, satisfactory. The theory which is most satisfactory from a fundamental standpoint treats turbulence as a statistical problem but Schlichting goes so far as to question whether a rational theory of turbulence, on this, or any other, basis can ever be fully explored in view of the extreme complexity of such flows. However, none of these theories have anything to say upon the problem of why the flow becomes turbulent.

We now proceed to examine those theories which seek to predict and explain the phenomenon of transition from laminar to turbulent flows.

Prandtl (1914) had shown, by means of his experiments on spheres, that turbulence was possible in any boundary layer and, beginning in 1921 developed a semi-empirical theory of transition. It was not until later that more rational theories of transition were developed and it is to this later work that we must turn our attention.

Prandtl had shown that the phenomenon of separation was closely related to whether the flow was turbulent or laminar. G.I. Taylor (1936) theorised that transition was caused by separation, either momentary or permanent, in the laminar layer. Therefore transition should be governed by the Karman-Pohlhausen parameter for laminar separation

(1921). Taylor was able to relate this parameter to measurable free stream quantities, scale and intensity, and thus was able to relate the pressure forces causing intermittent separation to free stream quantities. Taylor's theory predicted that the parameter $\left[\frac{v'}{U}\left(\frac{x}{L}\right)^{1/5}\right]$ would determine at what R_x value the boundary layer will undergo transition. The theory applied only to isotropic free stream turbulence. Taylor confirmed that this parameter does, in fact, control transition provided that the free stream turbulence is fairly high, the experimental data ranging over flat plates, spheres, and elliptic cylinders.

In the post war era this theory has met with several objections, the major one being that separation has not been proven to be necessary for transition.

However, some workers now incline to the view that one must consider transition as being due to several possible causes and that Taylor's theory describes one of the effects which contribute to transition.

The latest theoretical approach is due to Emmons (1951). In an experimental study on a water table analogy to supersonic flow he observed that the transition front was of a very intermittent nature. He points out that a disturbance may be introduced into the laminar boundary layer in a number of ways.

but, once there, will disturb the boundary layer. If this disturbance is large enough it will cause a localised transition to turbulence. This spot, or burst, of turbulence will fan out as it is convected downstream, in the manner described by Schubauer and Klebanoff (1955) and, the farther downstream one observes, the more fully turbulent will appear the flow. That is, if one measures with a macroscopic instrument, turbulence will become more and more fully developed, while if one measures with a microscopic instrument the percentage of time during which the flow is turbulent will become larger. Emmons develops a theory which predicts what percentage of time the flow at each position on the plate will be turbulent. Much more data on the initial size, rate of production, and rate of growth of these spots is needed, together with information on how these parameters are affected by free stream turbulence.

Thus Emmons' theory allows us to predict the conditions in the transition region on a statistical basis, but throws little light upon the cause of the breakdown to turbulence.

The most fruitful theory regarding the problem of how disturbances in the laminar layer achieve sufficient magnitude to cause transition is due to Tollmien and to Schlichting and since their work forms the basis of the present work we will discuss

it more fully than the foregoing theories.

(b) Theory of Laminar Oscillations.

(a) Basic Equations.

Starting in 1931 the problem of the stability of the laminar boundary layer was investigated from a theoretical standpoint. The Navier Stokes equations are solved for the case where small perturbations are impressed upon the large scale solution for the boundary layer.

The first papers were published by W. Tollmien (1931, 1936) and by H. Schlichting (~~1932~~, 1933, 1935) and the results of these workers have been corrected, but not essentially changed, by C.C. Lin (1952).

The theoretical work, which will now be indicated in outline, treats, in general, only two-dimensional flow with two-dimensional disturbances. The basic flow is assumed to be steady and a function of y only. The basic flow in the boundary layer is then

$$U = f(y) \; ; \qquad V = 0$$

The disturbances, which are a function of time as well as of x and y, become

$$u = f_1 (x,y,t)$$

$$v = f_2 (x,y,t)$$

The components of the total velocity then become (U+ u) and v. Since u and v are small the Navier Stokes equations become, neglecting squares and products of disturbance velocities and of their differential coefficients,

$$\frac{\partial u}{\partial t} + U\frac{\partial u}{\partial x} + v\frac{\partial U}{\partial y} = \nu\left(\frac{\partial^2 U}{\partial y^2} + \frac{\partial^2 u}{\partial x^2} + \frac{\partial^2 u}{\partial y^2}\right) - \frac{1}{\rho}\left(\frac{\partial P}{\partial x} + \frac{\partial p}{\partial x}\right) \quad (1)$$

$$\frac{\partial v}{\partial t} + U\frac{\partial v}{\partial x} = \nu\left(\frac{\partial^2 v}{\partial x^2} + \frac{\partial^2 v}{\partial y^2}\right) - \frac{1}{\rho}\left(\frac{\partial P}{\partial y} + \frac{\partial p}{\partial y}\right) \quad (2)$$

where p represents the pressure due to the disturbances and P is the pressure due to the basic flow.

The equation of continuity being

$$\frac{\partial u}{\partial x} + \frac{\partial v}{\partial y} = 0 \quad (3)$$

By subtracting from equations 1 and 2, respectively, the corresponding Navier Stokes equations for $u = v = p = 0$, we obtain two equations in terms of the perturbation only:

$$\frac{\partial u}{\partial t} + U\frac{\partial u}{\partial x} + v\frac{\partial U}{\partial y} = \nu\left(\frac{\partial^2 u}{\partial x^2} + \frac{\partial^2 u}{\partial y^2}\right) - \frac{1}{\rho}\frac{\partial p}{\partial x} \quad (4)$$

$$\frac{\partial v}{\partial t} + U\frac{\partial v}{\partial x} = \nu\left(\frac{\partial^2 v}{\partial x^2} + \frac{\partial^2 v}{\partial y^2}\right) - \frac{1}{\rho}\frac{\partial p}{\partial y} \quad (5)$$

These two equations, 4 and 5, are the fundamental hydrodynamic equations for small disturbances on which are based all stability theories.

(b) Solution for the Laminar Boundary Layer.

Lord Rayleigh (1887) was the first to outline a general mathematical theory which has been contributed to by many workers.

Tietjens (1925) was the first to apply Rayleigh's theory to a velocity profile intended to represent flow along a wall, but his solution suffered from serious limitations due to his profile being formed of a series of straight lines.

Tollmien and Schlichting successfully applied the theory to curved profiles and their most complete solutions, which will now be indicated in outline, apply to an approximation of the Blasius distribution.

From the basic equations, 4 and 5, the pressure terms are eliminated by differentiating with respect to y and x, respectively, and subtracting the second from the first. The result is:-

$$\frac{\partial^2 u}{\partial y \partial t} + U\frac{\partial^2 u}{\partial x \partial y} + \frac{\partial U}{\partial y}\frac{\partial u}{\partial x} + v\frac{\partial^2 U}{\partial y^2} + \frac{\partial v}{\partial y}\frac{\partial U}{\partial y} - \frac{\partial^2 v}{\partial x \partial t} - U\frac{\partial^2 v}{\partial x^2} = \nu\left(\frac{\partial^3 u}{\partial x^2 \partial y} + \frac{\partial^3 u}{\partial y^3} - \frac{\partial^3 v}{\partial x^3} - \frac{\partial^3 v}{\partial y^2 \partial x}\right) \tag{6}$$

The disturbance velocities may be expressed in terms of a stream function ψ such that

$$u = \frac{\partial \psi}{\partial y}, \qquad v = -\frac{\partial \psi}{\partial x} \tag{7}$$

We wish to search for a periodic solution to the disturbance equations, and any such solution can be represented by a Fourier series. As equation 6 is linear and homogeneous in u and v, its solution may be investigated by using a single term of the series. This may be done by supposing a periodic disturbance so that the stream function becomes

$$\psi = F(y)\, e^{i(\alpha x - \beta t)} = F(y)\, e^{i\alpha(x - ct)} \tag{8}$$

where F(y) represents the initial amplitude of the

stream function, and α is a wavenumber. Since β and hence c, are generally complex equation 8 may be written

$$\psi = F(y)e^{i(\alpha x - (\beta_r + i\beta_i)t)} = F(y)e^{i\alpha(x-(c_r+ic_i)t)} \quad (9)$$

where β_r is the angular frequency of the disturbance and β_i is the coefficient of damping, or of amplification.

Equation 6 is now written in terms of the stream function, substituting the form 8 (b), and the result is

$$(U-c)(F''-\alpha^2 F) - U''F = \frac{\nu}{i\alpha}\left(F'''' - 2\alpha^2 F'' + \alpha^4 F\right) \quad (10)$$

where primes denote differentiation with respect to y. This is a homogeneous linear equation of the fourth order with a general solution of form

$$F = C_1 F_1 + C_2 F_2 + C_3 F_3 + C_4 F_4 \quad (11)$$

The form of the particular solutions, F_1, F_2, F_3, F_4, depends on the boundary layer profile assumed.

Both Tollmien and Schlichting approximated to the Blasius distribution by a straight line anda parabola; This gave an adequate approximation for U itself, but for U' and U'' the values were taken directly from the Blasius solution.

As equation 10 cannot readily be completely solved, certain approximations must be made concerning the viscosity terms.

The equation is rewritten in a dimensionless

form, using the Reynolds number, R, as one of the parameters introducing y/δ^* as a new independent variable and putting $F = U_0 \delta^* \phi$. The result is:-

$$\frac{U-c}{U_0}\left(\phi'' - \alpha^2\delta^{*2}\phi\right) - \frac{U''\phi}{U_0} = \frac{1}{i\alpha\delta^* R}\left(\phi'''' - 2\alpha^2\delta^{*2}\phi'' + \alpha^4\delta^{*4}\phi\right) \tag{12}$$

where primes now denote differentiation with respect to y/δ^* . It is shown that the effect of the friction terms is negligible except at the surface and at a plane where the wave velocity is equal to the local stream velocity. Tollmien (1931) has shown that c must always be less than U_0 , thus a plane with U = c will always be found in the boundary layer.

Excluding this point (for the assumption that V = 0 virtually reduces the problem to one dimension) and the surface, we can obtain two particular solutions ϕ_1 and ϕ_2 by solving the frictionless equation

$$\frac{U-c}{U_0}\left(\phi'' - \alpha^2\delta^{*2}\phi\right) - \frac{U''\phi}{U_0} = 0 \tag{13}$$

These solutions are expressed as power series developed about y_c , where y_c is the position of the critical point U = c. While ϕ_1 is regular throughout the boundary layer, ϕ_2 has a singularity at the critical point and must be corrected by means of a second approximation to equation 12, obtained by neglecting all but the largest of the friction terms. A new independent variable, η , defined by

$$\frac{y-y_c}{\delta^*} = \left(\alpha\delta^* R \frac{U'_c}{U_0}\right)^{-1/3}\eta = \varepsilon\eta$$

is introduced which enables the behaviour of the

equation in the vicinity of $y = y_c$ to be examined and indicates the form of ϕ_2 to be used for $y - y_c < 0$ A new homogeneous equation is also obtained which provides particular solutions ϕ_3 and ϕ_4. As ϕ_4 increased rapidly with y, one sets C_4 equal to zero and the general solution to equation 12 becomes

$$\phi = C_1 \phi_1 + C_2 \phi_2 + C_3 \phi_3 \qquad (14)$$

Now the stability problem is one in which the boundary conditions afford sufficient equations between the solutions at the boundaries to determine the values of the parameters for which equation 12 is satisfied, those values being the characteristic values.

Using the boundary conditions at $y = 0$ and at $y = \delta$ we obtain three equations for the boundary solutions, which provided $\phi \neq 0$, yield a determinantal equation.

Upon solving this equation it may be arranged such that one side is a function of η_0, that is the value of η at the surface, while the other side is a function of the parameters $\alpha\delta^*$ and c/U_0.

Thus we may write the solution as

$$G(\eta_0) = E(\alpha\delta^*, c/U_0) \qquad (15)$$

noting that η is a function of $\alpha\delta^*$ and R. Since equation (15) is complex it may be separated into two equations, between which any one of the three parameters $\alpha\delta^*$, R and c/U_0 may be eliminated and a relation found between the other two.

This has been done by both Tollmien and Schlichting for the case where c is real. This corresponds to a disturbance which is neither amplified or damped and results in the curve shown in figure I. This curve actually forms a closed loop as both branches meet at ∞.

A disturbance whose characteristics fall within this loop will be amplified while any other disturbance will be damped.

Schlichting has extended his calculations to include small amplifications and has calculated also the total amplification on proceeding from branch I to branch II of the neutral curve.

In order to complete the investigation it is necessary to consider a solution which will provide the constants of integration for equation 14. Schlichting has obtained the solution for neutral oscillations on a flat plate. He was thus able to calculate the relative values of u' and v' and their distribution across the boundary layer (fig. 2). He also investigated the correlation between u' and v' and the energy balance.

Having thus briefly indicated the theory of laminar oscillations let us consider the predictions which it makes from an experimental viewpoint.

Consider the case of a disturbance being injected into the boundary layer at a Reynolds number R, and let this disturbance have equal

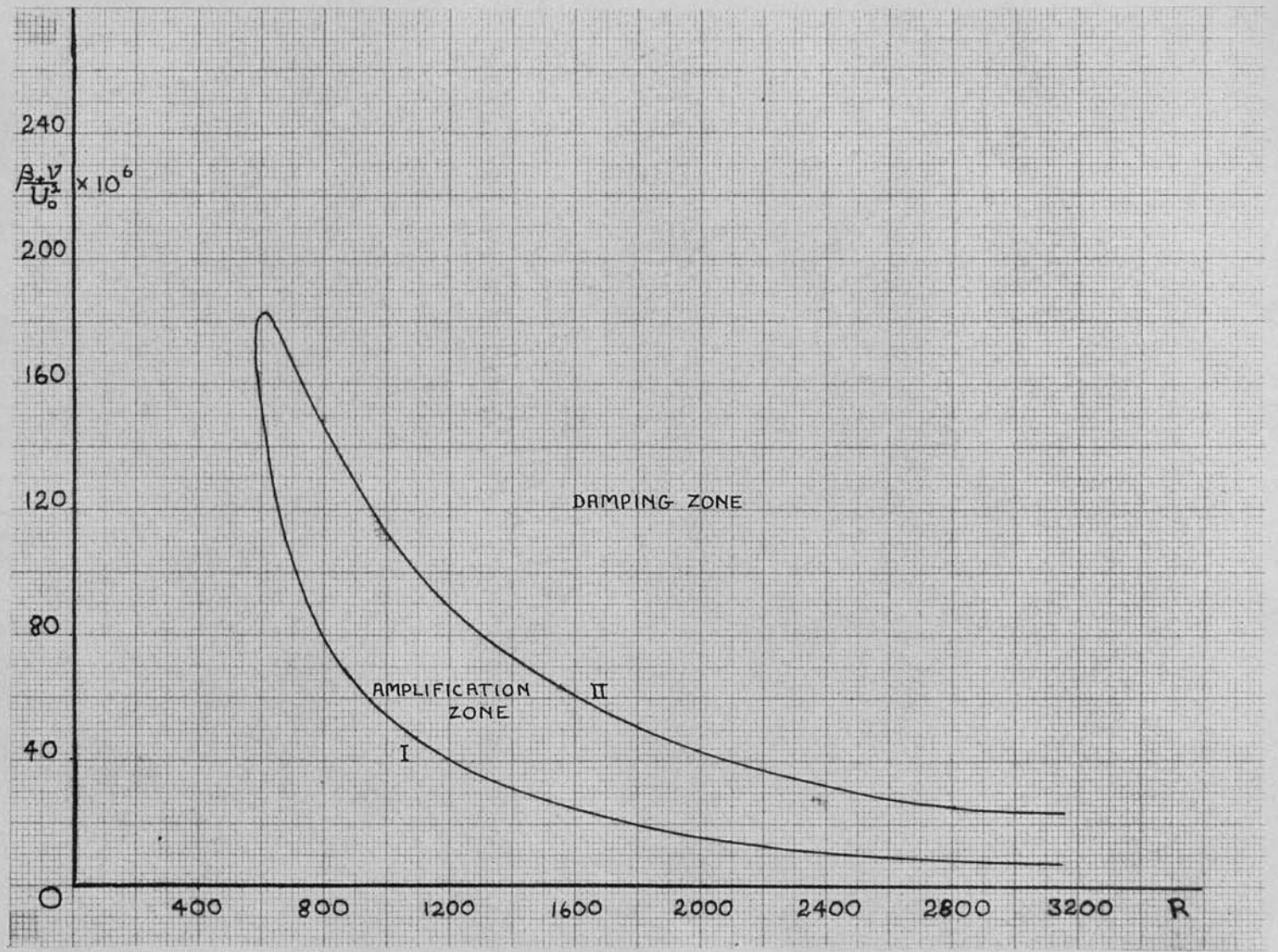

FIGURE 1

Zone of Amplification enclosed by neutral curve, after Schlichting.

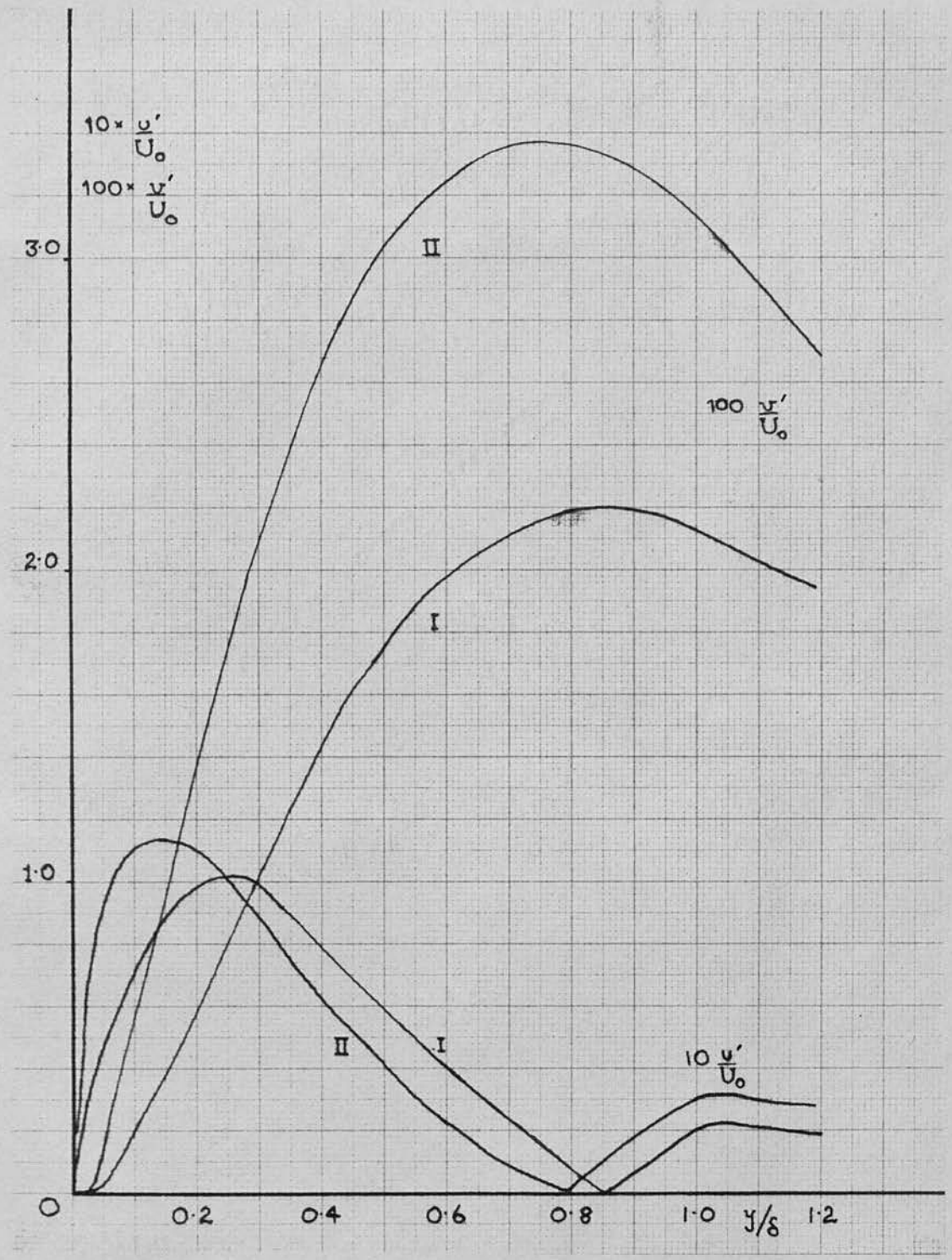

FIGURE 2.

Distribution of u' and v' through boundary layer, after Schlichting. Drawn for average $u'/U_0 = 0.05$ from $y/\delta = 0$ to $y/\delta = 1$.

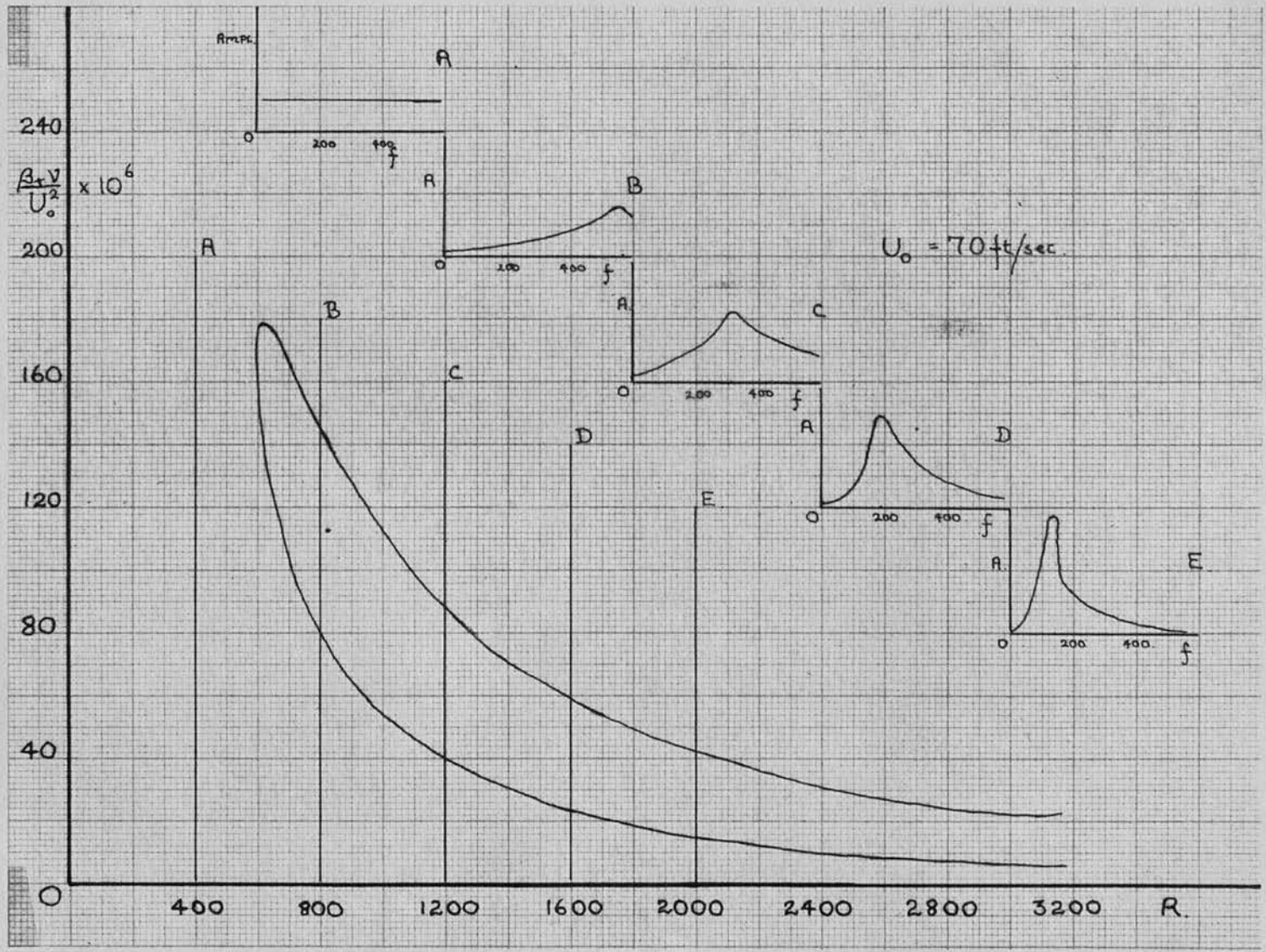

FIGURE 3

Diagrammatic representation of modification of spectrum by Neutral curve.

amplitudes at all frequencies as indicated in figure 3 If we plot the amplitude distribution as we proceed to greater Reynolds numbers we find that the distribution develops a more and more sharply defined peak, the frequency of this peak being the frequency which has received maximum amplification at the particular Reynolds number chosen. Thus if we experiment with a frequency analysing apparatus we should observe that the peak frequency becomes more sharply defined and of lower frequency as we move downstream. This peak frequency, taken with the Reynolds number at which it was obtained should give an experimental point on the neutral curve.

Alternatively, if we inject a disturbance of a single known frequency we can follow its progress downstream and, by noting the point of maximum amplification, we can obtain points on branch II of the neutral curve. It should also be possible to obtain points on branch I by noting the lowest amplitude before amplification commences.

(c) Experimental Support.

The theoretical treatment met with a considerable amount of adverse criticism, largely based upon the fact that it assumed a non-thickening boundary layer, and also because no workers were able to detect the laminar oscillations. However, this situation was reversed when Schubauer and Skramstad (1947) published a classic paper in which they provided ample

experimental support for the theory. Their investigation was conducted with hot wire equipment of a simple nature and the success of their work must largely be attributed to the unusually low free stream turbulence which they were able to utilize. They reduced the turbulent velocities to 0.03% of the free stream velocity and, while it has since been shown that laminar oscillations may be detected with a turbulence level of 0.42%, their results suggest that earlier workers failed to detect the oscillations because the initial disturbances were too large.

They were able to detect natural oscillations and, by measuring their frequency, could obtain experimental points on the neutral curve of the stability theory. They also studied artificial mono-frequent oscillations which were introduced into the boundary layer by means of a vibrating ribbon, held very close to the surface, and found results in complete accord with the theory. Further, they were able to investigate the distribution of u' and v' across the boundary layer, and again found good agreement. Their main experimental data are compared with the theoretical curves in figures 4 and 5.

While the investigation was not confined to the above results, those quoted are sufficient to clearly indicate the astonishing accuracy of the theoretical treatment.

Schubauer, noticing several interesting points

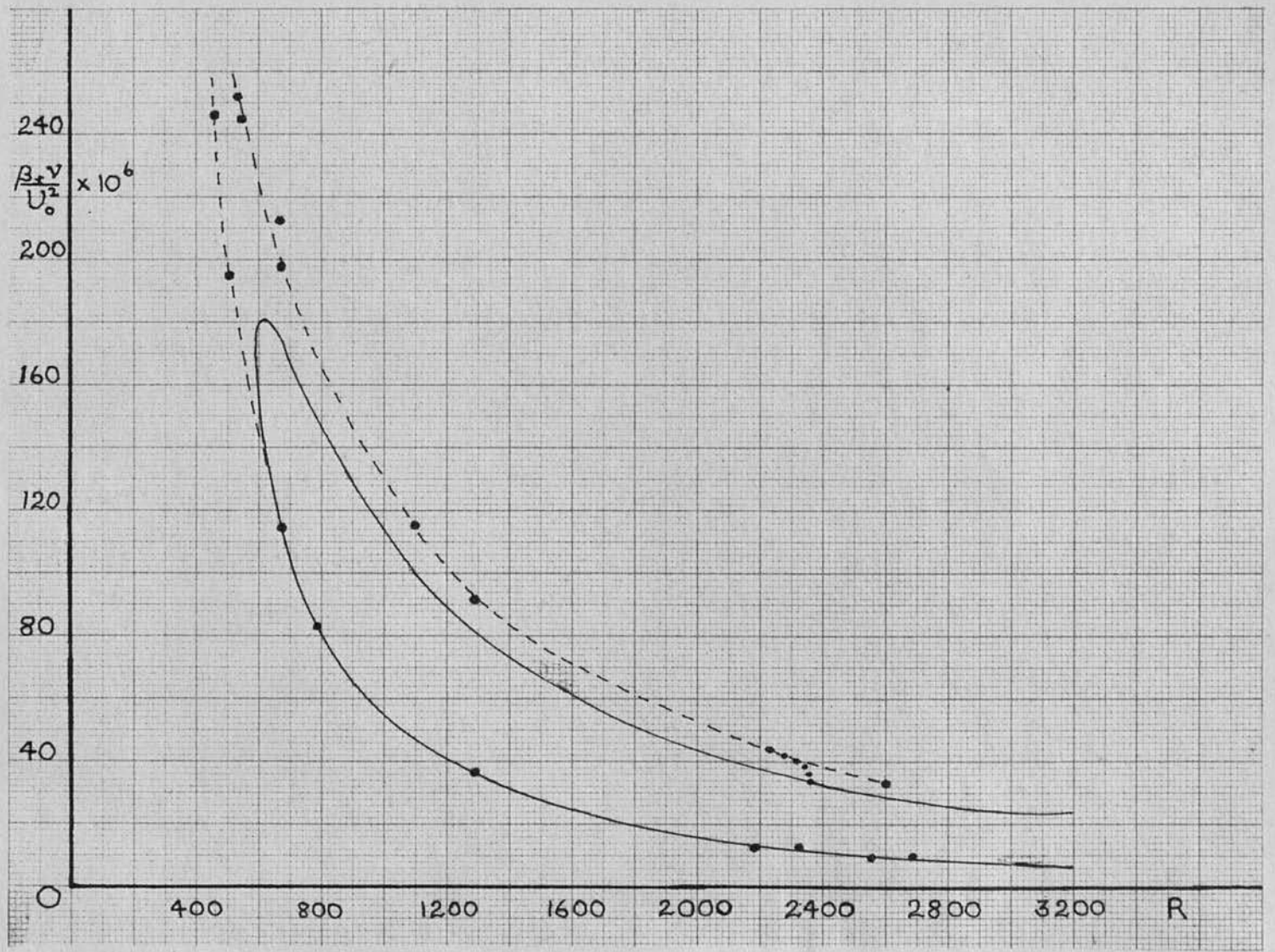

FIGURE 4

Experimental verification of neutral curve by Schubauer and Skramstad. Solid curve due to Schlichting.

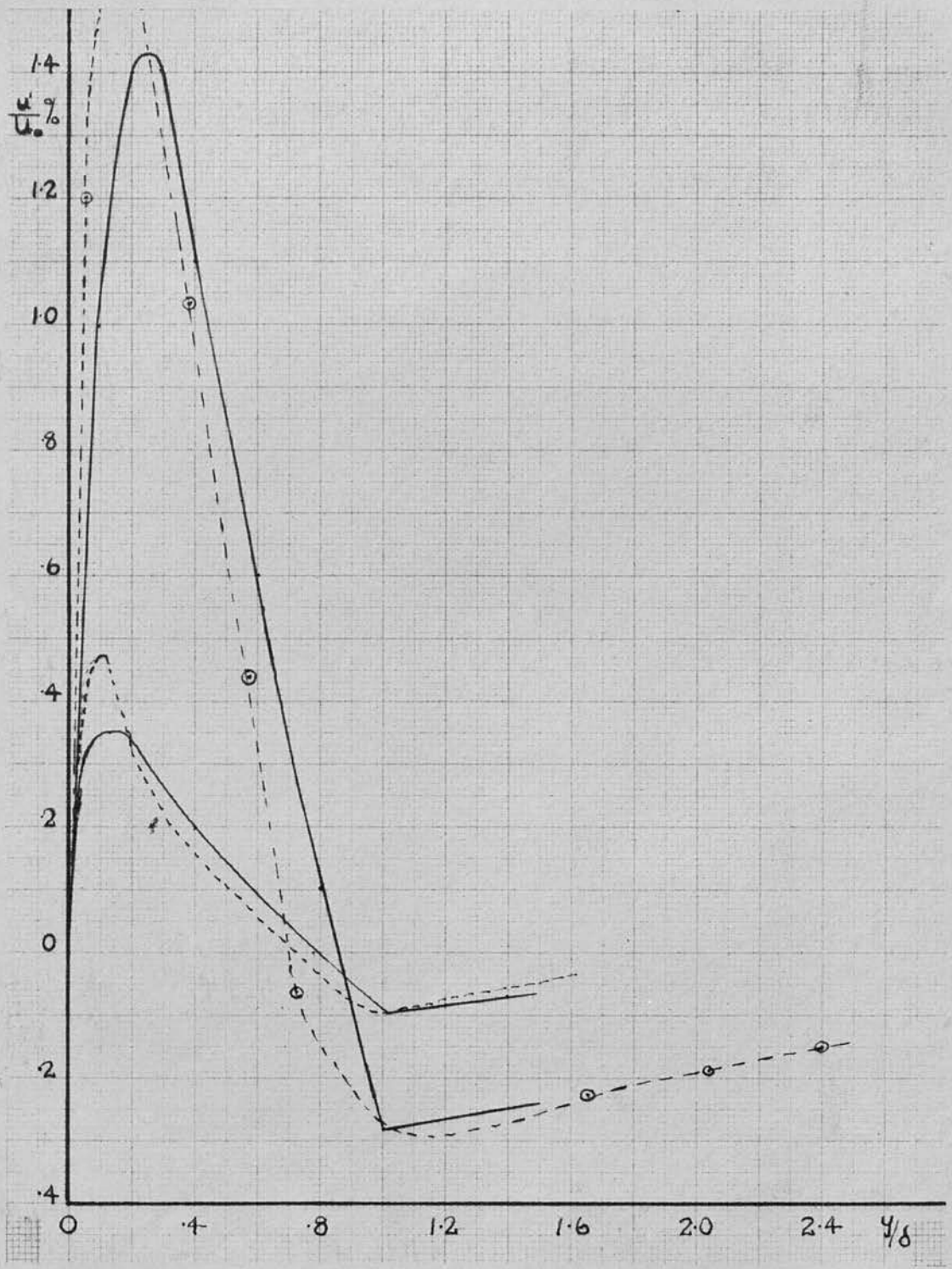

FIGURE 5

Experimental verification of distribution of u' through boundary layer by Schubauer and Skramstad. Experimental and theoretical curves normalised to same area under curve.

in the transition region, continued his work in conjunction with Klebanoff (1955) and investigated the properties of artificially excited 'spots' of turbulence. This work has already been referred to and has contributed much to our knowledge of the manner of growth of such spots.

I. 3 Conclusions.

We have now outlined the theoretical and experimental state of the subject and can assess the situation as it appears at present.

It is certain that the laminar oscillation theory of Tollmien and Schlichting governs the amplification, or decay, of a disturbance which finds its way into the laminar boundary layer, provided that the level of free stream turbulence is low. If the free stream turbulence is high, then transition appears to depend on separation, as proposed by Taylor. It is probable that the truth lies in an admixture of both theories.

Laminar oscillation theory has nothing to say upon the problem of the actual transition. It is tacitly assumed that when the oscillations reach a sufficient amplitude breakdown will occur and turbulence will result. The work of Emmons, and of Schubauer and Klebanoff has shown us that this breakdown is complete and spontaneous, and may occur over a range of Reynolds numbers. In short, that the concept of a transition region is a statistical picture, the flow being either turbulent or laminar

at a given point. It might also be supposed that, following Taylor, the criterion for breakdown to turbulence is that the laminar oscillations should reach an amplitude sufficient to cause momentary separation.

If we examine the frequency characteristics of the flow we find, in the laminar region, at a given Reynolds number, a predominant frequency, this frequency gradually decreasing as the Reynolds number increases. The flow then undergoes transition and the spectrum becomes characterized by much higher frequencies than have hitherto been observed. There is, however, still a considerable low frequency content.

If we consider the solution of a second order differential equation, (which is not too far removed from the fourth order equation which describes the flow) we find a very similar behaviour. The equation may admit of one solution until a critical value is passed when two solutions, a high and a low frequency solution are possible. As we proceed to higher values these two solutions gradually approach each other and finally blend into one solution.

While it is not supposed that a solution exists as such for the boundary layer it is possible that a similar phenomenon takes place, and that the two branches may describe a laminar or turbulent state existing in the boundary layer, the eventual blending of the two solutions corresponding to the establishment of the fully turbulent region.

A solution to the equations of motion would have to admit of many frequencies in the transition region and one can suggest a band of frequencies, centred about a preferred frequency as being a possible answer.

In order to investigate such an idea it was decided to develop a new instrument which would respond mechanically to disturbances in the boundary layer. This was to be designed to respond to disturbances at right angles to the main flow and to the flat plate, (that is, to v fluctuations.) Such a system will have certain natural frequencies and use can be made of these, provided they can be arranged to fall within the desired frequency range. The system may also be used at frequencies other than its natural frequency but the response will be much impaired in such a case.

Thus the instrumental problem resolved itself as follows:- A mechanical response to boundary layer disturbances was to be obtained, either by using a system on resonance or off resonance; this response had then to be converted into some signal suitable for observation, either visually, or by means of a recording device.

Having developed such a system its performance can be checked by verifying or otherwise, the laminar oscillation theory. If this proves successful then the measurements can be extended to the transition region where the relative value of both high and low

frequencies can be assessed, with a view to shedding further light on a possible solution to the equations.

Chapter II.

Construction and Calibration of the Wind Tunnel.

II. 1 Introduction

As no wind tunnel was available in Edinburgh when this work was commenced the first steps were to design, construct and calibrate a suitable tunnel.

The accomodation consisted of a room, 44' x 18' x 10½', which was later to be enlarged, by the removal of a temporary wall, to 50' x 26' x 10½'. The work was commenced in October 1955 and was finally completed in June 1958, although the tunnel had been in operation for some eighteen months prior to the latter date. There were several conflicting factors which influenced the basic design of the tunnel.

From the financial viewpoint it had to be relatively small and preferably of an open circuit type, but yet as flexible as possible if it were to form the basic equipment of a fluid mechanics section. From the standpoint of our immediate investigation it should have a low free stream turbulence level and also have considerable span in the working section in order to give an uncontaminated flow on a flat plate mounted to span the tunnel.

II. 2 Design and Construction

When the above requirements were analysed it became apparent that the construction of a very low turbulence tunnel was excluded, both on grounds of

space and of cost.

In view of this it was decided to modify an already well tried general purpose tunnel. This tunnel, N.P.L. Design No.A155,is an open circuit wind tunnel with an 18" octagonal working section, a contraction ratio of 3.16: 1 and with a two-bladed fan driven by a 4 H.P. motor giving at 3000 r.p.m. a wind velocity of approximately 100 ft./sec. in the working section. This design, shown in figure 6,was modified as follows:-

The basic measures which can be taken to ensure low turbulence are, firstly, that a large contraction ratio be provided, secondly, that the flow be smoothed by wire mesh screens preceding the contraction section and lastly that adequate settling lengths be allowed between the screens and the contraction section and also after the contraction. To these ends extra sections were included before the contraction ~~ratio~~ to provide space for the installation of screens and to allow the flow to settle after passing through the screens. An extra settling length was also provided after the contraction section with the purpose of removing the flat plate beyond any pressure fluctuations due to the contraction and also to provide a section in which diverging walls could be commenced with a parallel section, should such a device prove necessary to adjust the pressure gradient on the flat plate. In view of the power absorption

of the screens, which work out about 1/3 H.P. per screen at 80 ft./sec., and of extra sections the two bladed fan was replaced by a four bladed unit driven by a 7.5 H.P. motor. The modified design is shown in figure 7.

The tunnel was pre-fabricated in easily manageable sections, the frames being made of white wood and the tunnel walls of hardboard, which was well supported to prevent any appreciable panel vibrations. The working section was made from ¼" Perspex sheet, cemented together to form an octagonal cylinder.

One of our major problems was to be the elimination of spurious vibrations, as far as this was possible, and precautions were taken to this end during the erection of the tunnel. The tunnel room itself, being in the basement, is of very solid construction, having 7" reinforced concrete walls, floor and ceiling. Each section of the tunnel was mounted on 2" angle iron legs which were bedded in heavy concrete slabs, insulated from the floor by layers of felt, and located by steel pegs sheathed in rubber tubes, (see fig. 7). Each section is bolted to the next, forming a solid unit except for a break between the working section and the diffuser. This break, (in which the walls are of canvas), allows a transition from an octagonal to a sixteen sided section and also serves to insulate the main body of

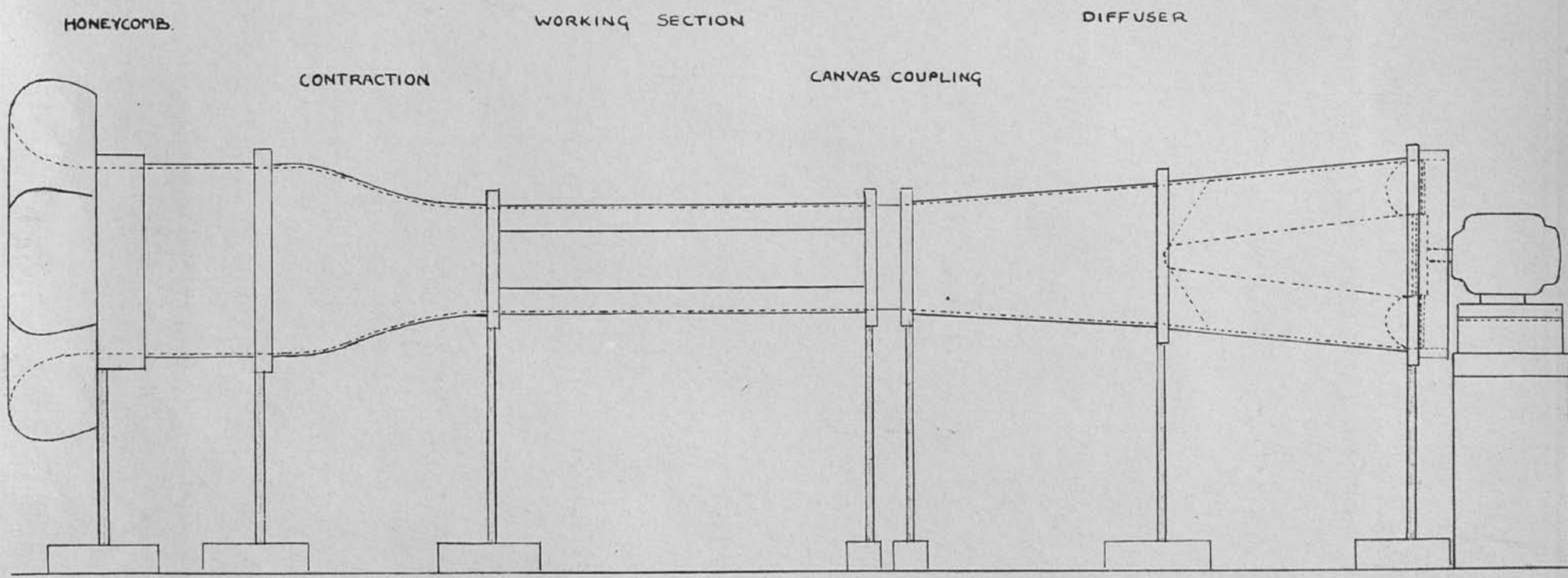

ELEVATION OF N.P.L. TUNNEL

FIGURE 6.

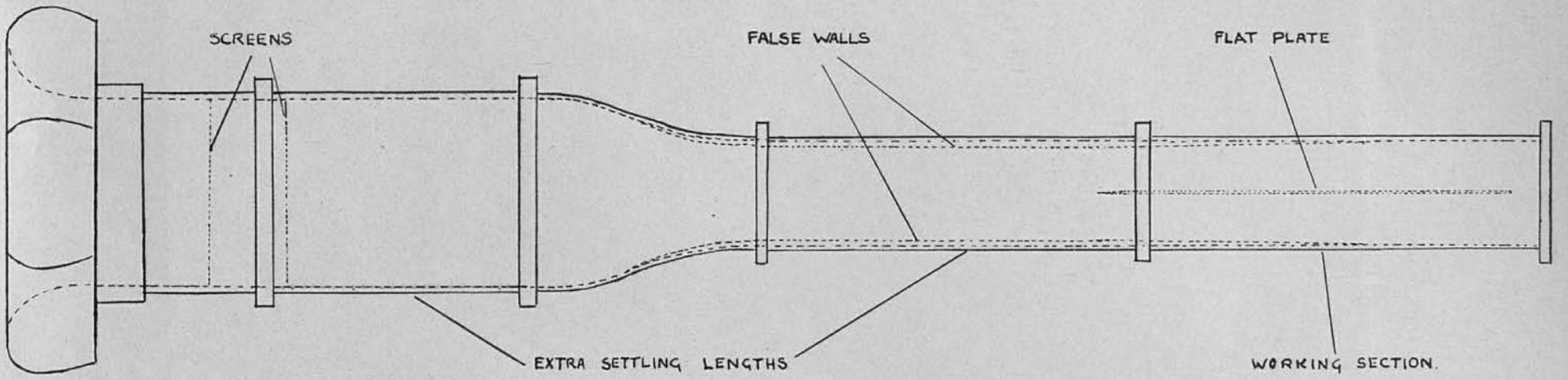

PLAN VIEW OF ACTUAL TUNNEL

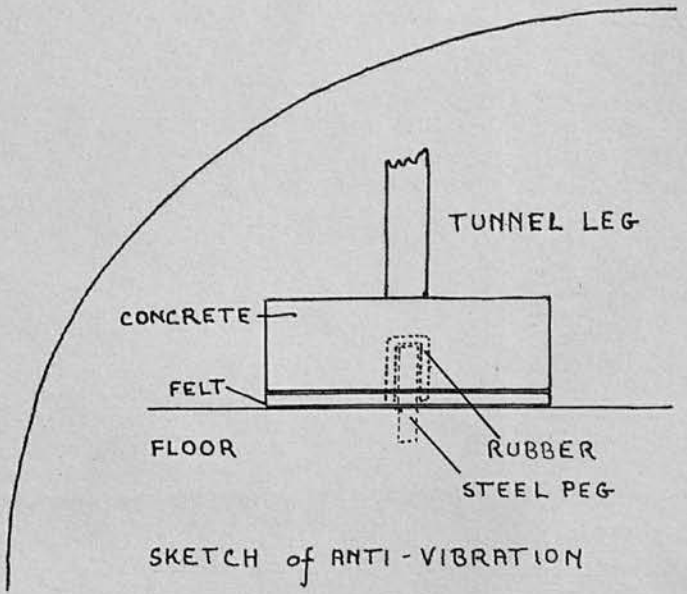

SKETCH of ANTI-VIBRATION MOUNT

FIGURE 7.

the tunnel from vibrations which might be set up in the diffuser by the fan.

Immediately following the inlet flare is a honeycomb straightener of hexagonal brass tubes, 4" long and $\frac{3}{8}$" from face to face, and this is followed by phosphor bronze screens made from 32 S.W.G. wire at 30 wires to the inch. The relative location and optimum number of screens were determined when calibrating the turbulence level.

During the assembly of the tunnel all internal screw heads, of which there were several thousand, were flushed off and the internal surfaces were highly polished with a silicone polish. The joins between each section were sealed internally with sellotape, leaving the whole assembly with a very good internal finish and with relatively few leaks to disturb the flow after the contraction.

It was found that the simplest (and most economical) method of producing a continuously variable speed control for the fan was to generate our own D.C. and use this to drive a D.C. motor directly coupled to the fan. A three phase 7.5 H.P. motor was directly coupled, by means of a gear and chain coupling, to a 6 K.W. D.C. generator, considerable care being taken to align the motor and generator shafts on a common axis. This was achieved by first using an auto collimating device and checking this with a clock gauge mounted on one shaft with its probe bearing on the other. The whole unit was

mounted on a single reinforced concrete slab which was insulated from the floor in the same manner as the tunnel. The field of the generator was excited by an external D.C. supply which was fed into the field coils by means of a stepped potential divider. This external supply was also used to excite the field of the 7.5 H.P. fan motor at a constant level, the output from the generator being fed directly onto the fan motor armature and speed control obtained by use of the potential divider and of a small rheostat to give fine control. The fan, which was designed and manufactured by the Airscrew & Jicwood Co., was mounted directly on the fan motor shaft, the hub of the fan shielding the motor from the airstream.

The motor was mounted on a mild steel frame which was imbedded in a concrete slab, supported by a brick column and insulated from the floor in the usual way.

The photographs in figures 8 and 9 show the completed tunnel, which was symmetrically placed in the space available when it was erected. Although the velocity of the return flow through the room was low, being approximately 1 ft./sec., care was taken at all times to prevent any undue asymmetry or blockage in the room.

In an attempt to minimise the amount of dust in the tunnel room an exhaust fan was arranged to blow air into the room through an oiled steel wool cleaner.

FIGURE 8

View of Wind Tunnel from Inlet End.

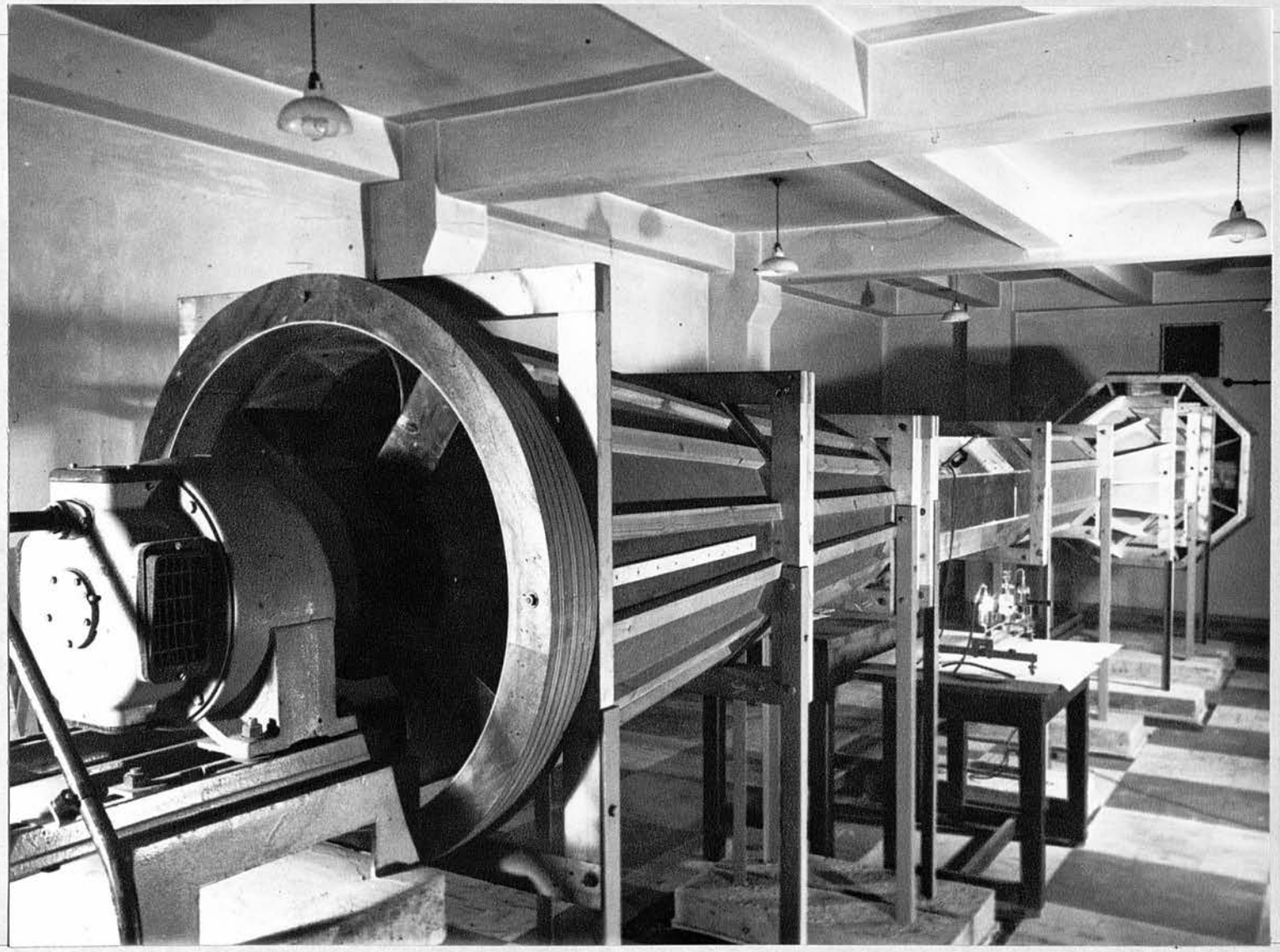

FIGURE 9

View of Wind Tunnel from Diffuser Exit.

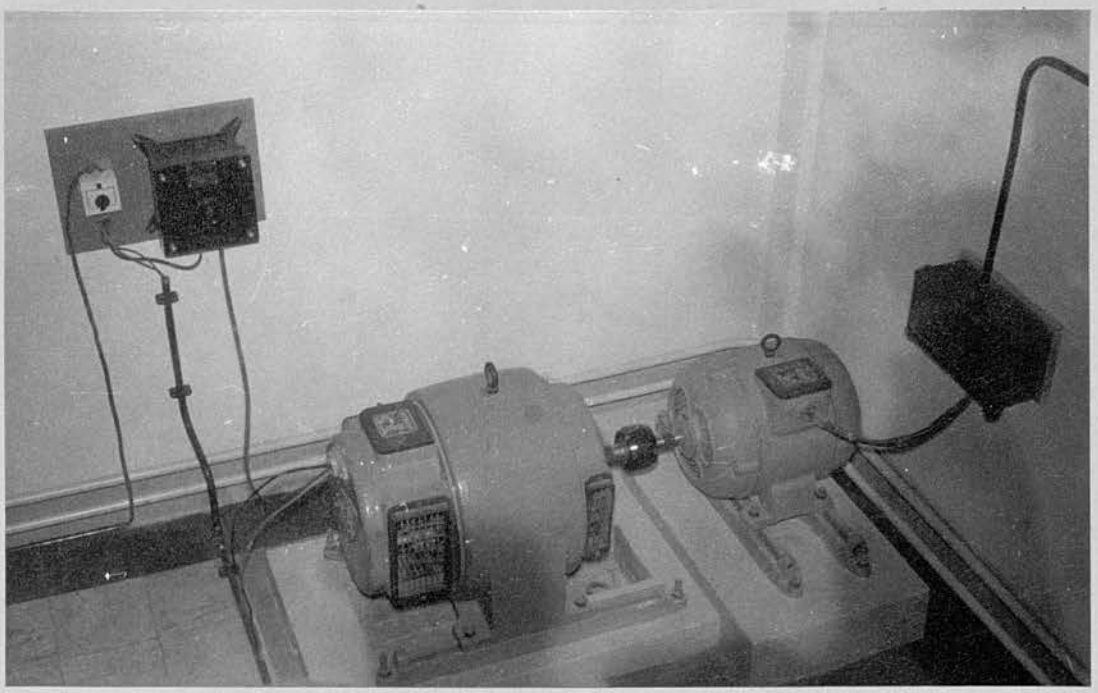

MOTOR - GENERATOR SET.

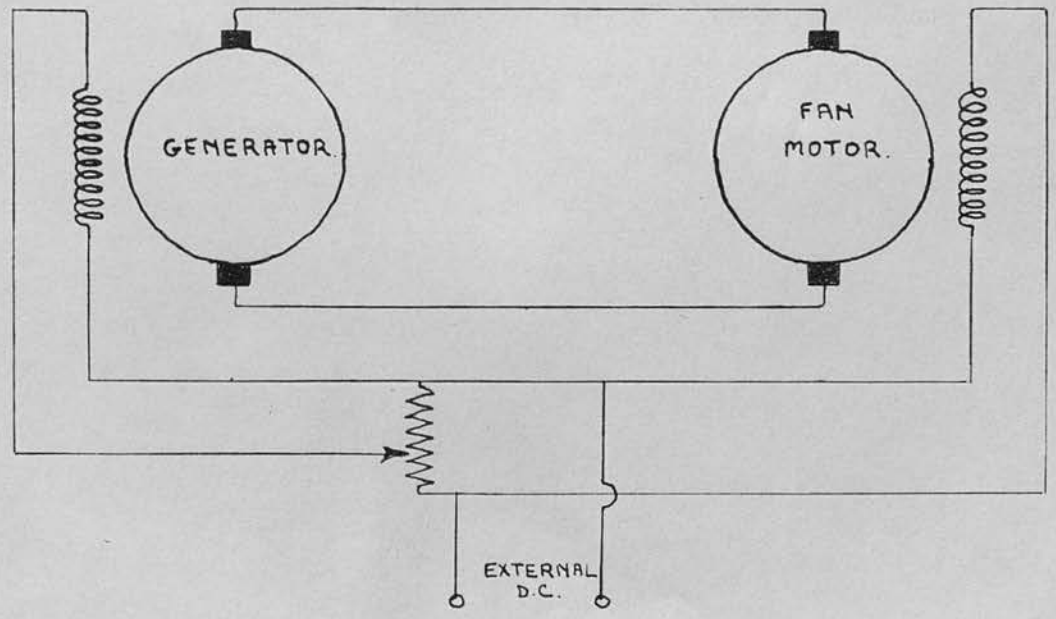

SPEED CONTROL CIRCUIT.

FIGURE 10.

This had the effect of keeping the room at a slightly positive pressure relative to the exterior and may have helped to exclude dust. It was still necessary to clean the screens in the tunnel at regular intervals.

II. 3 Calibration of Wind Tunnel

(a) Calibration for Wind Speed & General Flow in Tunnel

As has already been described the speed control on the tunnel is effected by means of varying the voltage applied to the generator field coils. This is done by means of a potential divider, provision being made for 25 increments of voltage between zero and maximum. A further variable resistance was included in the circuit to provide fine control between the steps of the potential divider (see figure 10).

The wind speed in the tunnel was measured by means of an N.P.L. Standard pitot static tube, used in conjunction with a Chattock gauge. The parameters with which the wind speed couldbe compared are, for our purposes, either the voltage applied to the generator coils or the R.P.M. of the fan. Both were measured, the former with a voltmeter and the latter with a stroboscope. Several curves were obtained for varying numbers of screens in the tunnel and these are shown, as a function of R.P.M. in figure 11. It was found, through experience, that once the equipment had warmed up, the drift in wind speed

during a run of twenty minutes was not more than 1%, and usually less than this. It had been intended to construct a wind speed control balance, based on N.P.L. design No.A236, but in view of the stability, and of the shortness of the period required for photographic recording, it was felt that this could be deferred, as a later refinement. The balance is now being constructed.

The calibration was checked from time to time during the work, especially when any modifications were undertaken. For most of the work it proved sufficient to set the potential divider to a given position on its scale. Thus, for example, position 16 corresponded to 70 ± 1 ft./sec.

The flow in the working section was next investigated by means of several traverses across the tunnel with a pitot static tube. The velocity was found to be uniform over the whole cross section, except for the boundary layers. The pressure gradient in the working section was determined by means of a pitot traverse down the axis of the tunnel. This revealed a considerable negative pressure gradient which would have an adverse effect on laminar oscillations. In order to correct this false walls of 1/16" Perspex were designed and fitted to the vertical walls of the tunnel. These were commenced in the contraction section at the point of inflexion and were allowed to have a parallel section in the

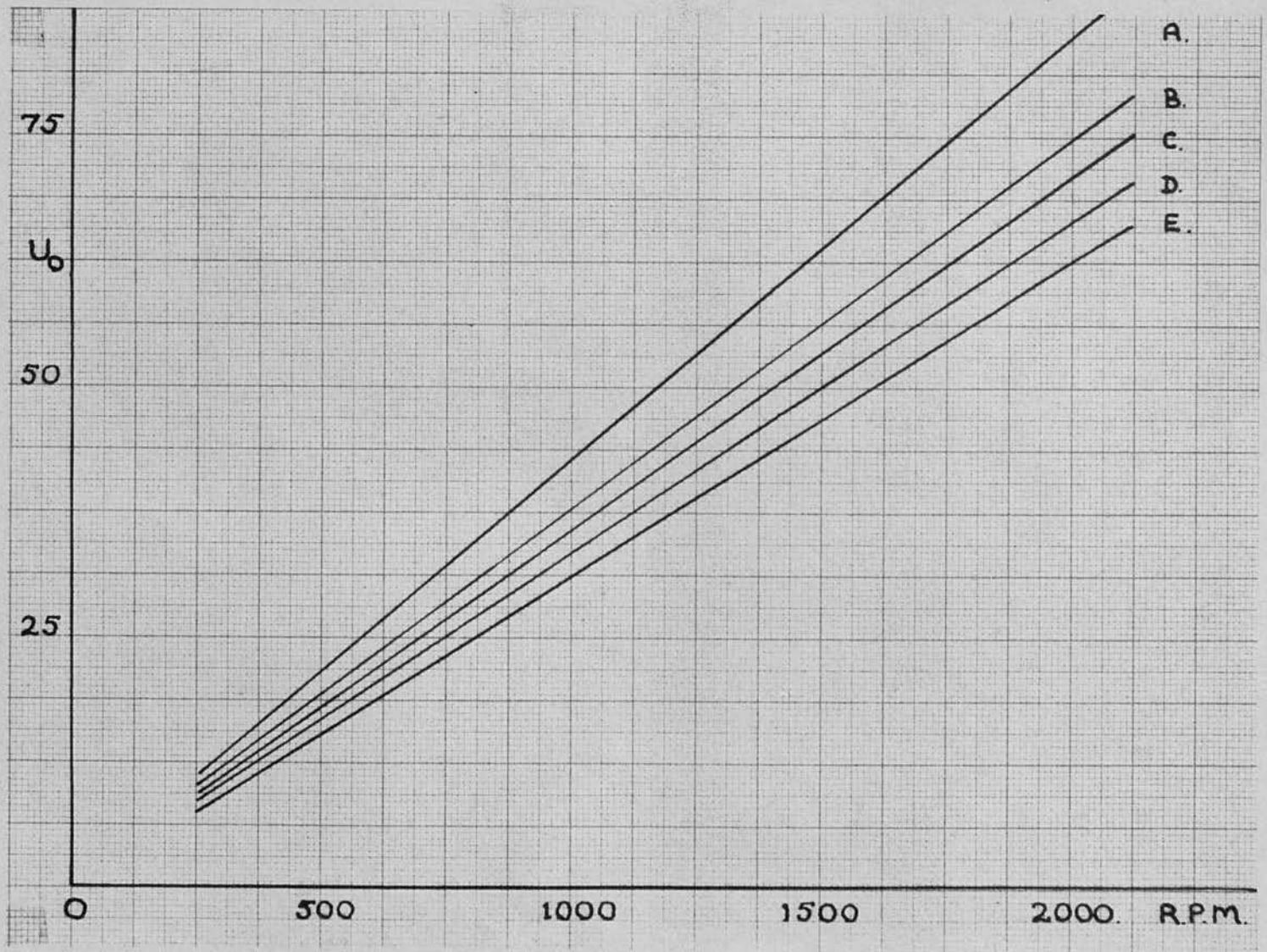

FIGURE 11

Variation of Windspeed, U_o, in ft./sec. with fan R.P.M.

A. Clean Tunnel
B. One Screen
D. Two Screens
E. Three Screens
C. Two Screens and False Walls.

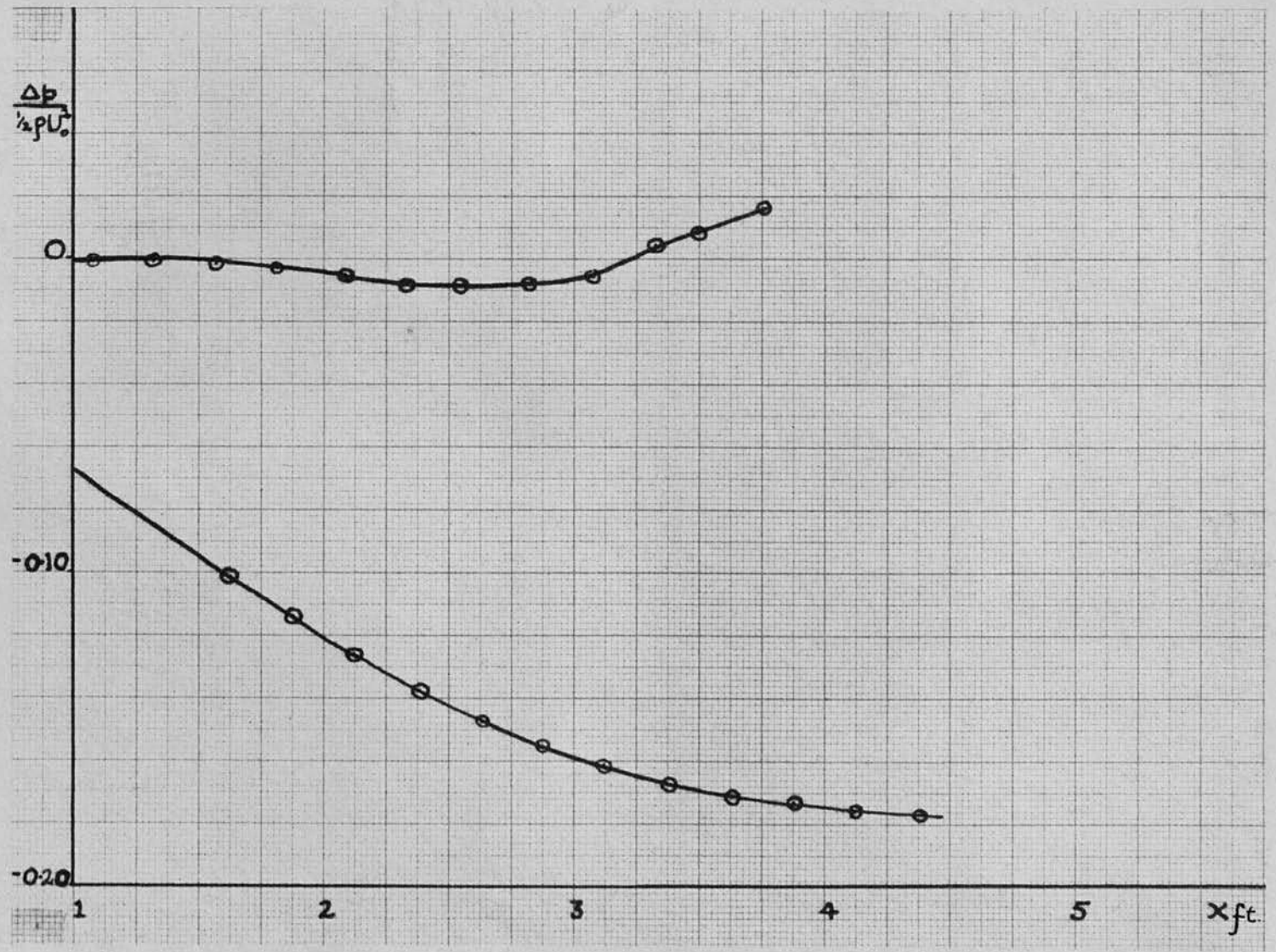

FIGURE 12

Original and modified pressure gradients on the flat plate. Pressure variation, as a fraction of total head, versus distance on flat plate in feet.

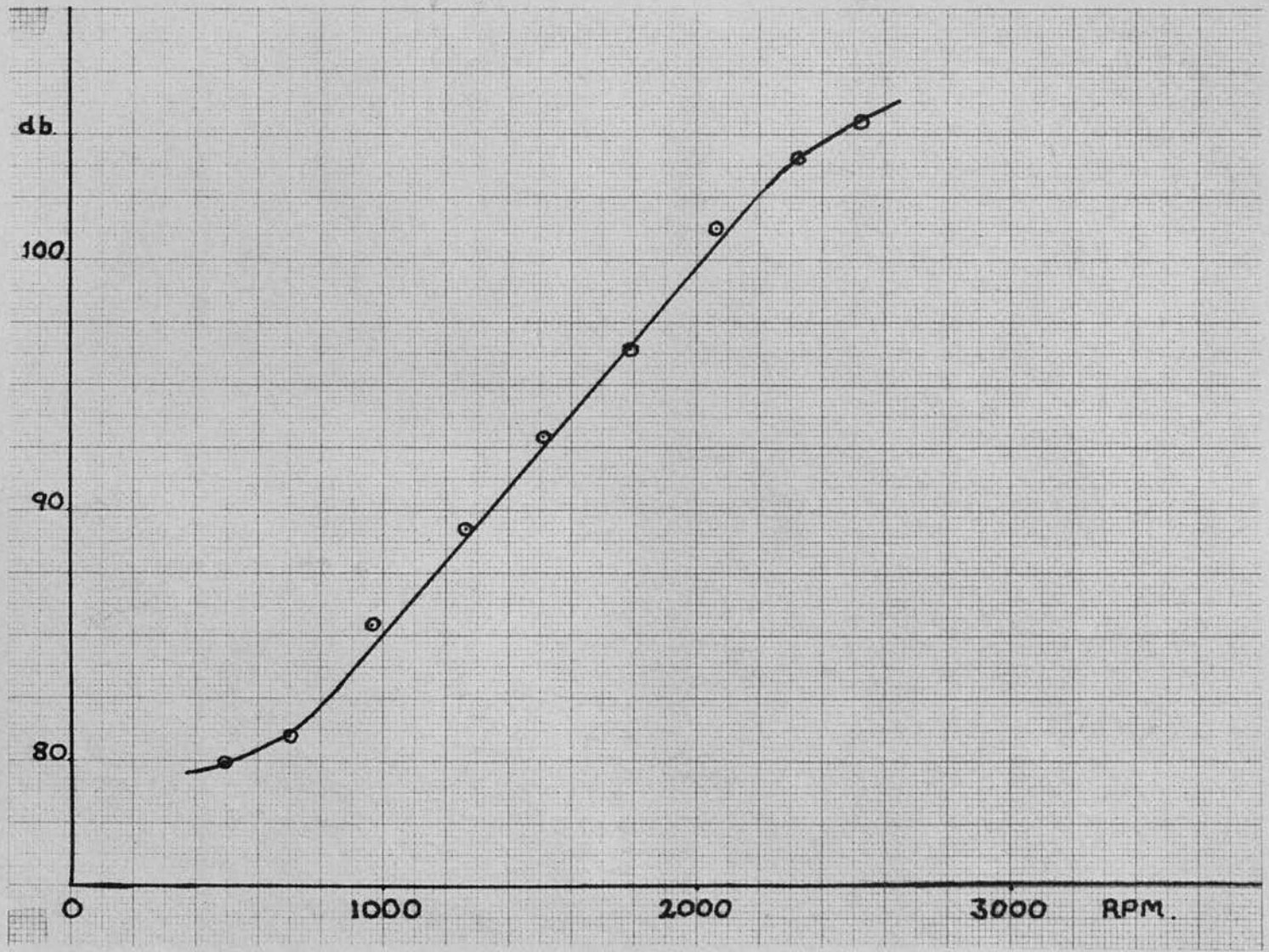

FIGURE 13

Noise Level in db, measured at the working section, as a function of fan R.P.M.

settling length. They were then arranged to diverge at the appropriate angle until they met the tunnel wall near the rear of the working section. The modified pressure gradient was effectively zero over the working region. The original and modified pressure gradients are shown in figure 12.

The noise level in the tunnel room was measured as a function of wind speed. As figure 13 shows the noise level, measured on the 'flat-response' range of a meter, rose linearly with wind speed. The level due to the generator alone was about 80 db while at a windspeed of 90 ft/sec it had risen to 110 db. If we take zero intensity to be 0.0002 dynes/cm., and knowing that the intensity I is given by $I = \frac{1}{2}\rho c U^2$, where c = velocity of sound and U = velocity of the particle, then 106 db corresponds to a velocity of 0.0145 ft/sec which gives an equivalent turbulence level of 0.0165%. Thus the turbulence which can be attributed to noise is lower, by an order of ten, than the actual free stream turbulence, which is later shown to be 0.3%. In practice the tunnel was used at 70 ft/sec for most purposes, which gave a noise level of 100db.

(b) Calibration for Free Stream Turbulence.

In order to assess the suitability of the tunnel for detecting laminar oscillations it is necessary to determine the value of the free stream turbulence, and to reduce it to a minimum.

The method used, due to G.I. Taylor (1935), was

to measure the temperature distribution in the wake of a heated wire.

The theory supposes that if a line source of heated particles is placed at right angles to an air stream then the temperature distribution in the wake will be governed by two distinct effects. First, diffusion by true conductivity from the heated particles and secondly, diffusion due to the turbulent nature of the flow. It is shown that, subject to certain restrictions, the distribution of heated particles due to both causes follows a normal error law.

Thus the temperature distribution in the wake of the heated wire must follow an error curve, so that we can represent the results by a formula of type

$$\bar{y}^2_{obs} = \bar{y}^2_{turb} + \bar{y}^2_0 \qquad (1)$$

that is, the observed mean square deviation is equal to the sum of the mean square deviations due to each separate cause.

Since the temperature, θ, in the wake obeys an error law we have

$$\theta = \theta_0 e^{-\left(\frac{y^2}{2\bar{y}^2}\right)} \qquad (2)$$

from which it can be shown that the breadth $y_{\frac{1}{2}}$ at $\theta = \frac{1}{2}\theta_0$ is related to the mean square deviation by

$$y_{\frac{1}{2}} = 1{\cdot}177\sqrt{\bar{y}^2} \qquad (3)$$

It can also be shown that, in a non turbulent stream, the diffusion due to conductivity alone is represented by

$$y_0^2 = \frac{2Kx}{\rho\sigma U_0^2} \qquad (4)$$

where K = coefficient of thermal conductivity and σ

is the specific heat of air.

Thus, from a knowledge of $\overline{y}_o^2$ and the measured value of $\overline{y}_{obs}^2$, one can calculate $\overline{y}^2$ turb. from which the root mean square value for the turbulent velocities, at right angles to both the flow and the heated wire can be determined by using the relation

$$\frac{\sqrt{\overline{y}^2_{turb}}}{x} = \frac{\sqrt{\overline{v}^2}}{U_o} = \frac{v'}{U_o} \qquad (5)$$

This relation is subject to a condition that the correlation coefficient, R_ξ , between the velocity of a particle at time t and at time $t+\xi$ should be nearly equal to 1.0. Subject to this condition one has only to measure $\overline{y}^2$ obs. to determine v'/U_o

As a test of whether the condition R_ξ nearly equal to 1.0 was being met, one could investigate the temperature distribution curves obtained for deviations from the Gaussian curve, since such a curve should be observed only so long as the condition is satisfied.

The apparatus shown in figure 14 was constructed and used to carry out the investigation. AB is a nichrome wire, 0.001" in diameter, soldered across the tips of steel needles under sufficient tension to avoid sag when the wire is heated. The heating current was supplied through a Variac, which enabled the wire to be raised to any desired temperature. C is a Pallador thermocouple constructed of 0.001" diameter wire, the junction being a butt weld. The leads from the thermocouple are led down to D through glass lined hypodermic tubing, where junction is made

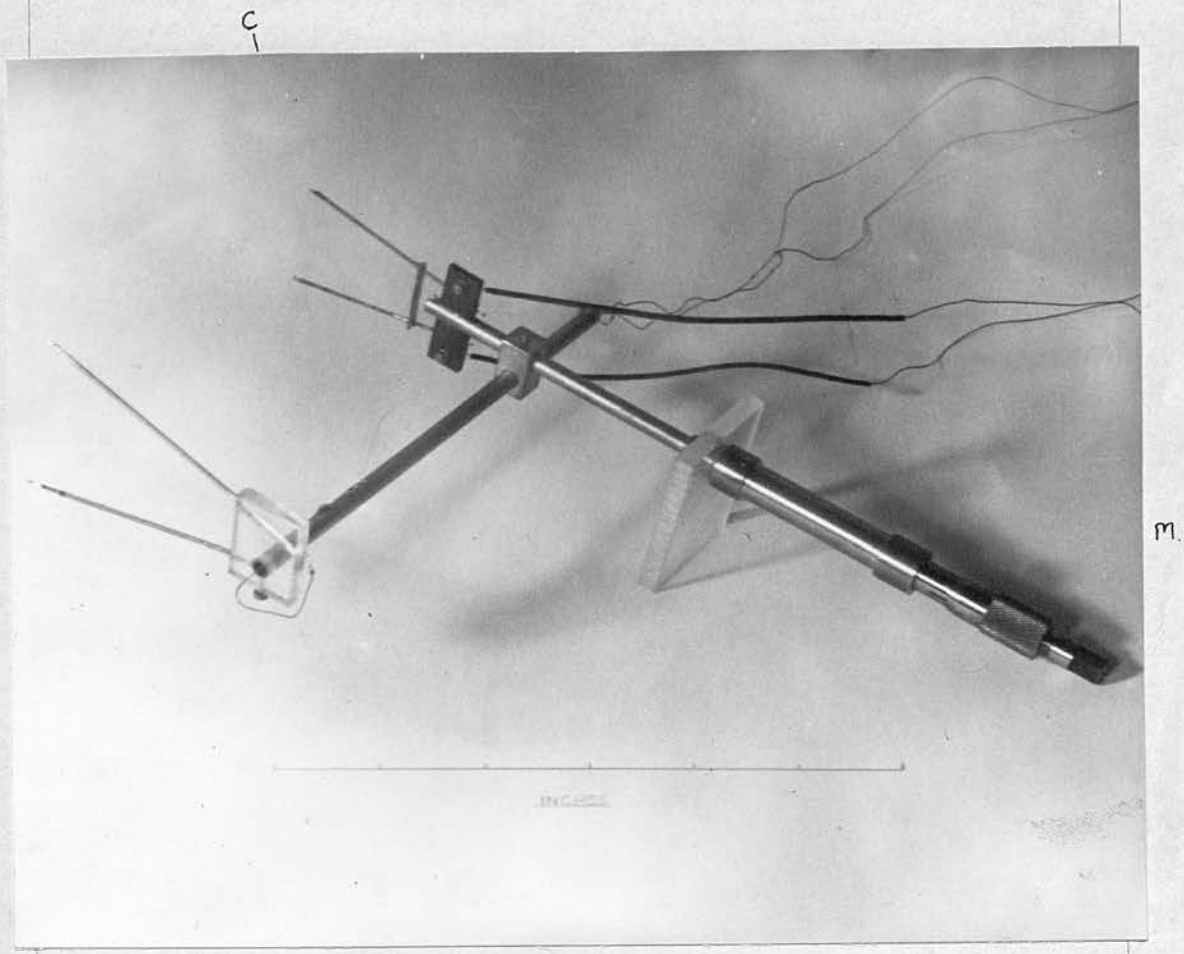

FIGURE 14

Apparatus for Turbulence Calibration

AB Nichrome wire 0.001" diameter

C. Pallador thermocouple

M, Micrometer

(a) Calibration curve for Pallador Thermocouple

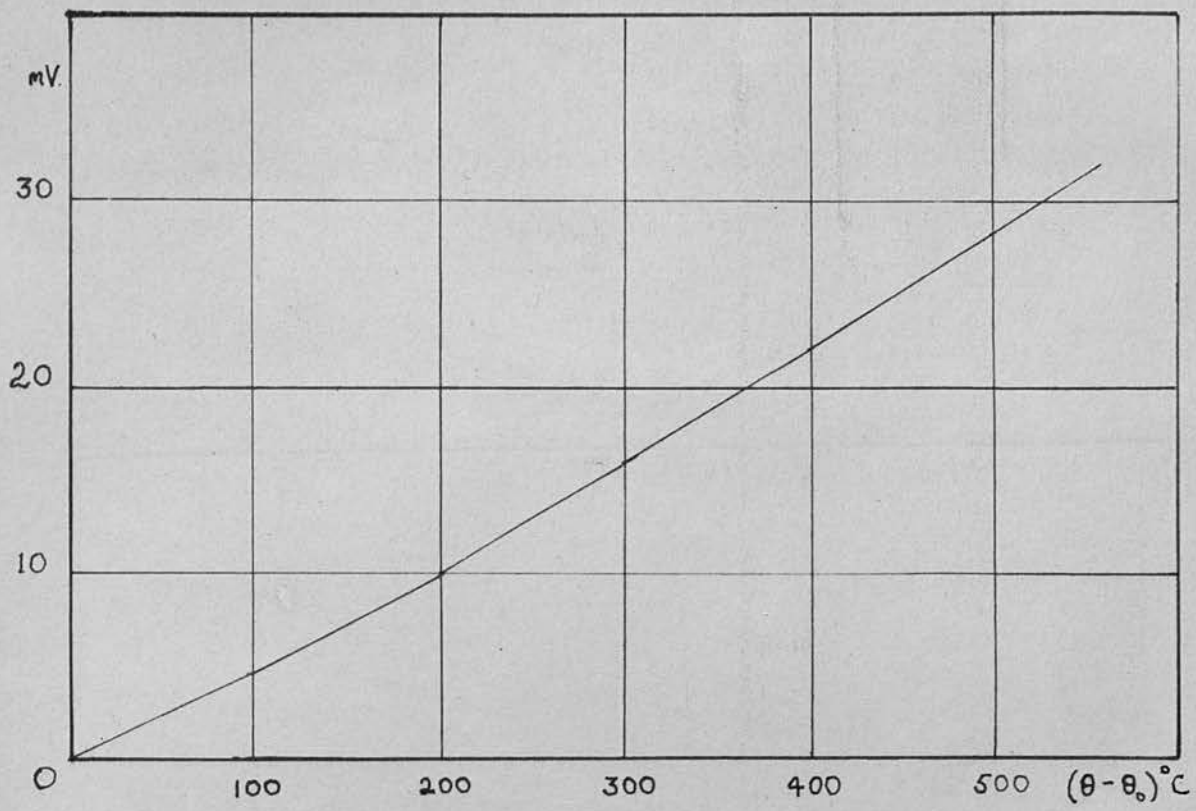

(b) Diagrammatic layout of turbulence determination equipment

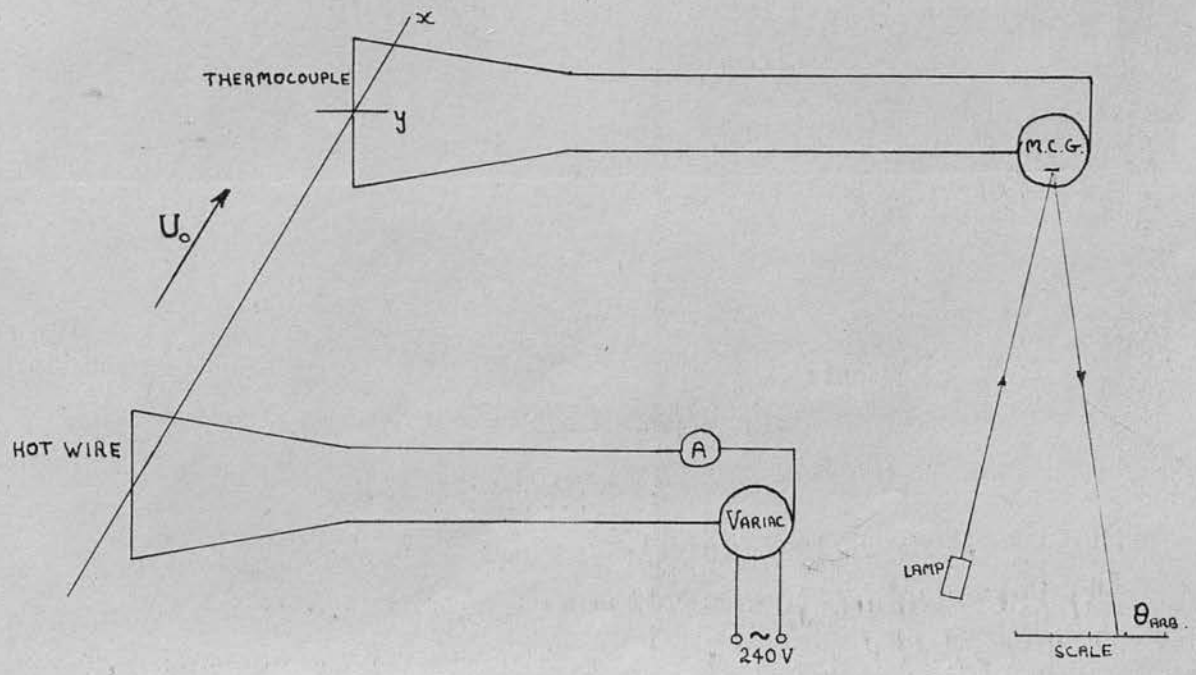

FIGURE 15

with copper wires to the exterior of the tunnel, the circuit being completed with a moving coil galvanometer. The thermocouple can be traversed across the wake of the hot wire by means of the micrometer M, the whole device being clamped to the tunnel wall. Provision is made for the longitudinal separation, x, of the hot wire and the thermocouple to be varied.

Since the resistance of the galvanometer was large compared with the rest of the thermocouple circuit it was sufficient to plot the observed deflections of the galvanometer as direct readings of temperature, the calibration curve of the thermocouple being linear over the range considered, as shown in figure 15. The procedure adopted was, first, to raise the temperature of the hot wire high enough to give a suitable deflection when $y = 0$, then to traverse the thermocouple across the wake, taking readings of the deflection at suitable intervals, which varied with x, until the whole curve had been traced out.

These readings were plotted as θ arb. against y, and the value of $\sqrt{\overline{y^2}}$ obs obtained either by measurement of $Y_{\frac{1}{2}}$ or by numerical integration using Simpson's Rule, when

$$\overline{Y}^2_{obs} = \frac{\int y^2 \theta \, dy}{\int \theta \, dy} \qquad (6)$$

The latter method was preferred, as small errors in reading or curve drawing on the steep sides of the curve could lead to appreciable errors in $Y_{\frac{1}{2}}$. In a sample set of cases the experimental points were

plotted on probability paper to test the condition that the curve should be Gaussian, a good fit being obtained. Figures 16 and 17 show a temperature distribution curve and a probability plot.

Having established the technique, the following cases were investigated:

(a) The effect of varying numbers of screens on the turbulence level.

(b) The effect of the relative location of the screens.

(c) The effect of wind speed.

The results are shown in figures 18 and 19. In figure 18 the region of the curves for $x < 2.5"$ is considered to be a wake effect from the heated wire but for $x > 2.5"$ the value obtained for the turbulence level is constant as would be expected if the level was isotropic. Thus, with no screens, the turbulence level, expressed as a percentage of the free stream velocity, is 0.44%, one screen reduces this to 0.31%, two screens at 6" spacing increase the level to 0.36%, 3 screens at 6" spacing reduce it to 0.29%, while 2 screens at 1 ft. spacing give 0.30%, a similar value being obtained for 3 screens at 1 ft. spacing. The anomolous results with 2 screens at 6" spacing is thought to be due to an interference effect between the screens although the Reynolds number, based on the wire diamter is well below the critical value of 40 for all tunnel speeds.

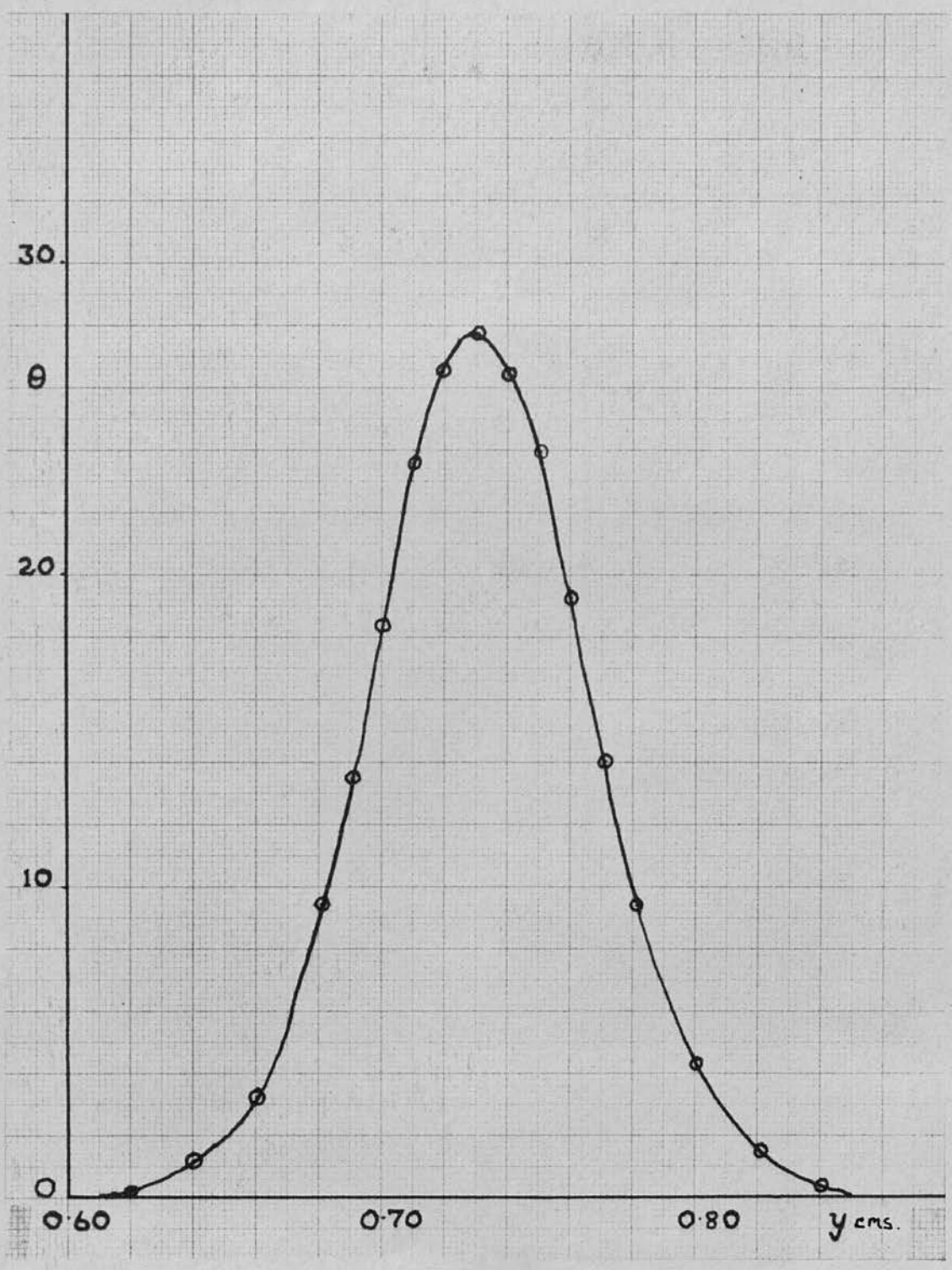

FIGURE 16

Temperature distribution in wake of heated wire. Temperature θ, plotted in arbitrary units, versus y, distance traversed across wake.

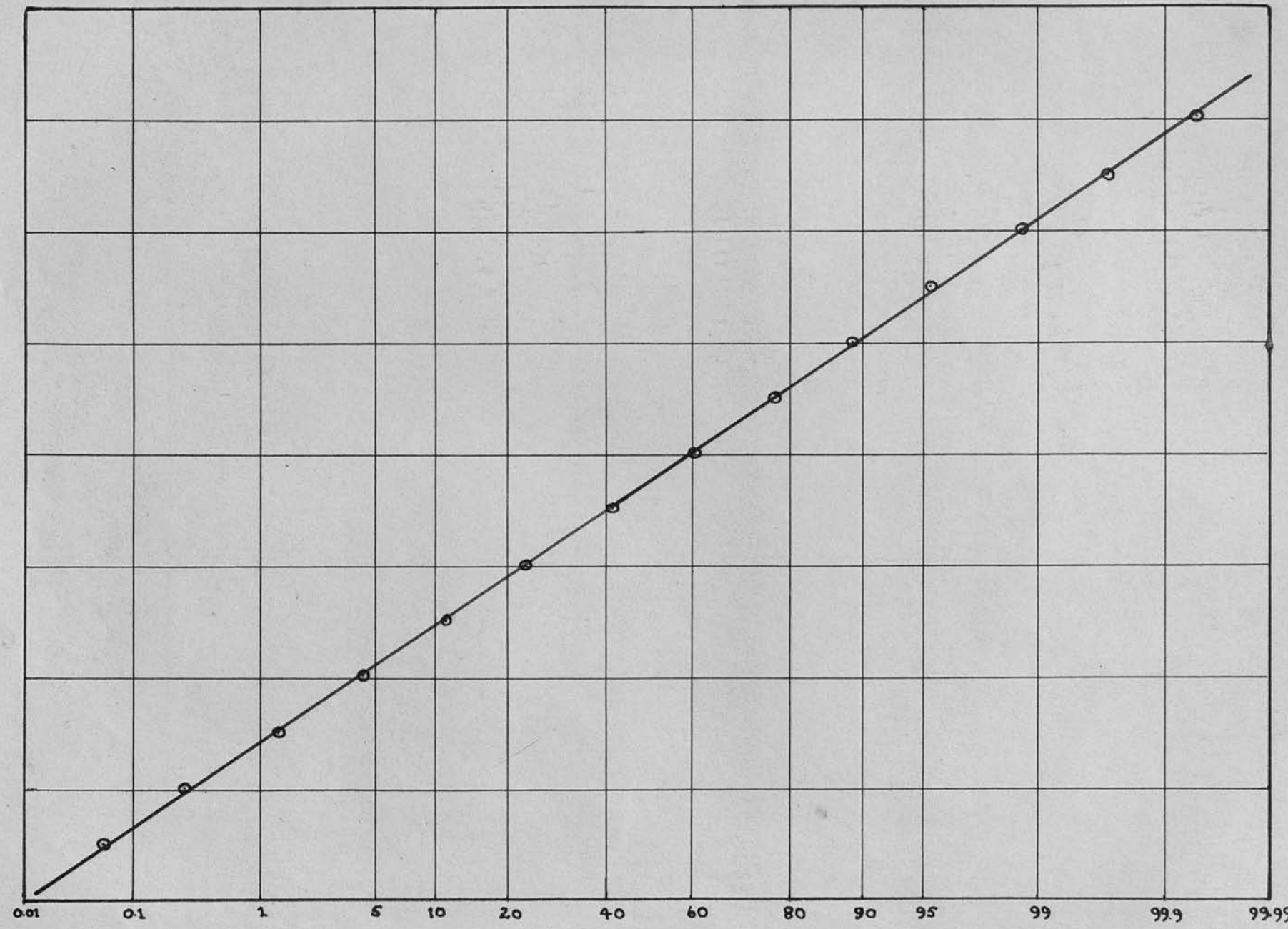

FIGURE 17

Probability plot of Temperature distribution curve.

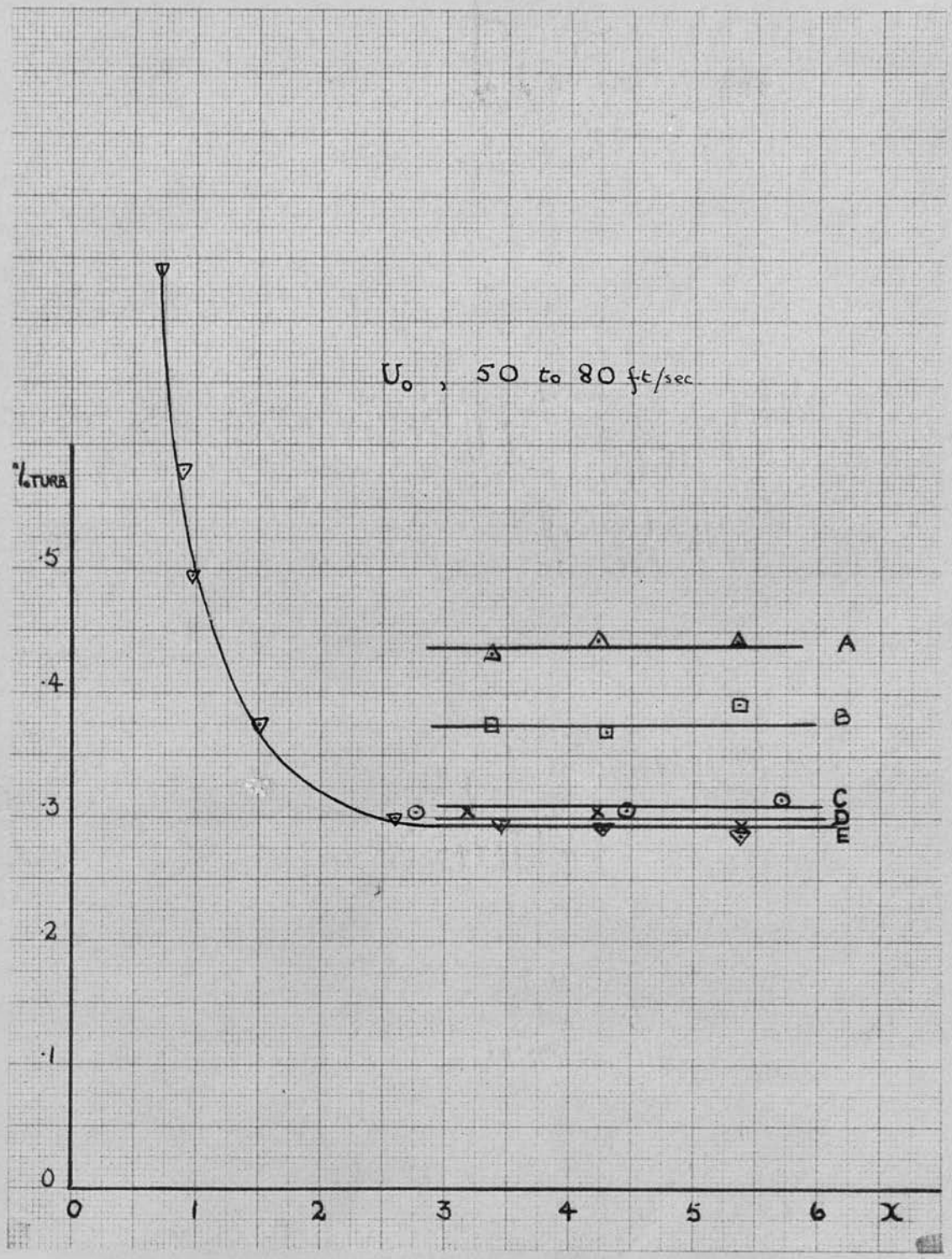

FIGURE 18

Percentage Turbulence as a function of the separation, x", of the hot wire and the thermocouple

A No Screens
B Two Screens at 6" separation
C One Screen
D Two Screens at 1 ft. separation
E Three Screens at 1 ft. separation.

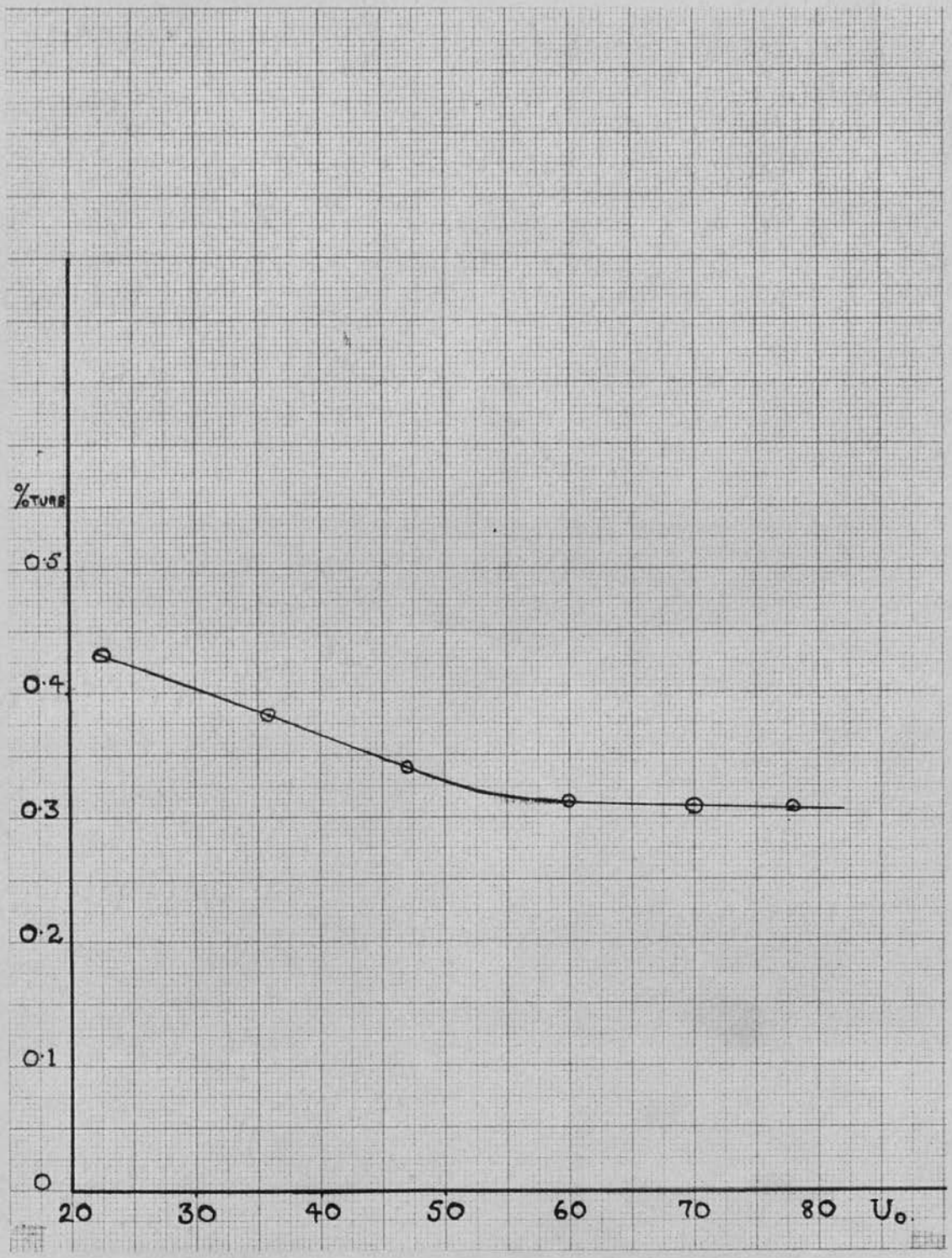

FIGURE 19

Percentage Turbulence as a function of Windspeed in ft./sec. ; One Screen.

Figure 19 shows that the wind speed affects the turbulence to a small extent, as is to be expected, since the efficiency of the straightener increases with wind speed. Over the working range of 50 ft/sec. upwards the change is small and can be neglected.

In considering these results we must bear in mind that the accuracy of the experimental method decreases rapidly as the turbulence level falls. At a turbulence level of 0.3% the turbulent diffusion accounts for 35% of the total diffusion while at 0.2% turbulence this has fallen to 10%. The method is thus being used at the limit of its application and, while the differentiation between the results for 1, 2 and 3 screens is real, the experimental error in each value is approximately 5 %. Batchelor (1945) shows that the effect of gauze screens on the transverse turbulence is to reduce the mean square values in the ratio

$$\frac{v_2'^2}{v_1'^2} = \left[1 - \frac{K}{10(1+\frac{2}{5}K)}\right]^2$$

where K is the pressure drop coefficient of the screen, defined by $K = \frac{P_1 - P_2}{\frac{1}{2}\rho U^2}$ and the subscripts 1 and 2 denote conditions before and after the screen. For the screens which we are using K is 3.25 which gives a reduction of 14% in the R.M.S. value of the transverse component for one screen, 18% for two screens, and 20% for three screens.

MacPhail (1944) has shown that the contraction ratio has little effect upon the transverse components, reducing the R.M.S. value by a factor of 2 in his

experiments with a 10:1 contraction ratio.

G.I. Taylor (1935) has shown that the turbulence generated by a honeycomb of mesh size M is given by

$$\frac{u'}{U} = \frac{1}{B + 5/A^2 x/M}$$

where x is the distance downstream of the honeycomb, B is a constant which becomes negligible for large values of $\frac{x}{M}$ and A has the value 2.1, so that

$$u'/U = 0.9\ M/x$$

If we assume that v'/U has a similar value and calculate the turbulence in the working section with one, two and three screens, using Batchelors formular, we obtain values of :-

$\frac{v'}{U_o}$ = 0.31%, 0.295%, and 0.285% respectively taking an $\frac{x}{M}$ value of 250, and assuming the contraction ratio to have no effect. As experimental information on the effect of the honeycomb is limited, and inconsistent, these figures agree well with the experimental results for screens 1 ft. apart, if we assume that the no screens result is high for some reason. The results with screens at 6" spacing are due to the second screen being in the wake of the first. The turbulence measurements for $x < 2.5$" demonstrate this effect in the wake of the hot wire. While these figures are high compared with the figure of 0.03% used by Schubauer and Skramstad it should still be possible to observe laminar oscillations, and in view of the other limitations of the tunnel it was decided to accept this figure.

Two screens were used at 1 ft. spacing as they gave a definite advantage over 1 screen, while 3 screens

gave very little improvement and considerably increased the noise level.

II. 4 Special Equipment

(a) Installation of Flat Plate

In order to study laminar oscillations we require a flat plate in the tunnel and this was installed during the assembly of the tunnel, since it would not interfere with the general calibration.

The flat plate itself was fabricated from a single sheet of $\frac{1}{4}$" Perspex, 6 ft. long and spanning the tunnel vertically. The leading edge was tapered on both sides on a milling machine over a distance of 4" to a knife edge at the leading edge. The shoulder formed at the rear end of the taper was hand polished until the transition could barely be detected by touch. The flat plate was bolted to 1" brass angle bars which were in turn bolted to the tunnel walls. This was done in such a way that a slight transverse tension was placed on the plate, especially at the leading edge, to prevent any warping due to stresses set up by the milling operation.

As the perspex portion of the working section is 5'6" long the flat plate was mounted with its leading edge 1 ft. upstream of the front of this section, that is, 4 ft. downstream from the rear of the contraction ~~ratio~~, an ample distance to allow for pressure fluctuations to die out.

A set of rails were provided at top and bottom

of the tunnel running parallel to, and 2" from, the flat plate, the brass angle bars providing one side of the rails. A carriage was constructed to run on these rails on four ball races, with provision for locating a boom at different stations. An instrument carried on this boom could be located at any desired x and z co-ordinates on the flat plate. Control over the co-ordinate was obtained by means of the device shown in figure 20. The boom on the carriage carried, at its upstream end, a further pivoted arm which bore upon the flat plate just upstream of the hinge. This arm was driven by means of a flexible cable and a micrometer outside the tunnel. The actual co-ordinate was read from a clock gauge mounted on the rear of this arm with its probe bearing on the flat plate backlash errors thus being avoided. Strong springs were provided at suitable locations. The carriage and flat plate mounts are shown in figure 21.

(b) Calibration of Flow on Flat Plate

Before experiments on laminar oscillations were commenced it was necessary to investigate the static flow pattern on the flat plate.

The carriage and boom were used to mount a variety of total head and static tubes with which the flow was plotted. The excess blockage provided by the carriage also served to ensure that the stagnation point remained on the working side of the plate.

Boundary layer profiles were first measured with

a total head tube, capable of being traversed through the boundary layer, and a static tube at $\frac{1}{2}$" outside the total head tube. Both tubes were made from 0.040" diameter stainless steel hypodermic tubing, the total head tube being flattened and ground at the end to form a slit 0.005" wide and 0.015" long, its centre being 0.007" from the surface when the tube was in contact with the surface. The static tube had four 0.008" holes drilled through the wall at 8 diameters from the closed end.

The profiles obtained are shown in figure 22 where the solid curve indicates the theoretical solution due to Blasius. Good agreement is obtained for x values of up to 3.25 ft. when the profile commences a change to the characterictic turbulent profile, which is well developed at 4.5 ft.

The exploration was continued by means of traverses along the plate with the total head tube in contact with the plate. The total head falls slowly as the x co-ordinate is increased until a turning point is reached and then increases rapidly, reaching a maximum at the rear of the transition region after which it again falls slowly. As indicated in figure 23 the first turning point is taken as the start of transition and the second as the end of the transition region. These traverses were carried out for several z values and a picture obtained of the laminar, transition and turbulent regions of the flow on the flat plate. Figure 24 illustrates the results of this

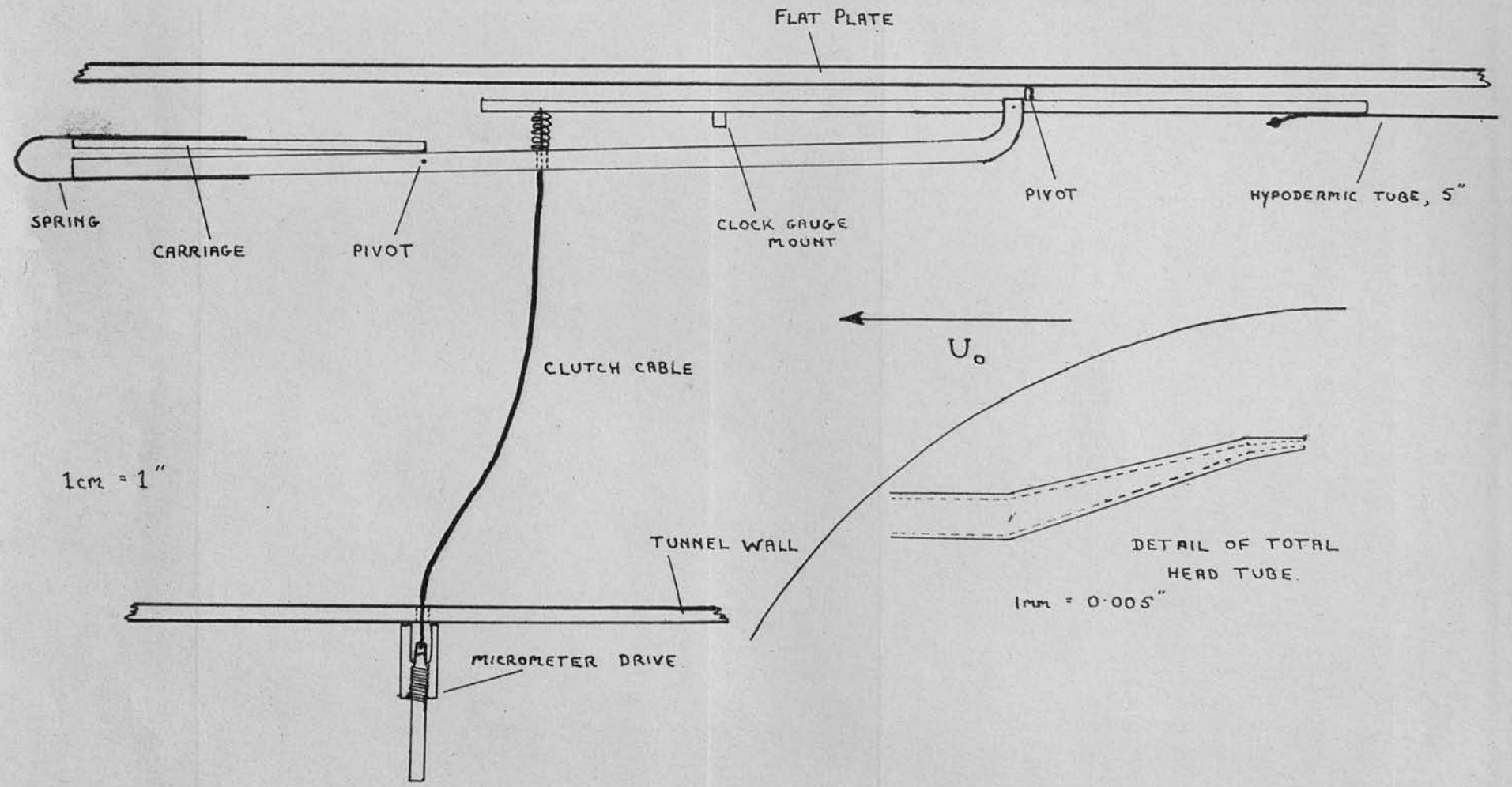

DETAIL OF BOOM AND CARRIAGE.

FIGURE 20.

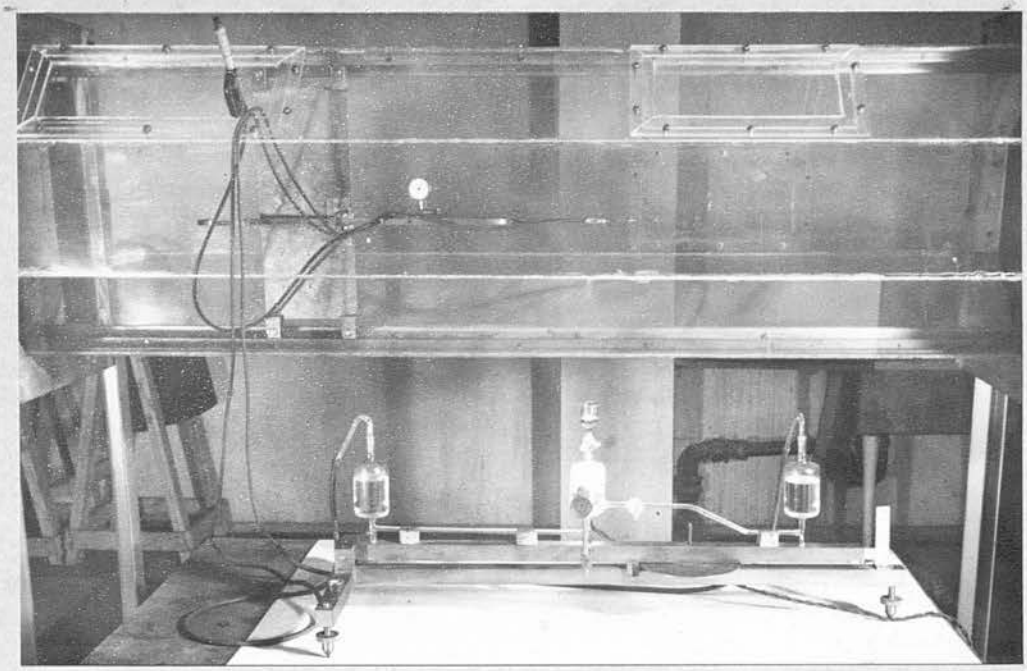

General View of Working Section.

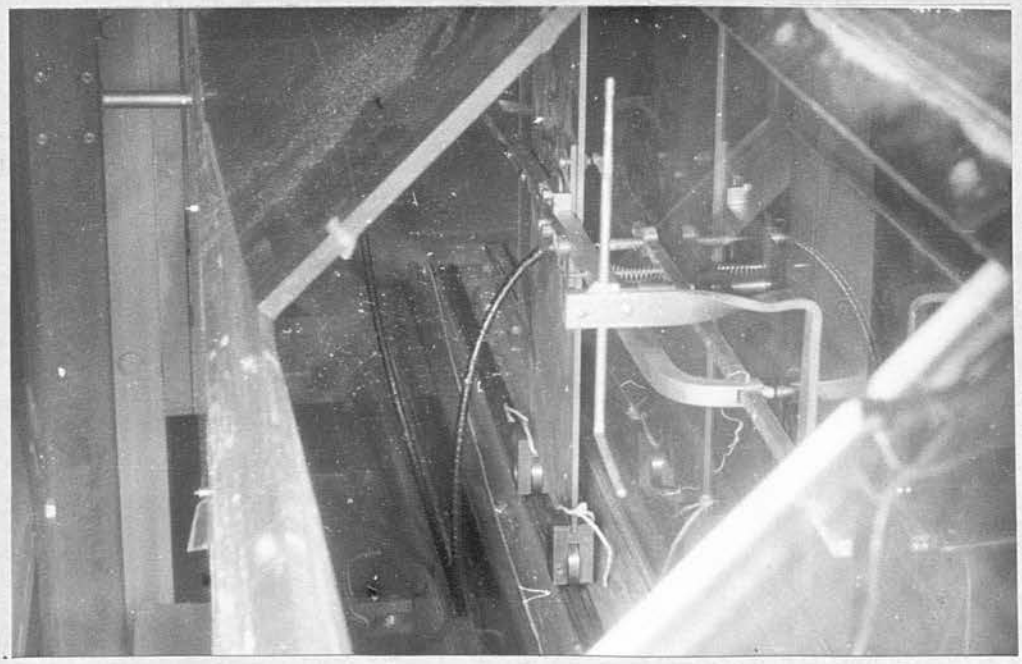

View of Boom and Carriage with small
Pitot-static tube mounted.

FIGURE 21

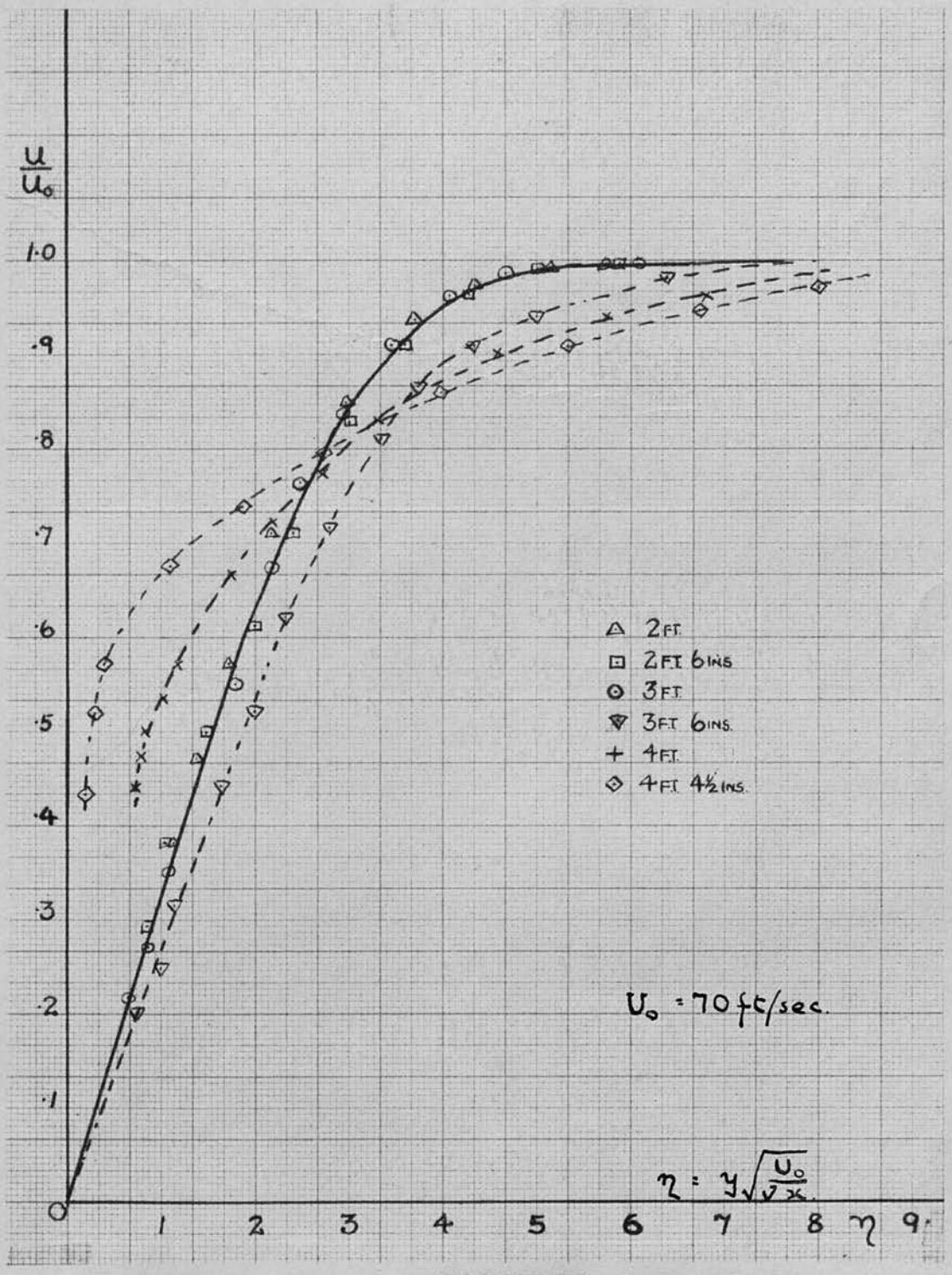

FIGURE 22

Boundary layer profiles for various x stations.
Blasius distribution represented by solid curve.

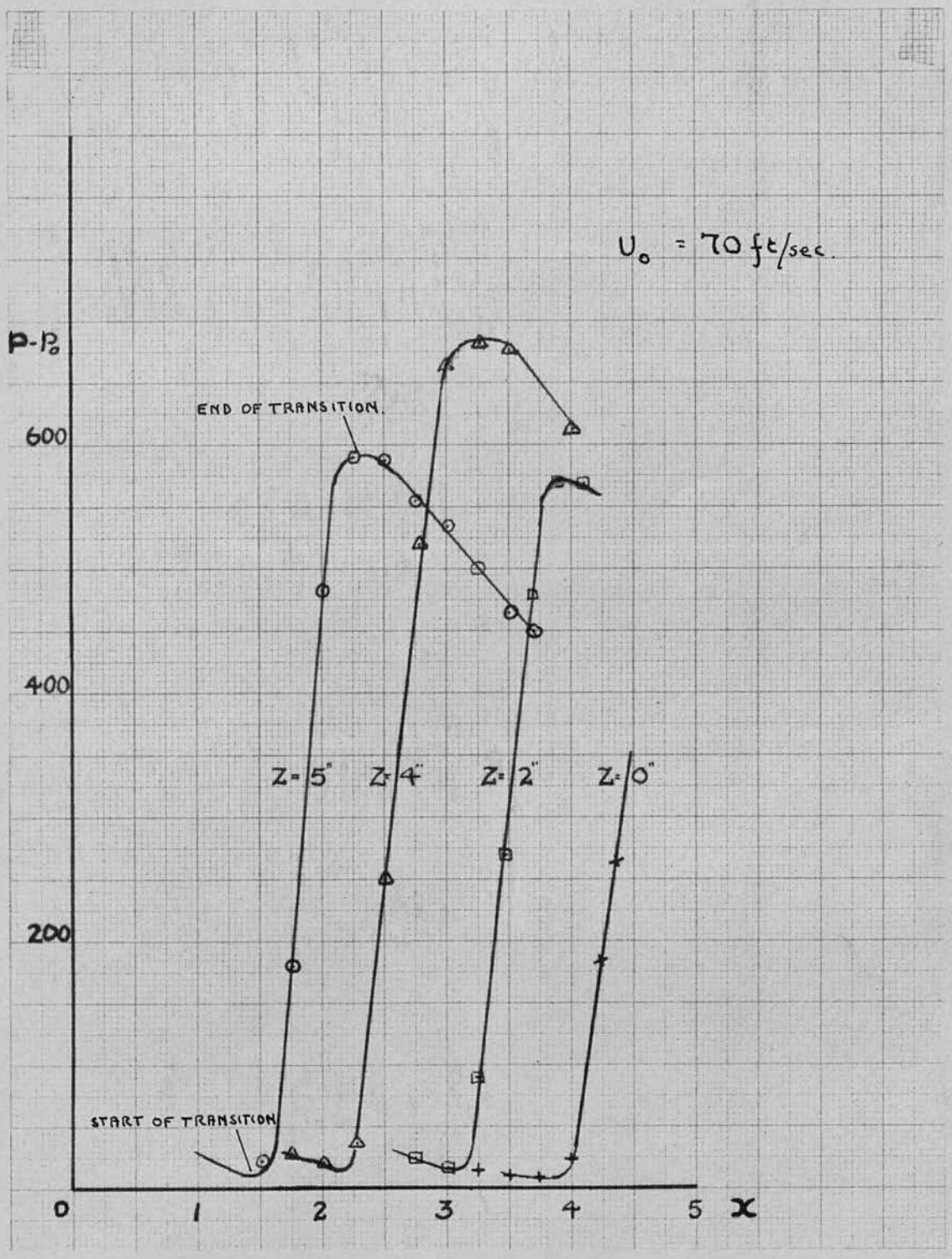

FIGURE 23

Variation of total head in arbitrary units, for various Z values. Measurement taken at 0.007" from plate.

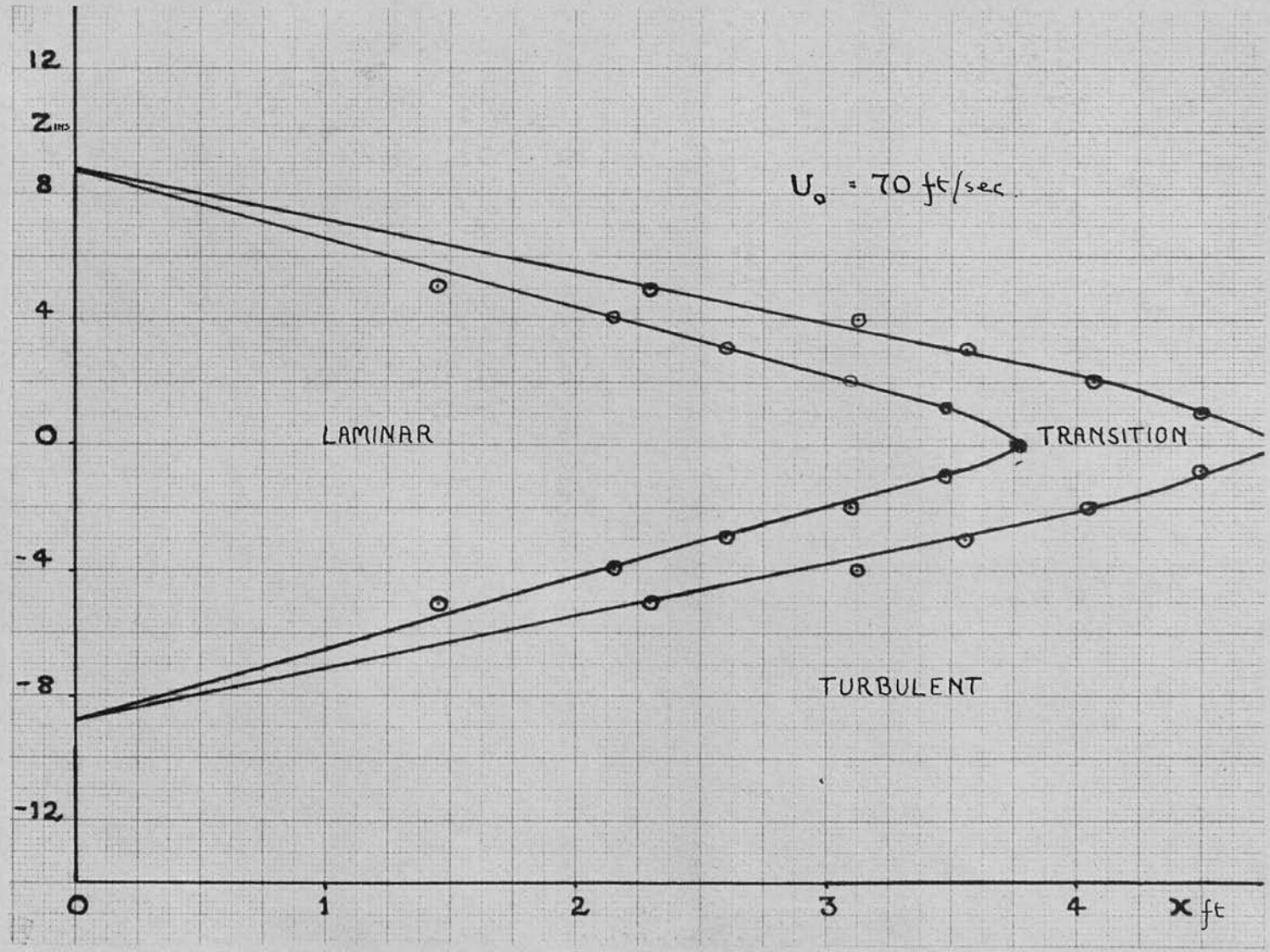

FIGURE 24.

Plan of static flow pattern in flate plate, showing laminar, transition, and turbulent regions.

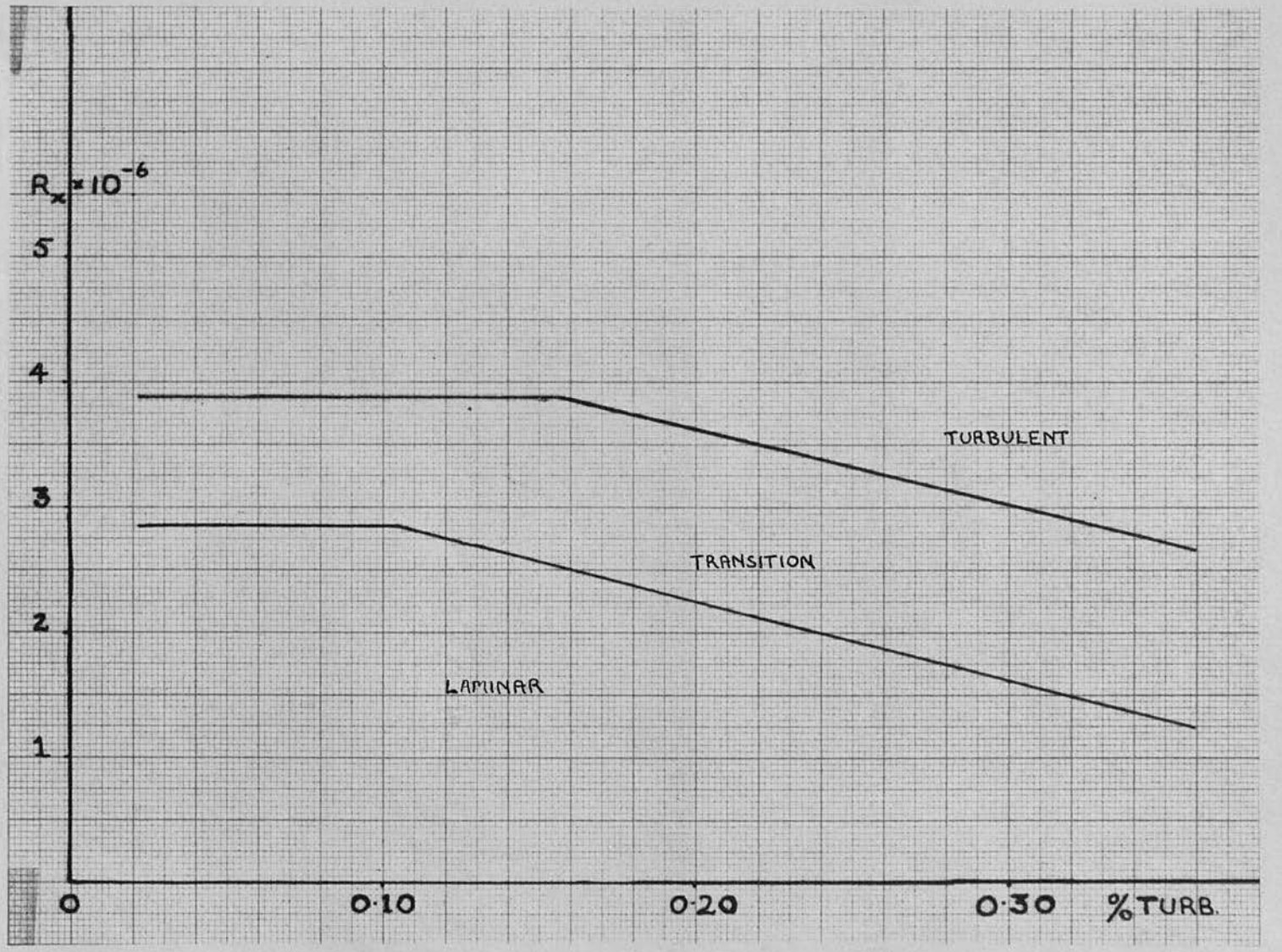

FIGURE 25

Transition Reynolds number as a function of free stream turbulence, after Schubauer and Skramstad.

exploration, which showed that the flow became turbulent due to the growth of turbulent wedges from the intersection of the leading edge and the tunnel wall. The half angle of the wedge, measured as $10\frac{1}{2}^{\circ}$, agrees well with the results of Tani and Sato (1956).

This completed the static exploration of the flow on the flat plate.

II. 5 Conclusions

In view of the measurements made in the preceding sections it is now possible to assess the suitability of the tunnel for detecting laminar oscillations and following their development into the transition region.

Transition, in such an experiment, may result from either the transverse contamination effect or from the free stream turbulence. Schubauer and Shramstad (1947), during their work, investigated the effect of free stream turbulence upon the transition Reynolds number and obtained the results reproduced in figure 25. While the flat portion of the curve for the % turbulence less than 0.1% is open to question the main portion is well supported and shows that, with 0.3% turbulence, which is our case, transition is completed at a Reynolds number of $R_x = 3.0 \times 10^6$ which gives, for $U = 100$ ft./sec., $x = 4.65$ ft. Thus, at the maximum wind speed which we can utilise the transition to turbulence is still governed by the wedges spreading from the leading edge extremities.

A reduction in the free stream turbulence would

not affect the static flow pattern on the plate to any marked extent, although it would make the observation of laminar oscillations a simpler procedure.

The effect of the relatively high turbulence level will be to mask the laminar oscillations to some extent so that we will not expect to observe the amplification and decay of a given frequency in such a clear cut fashion as Schubauer and Skramstad.

It should prove just possible by working at speeds above 85 ft/sec. to bring the front of the transition region upstream of the wedge fronts so that a marginal appraisal of the performance of the recording device in this region should be feasible.

Thus the tunnel though not ideally suitable for the project in hand will enable the device to be tested in the laminar region and, should results be sufficiently encouraging, the tunnel could either be modified or the equipment transferred to a more suitable tunnel.

Chapter 111

Development of Recording Device.

111. 1. Introduction

The basic requirements of the device has been outlined in chapter 1. This was that a mechanical response to velocity fluctuations perpendicular to the main flow should be obtained. A suitable method of recording this response is also necessary.

The conventional instrument for such measurements is the hot wire anemometer, the principle of which is to observe current, or voltage, variations as the rate of cooling of the wire varies with velocity. It can be shown that the rate of change of current with velocity, the resistance being constant is given by

$$\left(\frac{\partial i}{\partial u}\right)_R = \frac{i}{4\left(u + {}^{a}/_{b}\sqrt{{}^{u}/_{d}}\right)}$$

where a and b are functions of the temperature and of the fluid and d is the wire diameter. Thus the sensitivity increases as the velocity decreases. For small changes of velocity the response is linear.

The time constant of a hot wire is given by

$$t = \frac{Jms\,(\,\overline{R} - R_a)}{i^2 R_o^2 \gamma}$$

where J = mechanical equivalent of heat, m the mass of the wire, s the specific resistance, R the resistance at operating, air and zero temperatures and γ the temperature coefficient of resistance. This gives, for a platinum wire of 10^{-4}" diameter and 0.15" long a value of 10^{-3} seconds. This is the finest wire that it is convenient to work with and for recording of

frequencies above 1 Kc/sec elaborate compensating circuits must be included. The hot wire works well for low frequencies and no compensation is necessary at frequencies below 700 c/sec. It was a simple form of the instrument that Schubauer and Skramstad used to obtain their results.

A hot wire responds to the local velocity, so that a wire placed perpendicular to the main stream will respond to U + u and v, being shielded from W by the supports. The variable part of the local velocity is given by

$$(\delta V)^2 = 2u\,U + u^2 + v^2$$

As $u^2 + v^2$ is negligible compared with the first term a response proportional to u will be obtained. To measure v fluctuations a more complex arrangement is necessary. Two separate wires are mounted as a cross, or a vee, at 60° to each other and in the plane of u and v. The wires are connected with their outputs in opposition and, while a change in u and w has an equal effect on each, changes in v have an opposite effect and an output related to v is obtained. Thus, the hot wire, while an ideal instrument for measuring u fluctuations becomes more cumbersome when dealing with v fluctuations and a new technique measuring these directly is desirable.

A comprehensive review of hot wire technique and theory is given by Willis (1945).

Schubauer and Skramstad confirmed that v oscillat-

ions exist in the boundary layer but performed no quantitative measurements, so that a measurement of the neutral stability curve for v oscillations would provide further experimental support for the theoretical solution.

With this, and the ideas outlined in chapter 1 in view, methods were considered of obtaining a suitable response. The most promising approach appeared to be to suspend a light vane in the airstream and to observe the way in which it moved under the influence of the varying velocities. The main stream velocity $U + u$ is an effectively constant controlling force so that only v should affect the vane. A calculation of the wavelength of laminar oscillations, with $U_o = 60$ ft/sec., gives a minimum value of 0.5", so that a vane of less than half this dimension should follow the fluctuations accurately. The response to turbulent fluctuations, which are characterised by much higher frequencies, is more doubtful, as the vane will tend to integrate the fluctuations over its length. It may prove possible to obtain a suitable response by reducing the vane size in such a case.

Until the wind tunnel was completed it was decided to build a small tunnel and use it to investigate the properties of vanes, in particular their resonant frequencies, and to attempt to develop a theory to describe their behaviour and enable us to predict their performance in the boundary layer.

111. 2. Preliminary Investigations

A small wind tunnel with a 3" x 3" working section was constructed and is shown in figure 26. A contraction ratio of 16:1 was used in an attempt to obtain a fairly smooth flow, although no turbulence measurements were made. The fan was a centrifugal ~~impeller~~ one driven by a 3-phase motor, speed control being obtained by moving the fan in relation to the tunnel exit. A maximum speed of 40 ft/sec was obtained, measured with a small pitot-static tube which was later calibrated against a standard N.P.L. tube in the large tunnel.

A simple recording device was necessary to observe the motion of the vane and an optical lever method was adopted. A collimated beam of light was passed through a cylindrical lens of focal length 1 metre, placed just outside the tunnel wall, and the beam then reflected from the vane. The image was received at about 90 cms from the vane on the film of a moving film camera, no lens being used in the camera. The arrangement is shown in figure 27. It was necessary to work after sunset as the use of hoods to exclude stray light proved too cumbersome in a short term experiment.

In order to produce a reasonably sharp image the vane itself had to be a good plane mirror. It was found that microscope cover slips were sufficiently flat and, when silvered, gave a good image. Limitations

were imposed on the lens-object distance by the necessity of obtaining a sufficiently brilliant image. In most cases a distance of about 5 metres was used, giving an image less than 0.1 cms in lateral extent. The longitudinal extent was limited by a slit in front of the camera.

The cover slips were 0.007" thick so the vanes were mounted on wire of the same diameter. They were attached to the suspension by hinges which allowed freedom of rotation about the suspension, so far as this was possible. Thin wire, 0.001" in diameter, twisted round the suspension and glued to the vane edges, top and bottom, proved the most satisfactory, although difficulty was experienced in preventing the vane sliding down the wire. A stop formed of a small bead of glue on the wire solved the difficulty to some extent, but it was necessary to check the freedom of the vane frequently and to assist it at intervals by causing the vane to rotate continuously for a few minutes with the aid of a small air jet.

The suspension wire passed through small holes in the top and bottom of the tunnel and was clamped to a frame which surrounded the tunnel. The tension in the suspension could be adjusted by hanging weights on it before clamping the lower end. The frame carrying the suspension did not rest on the bench but was clamped to an overhead galvanometer table to isolate the vane and suspension from vibrations set up by the

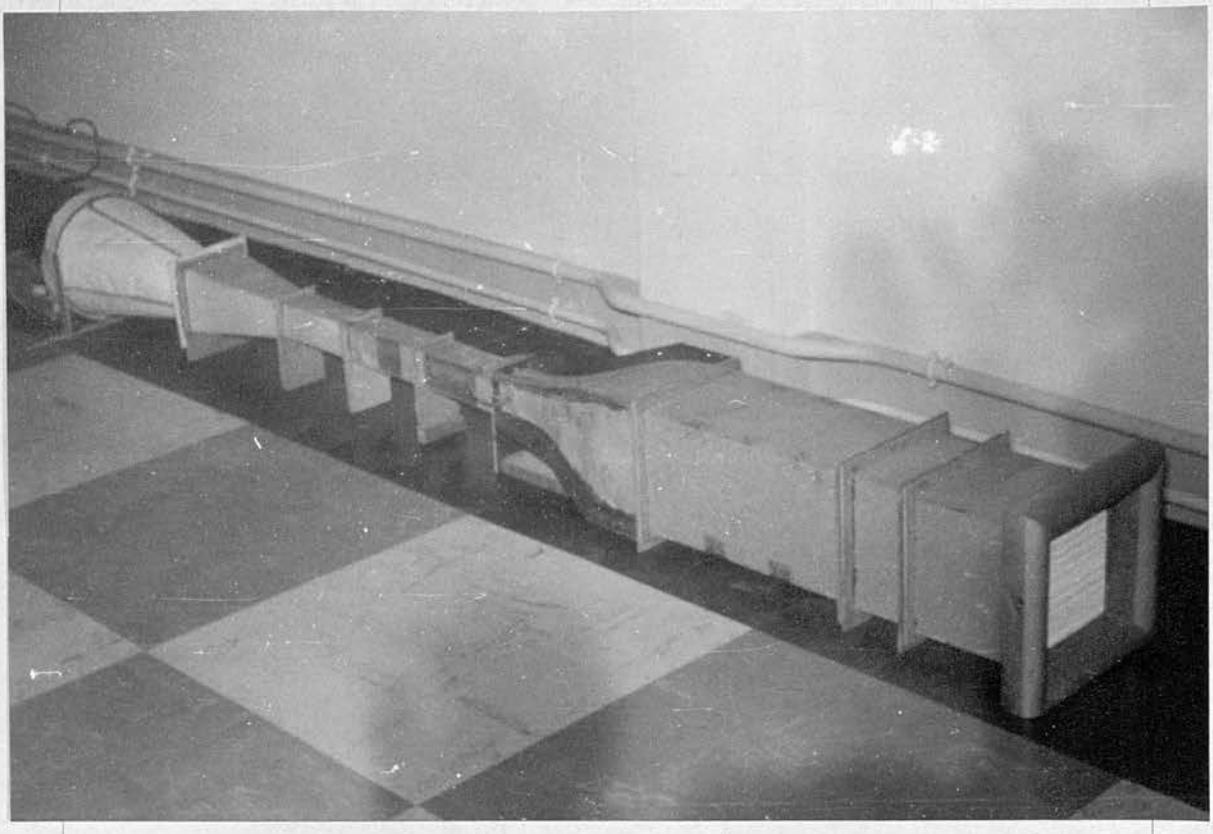

FIGURE 26

View of small tunnel used in preliminary investigations of vane behaviour.

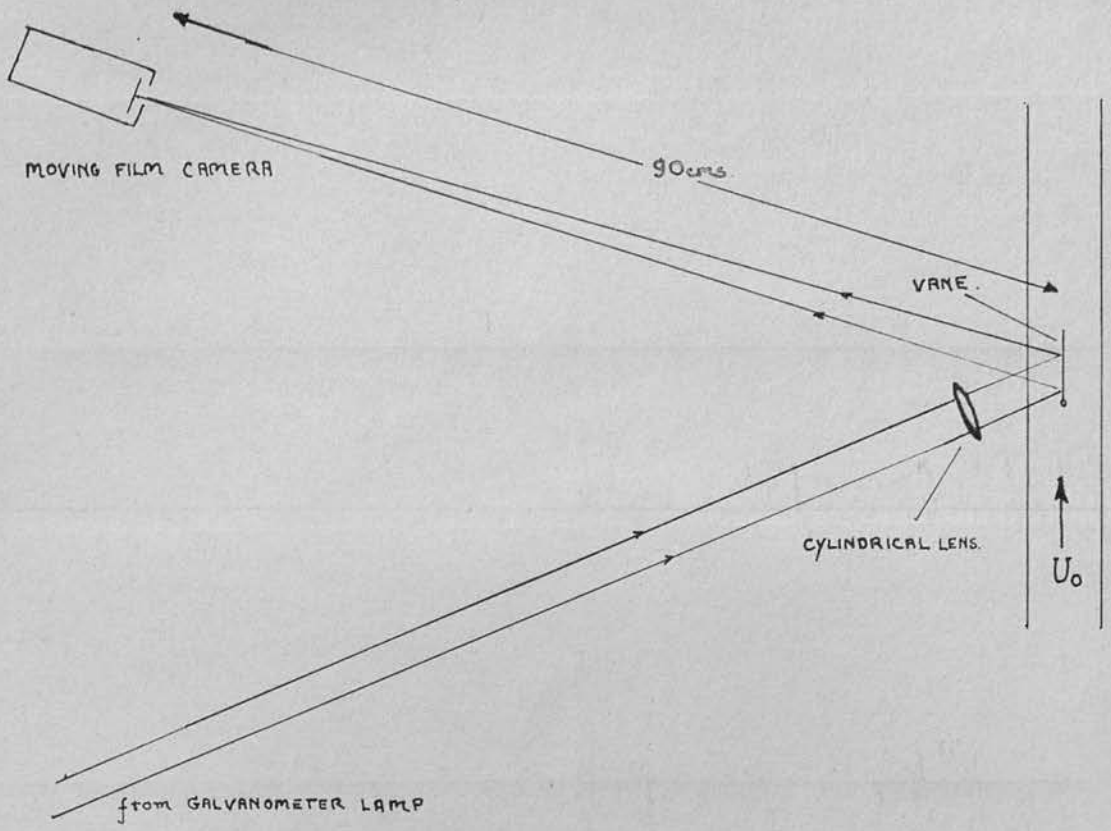

DIAGRAM of OPTICAL RECORDING.
(NOT TO SCALE)

FIGURE 27.

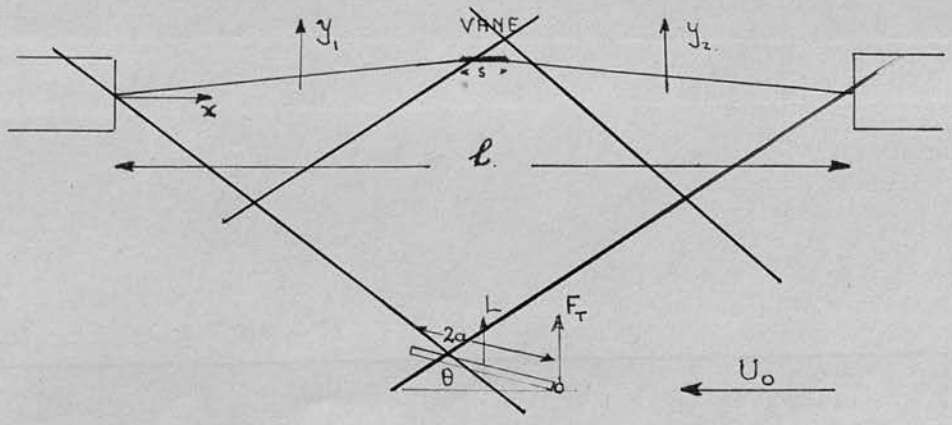

~~VANE LAYOUT for THEORETICAL TREATMENT~~

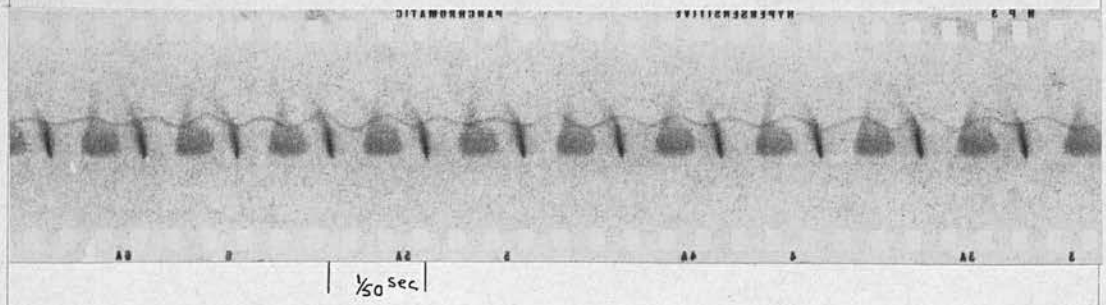

Low frequency 85 c/sec

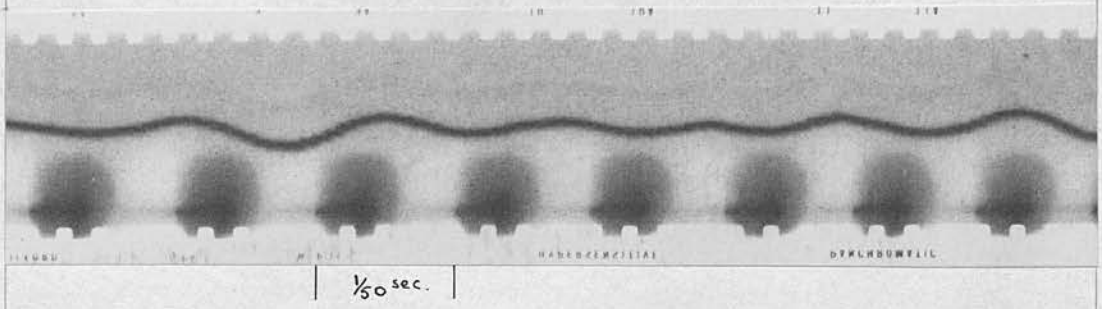

Low frequency 39 c/sec., High frequency 530 c/sec

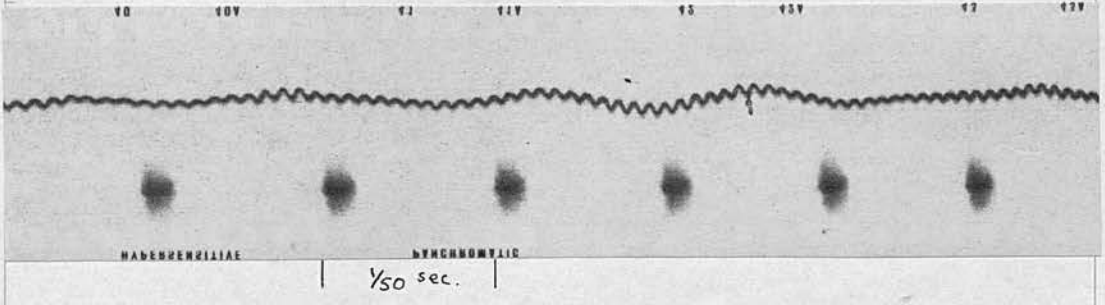

High frequency 530 c/sec.

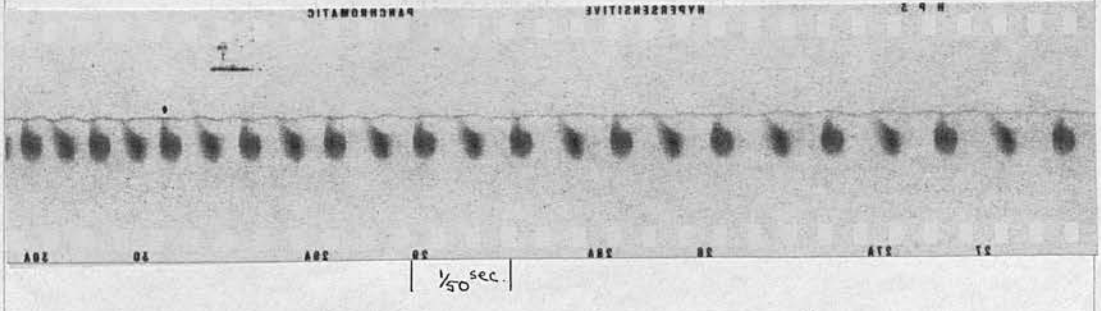

Tension increased, 580 c/sec

FIGURE 28
Typical records obtained in small tunnel showing high and low frequencies of system.

tunnel motor, the whole system being heavily weighted to reduce its resonant frequencies. Tests with a mirror on the frame showed that no detectable vibrations were set up by the normal equipment and tapping the frame showed its resonant frequency to be 7.8 c/sec.

Tests were now carried out with a vane and revealed that the system had two resonant frequencies which could be excited simultaneously, the lower frequency appearing to depend upon windspeed and the mass of the vane, while the higher one depended upon the tension in the suspension and also upon the mass of the vane. Figure 28 shows the type of record obtained in these experiments. By suitable development of the film, movements of 0.1 cm could be readily detected which correspond to an angular deflection of 5×10^{-4}° by the vane.

The lower frequencies measured were between 20 and 50 c/sec while the high frequency ranged from 100 to 1000 c/sec. A consideration of the neutral curve for a windspeed of U_o = 70 ft/sec shows that, to obtain points on the curve we require to record in the range 80 to 400 c/sec. The results, at this point were sufficiently encouraging to prompt a theoretical account of the behaviour of the vane to enable us to predict frequencies for vanes in the wind tunnel proper.

~~111. 3. Theoretical Solution for Vane Frequencies.~~

~~Consider the system shown in figure 27. A wire~~

111.3. Theoretical Investigation of Vane Frequencies.

The behaviour of the vane under the action of the aerodynamic forces and the constraining forces of the suspension was considered and the equations of motion were solved to obtain the natural frequencies of such a system.

The solution indicated that there were two resonant frequencies, a lower one, in which the aerodynamic forces on the vane determined the frequency, and a higher one in which the properties of the suspension determined the frequency. It was further shown that, provided the two frequencies were substantially different, the lower, or vane, solution was practically independent of the suspension system.

Inspection of the equations in this case showed that f/U should be constant, where f is the vane frequency and U the windspeed. It was also seen that $(s/M)^{\frac{1}{2}}$ is the relevant parameter in considering the effect of vane size and mass upon the resonant frequency, s being the span of the vane.

While the theoretical solution revealed the nature of the motion of the vane it was not sufficiently detailed to enable an accurate quantitative description of the motion to be made. As such a description was unnecessary for our purposes the theoretical investigation was not pursued. In the following section the aerodynamic constants are chosen to obtain a good fit

for the vane solution in the case of vane A, and these values are used in comparing the experimental results for vanes B and C with the theoretical predictions.

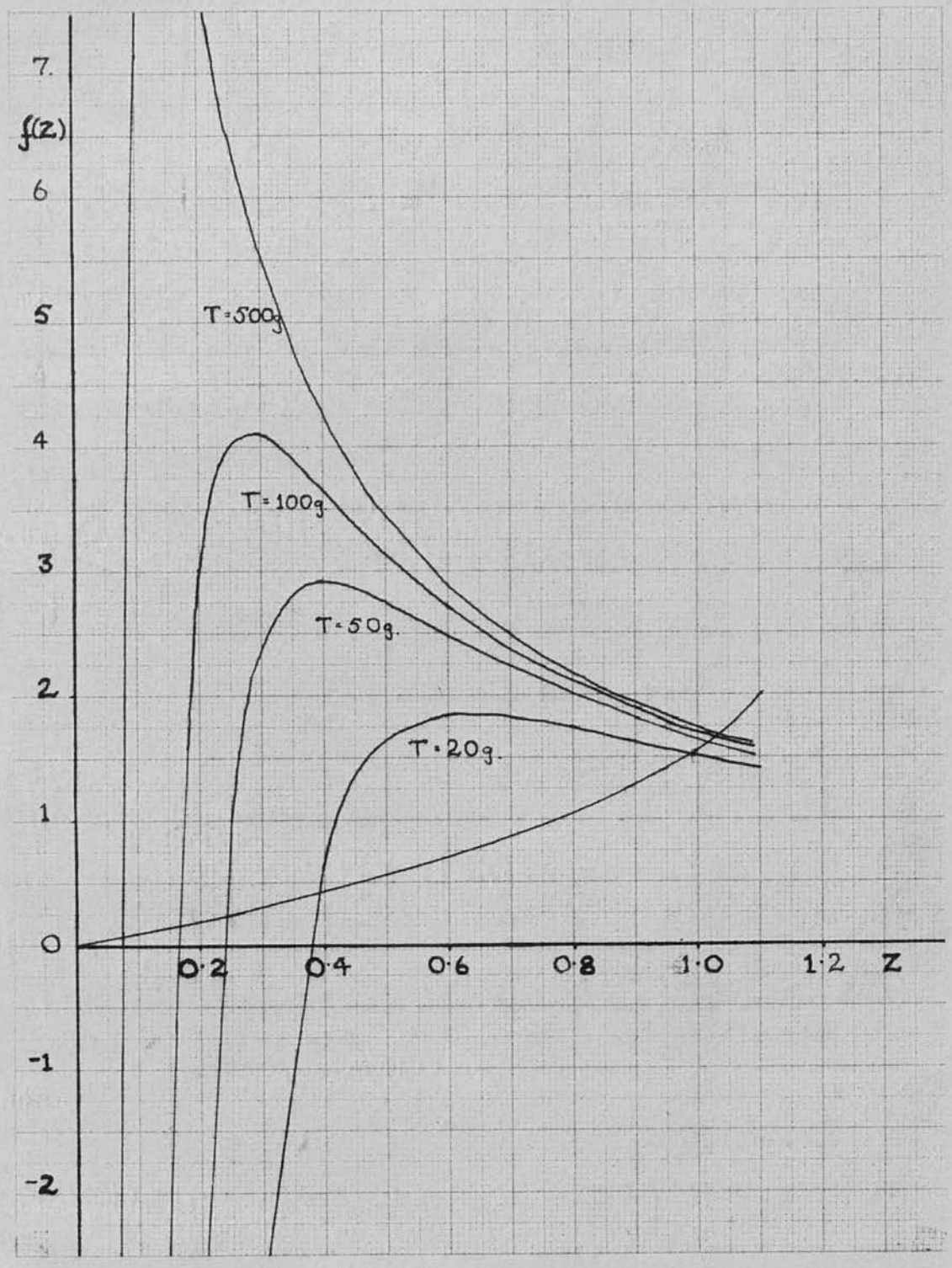

~~FIGURE 22~~

~~Solution to Equation 11 for vane A. The tension is allowed to vary, the windspeed being constant.~~

~~falling as l increases. An increase in M, the mass of the vane, decreases the frequency in a similar way, the line density λ having the same effect. The wind speed U has no effect, to a first order, on the wire frequency.~~

~~For the vane frequencies we find that the frequency increases linearly with windspeed while the mass decreases the frequency in proportion to $1/M^{\frac{1}{2}}$. The way in which the size of the vane affects the frequency depends on the way in which a change of size affects the mass, the appropriate parameter being $(S/M)^{\frac{1}{2}}$.~~

~~These predictions were now submitted to experimental test using the small tunnel.~~

111. 4. Experimental Support of Theory

Using the technique described in section 2 the variation of frequency with tension was investigated for two vanes, made from cover slips, with dimensions as given in table 1.

The complete solutions were completed for these vanes using ~~equations (14) and (11)~~ and the agreement between theory and experiment is shown in figures 30 and 31. Typical recordings, from which the experimental results were obtained are shown in figure 32.

It will be seen that agreement is better for vane B , which was the lighter. The ratio of the parameters $(S/m)^{\frac{1}{2}}$ for the vanes A and B gives 1.27 which is in good agreement with the ratio of the vane frequencies of 1.25.

TABLE 1.

VANE	A	B	C
Type.	Silvered Glass.	Silvered Glass.	Metal Foil and Mica.
Thickness.	0·007"	0·007"	0·0008"
M g.	0·060	0·017	0·019
2 a"	0·565	0·27	0·39
S"	0·375	0·175	0·315

gm wt.

Small tunnel.

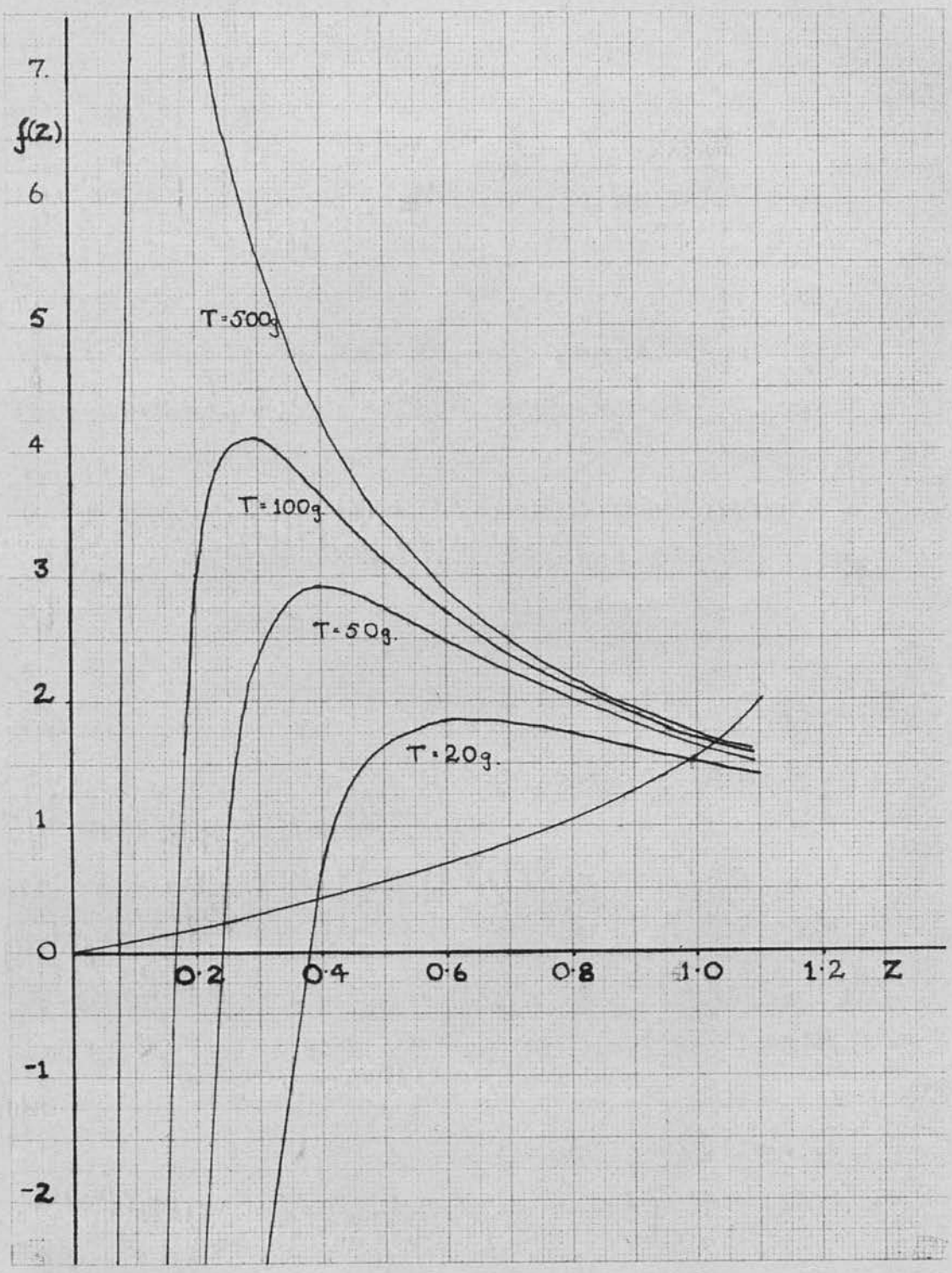

~~FIGURE 29~~

~~Solution to Equation 11 for vane A. The tension is allowed to vary, the windspeed being constant.~~

~~falling as l increases. An increase in M, the mass of the vane, decreases the frequency in a similar way, the line density λ having the same effect. The wind speed U has no effect, to a first order, on the wire frequency.~~

~~For the vane frequencies we find that the frequency increases linearly with windspeed while the mass decreases the frequency in proportion to $1/M^{\frac{1}{2}}$. The way in which the size of the vane affects the frequency depends on the way in which a change of size affects the mass, the appropriate parameter being $(S/M)^{\frac{1}{2}}$.~~

~~These predictions were now submitted to experimental test using the small tunnel.~~

111. 4. Experimental Support of Theory

Using the technique described in section 2 the variation of frequency with tension was investigated for two vanes, made from cover slips, with dimensions as given in table 1.

The complete solutions were completed for these vanes using ~~equations (14) and (11)~~ and the agreement between theory and experiment is shown in figures 30 and 31. Typical recordings, from which the experimental results were obtained are shown in figure 32.

It will be seen that agreement is better for vane B , which was the lighter. The ratio of the parameters $(S/m)^{\frac{1}{2}}$ for the vanes A and B gives 1.27 which is in good agreement with the ratio of the vane frequencies of 1.25.

When the large tunnel became available a lighter vane, C, was used to measure the variation of vane frequency with windspeed. The experimental points agree well with the theoretical line as shown in figure 33.

It was found that, with a short suspension, as used with vane C, that only the vane frequency was excited to a marked extent.

It also proved possible, using the ribbon technique described in chapter V, to investigate the shape of the vane resonance curves and a set of these obtained with vane C are shown in figure 34 for resonant frequencies of 60 to 90 c/sec. They were obtained by observing the response of the vane to a constant input at varying frequency. The recording equipment described in chapter IV was used to measure the output as vane C was only 0.0008" thick, and not suitable for use with the optical method. Figure 35 shows recordings of the response as the input frequency was varied from below to above the vane resonant frequency. It will be seen that the oscillations became purer, as well as increasing in amplitude, as resonance is approached. It proved more difficult to obtain quantitative measurements of response curves for vanes with resonant frequencies of 200 to 300 c/sec., the half width decreasing as the frequency increased. At 80 c/sec the Q value is 2.0, while at 300 c/sec it increases to about 10.

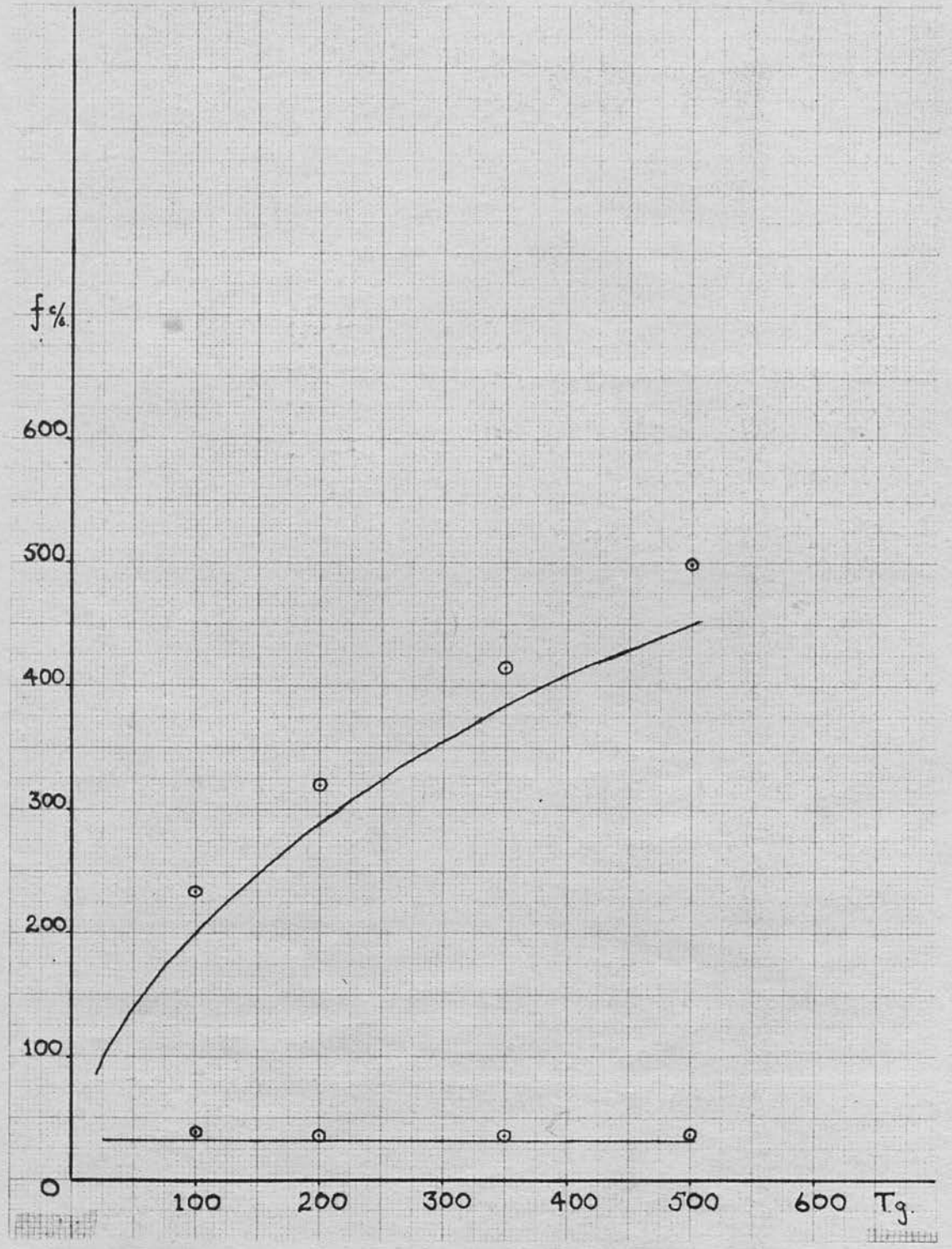

FIGURE 30

Comparison of theory and experiment for vane A. Solid lines denote theoretical solution. The experimental points were obtained in the small tunnel.

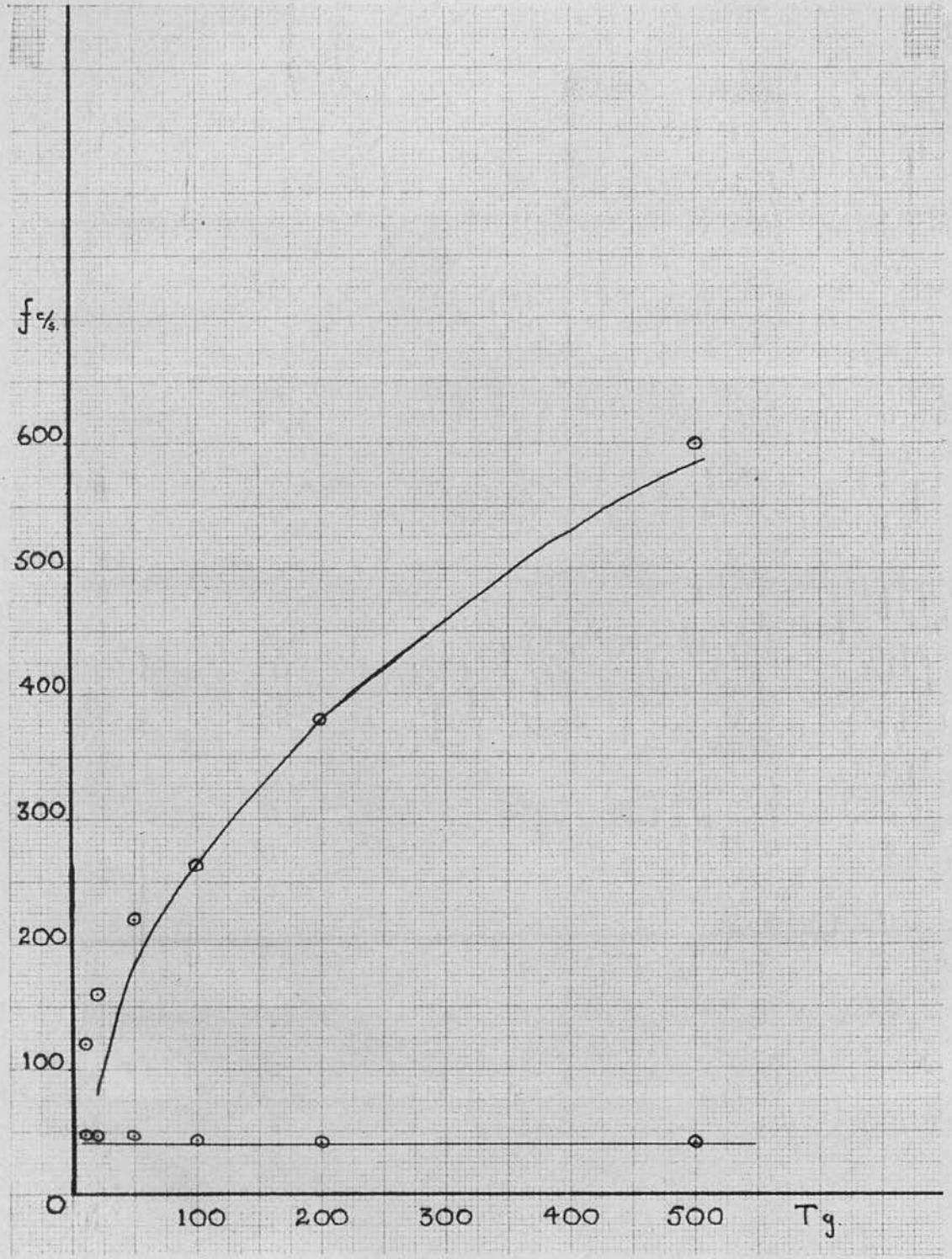

FIGURE 31

Comparison of theory and experiment for vane B. Solid lines denote theoretical solution. The experimental points were obtained in the small tunnel.

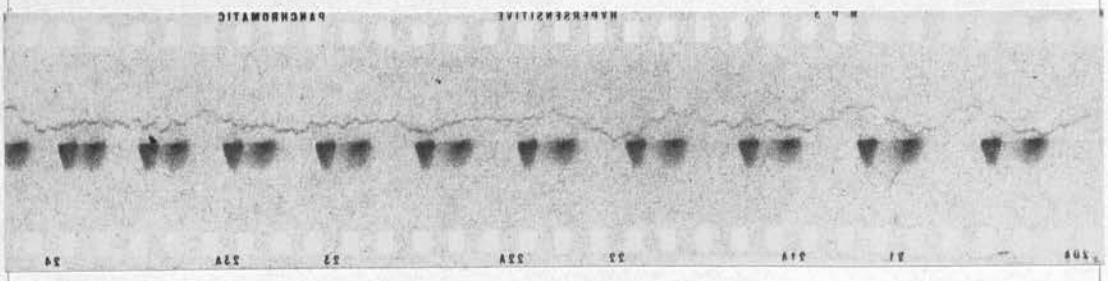

Vane A T = 100 g. U_o = 37.5 ft/sec
f = 235 c/sec 36 c/sec

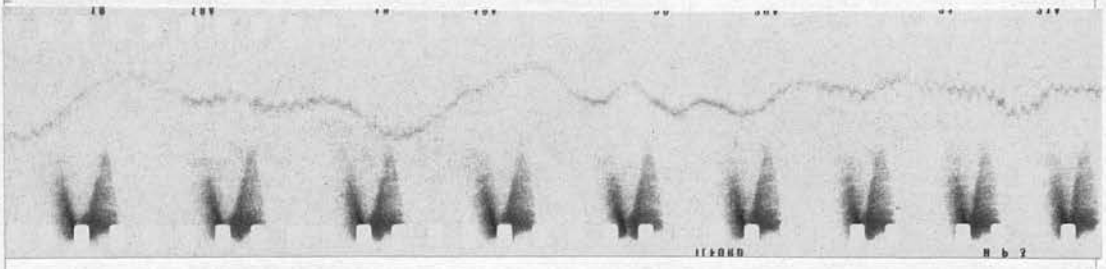

Vane B T = 500g. U_o = 37.5 ft/sec
f = 600 c/sec, 40 c/sec

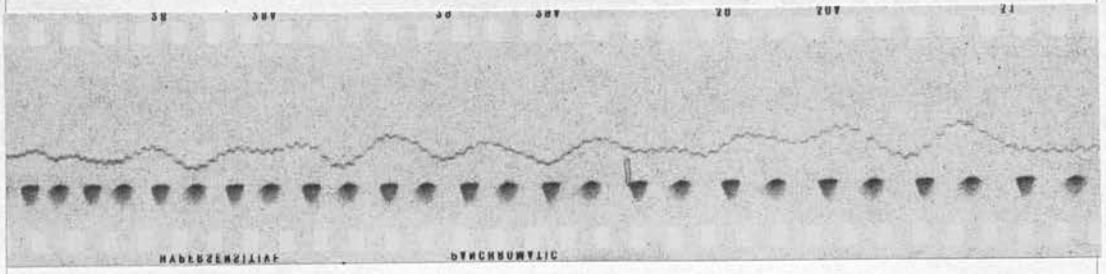

Vane B T = 200 g. U_o = 37.5 ft/sec
f = 380 c/sec, 42 c/sec

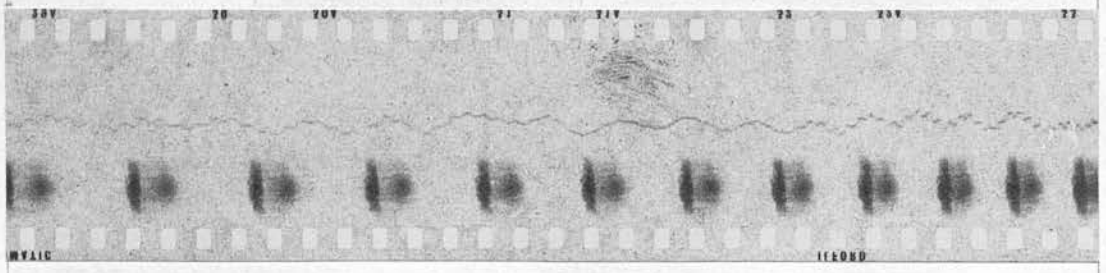

Vane A T = 200 g. U_o = 37.5 ft/sec
f = 320 c/sec, 35 c/sec

FIGURE 32
Typical recordings used to obtain results shown in figures 30 and 31.

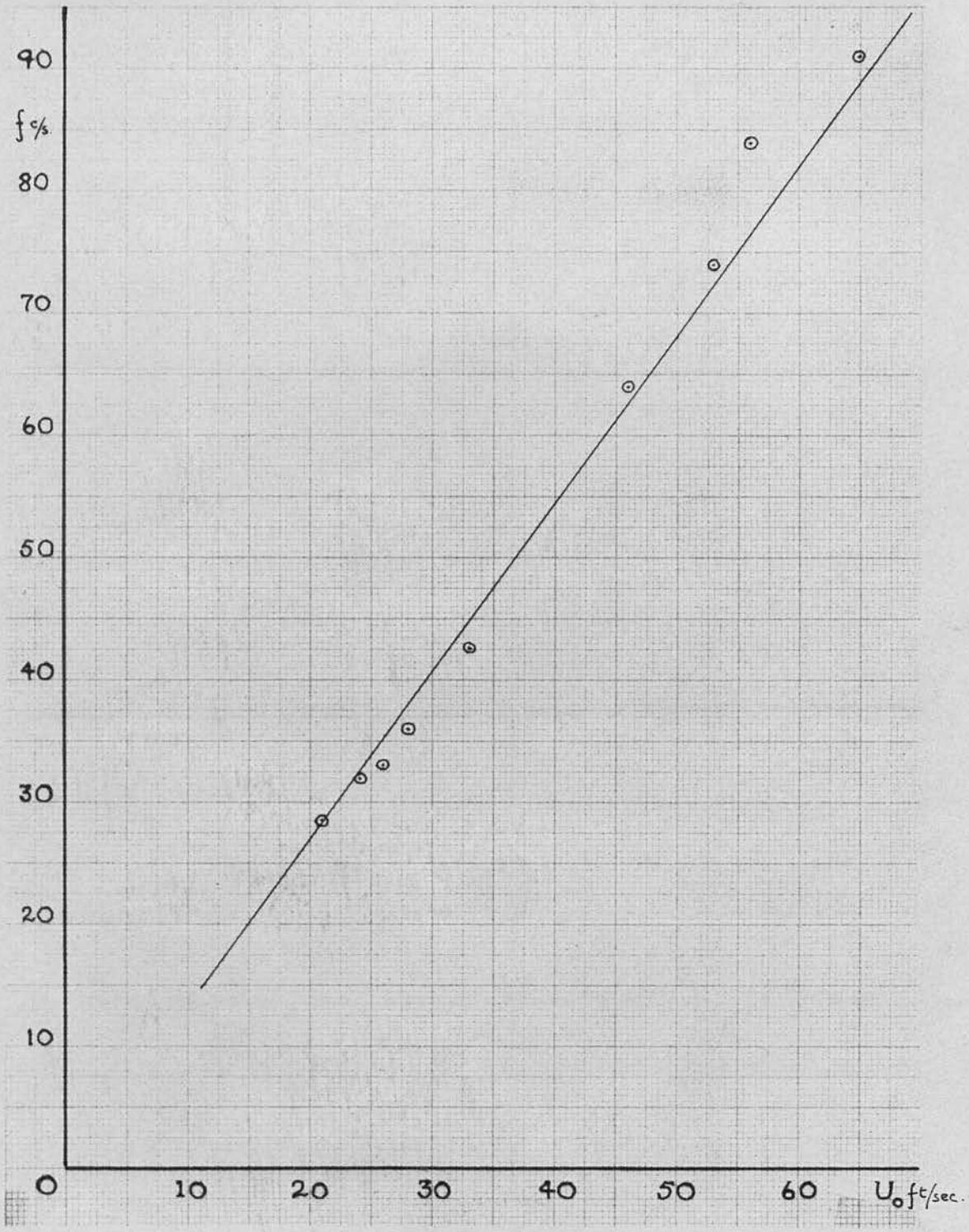

FIGURE 33

Variation of vane frequency with windspeed for vane C. The line denotes the theoretical solution, the experimental points being obtained in the large tunnel.

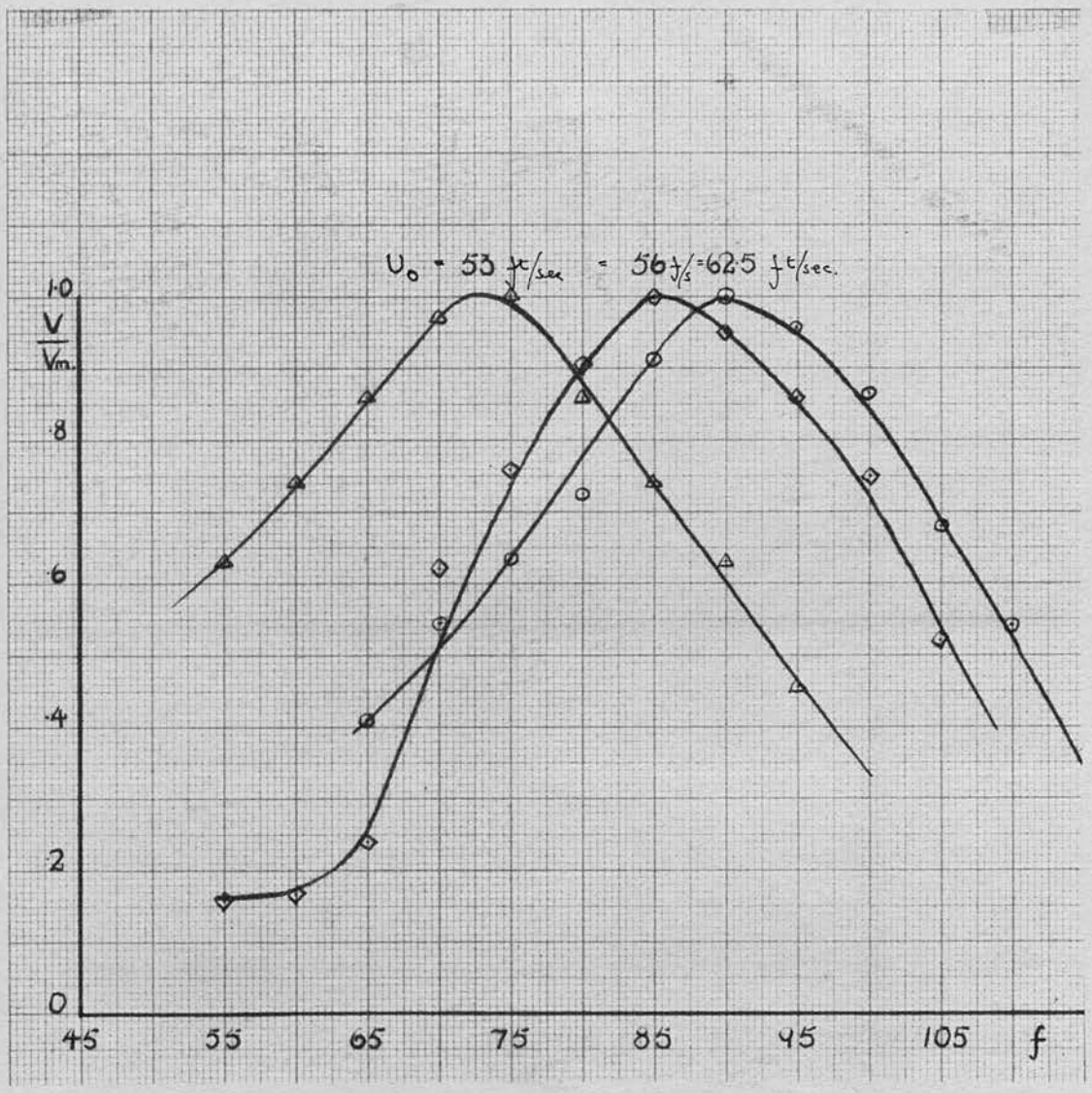

FIGURE 34

Response curves for vane C at varying windspeed. Obtained in large tunnel using electronic recording apparatus.

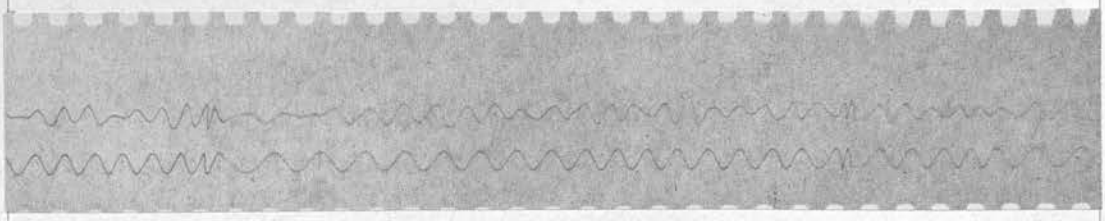

f = 60 c/sec U_o = 55 ft/sec

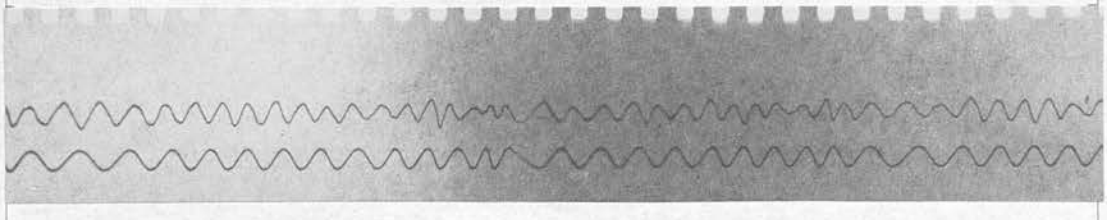

f = 70 c/sec U_o = 55 ft/sec

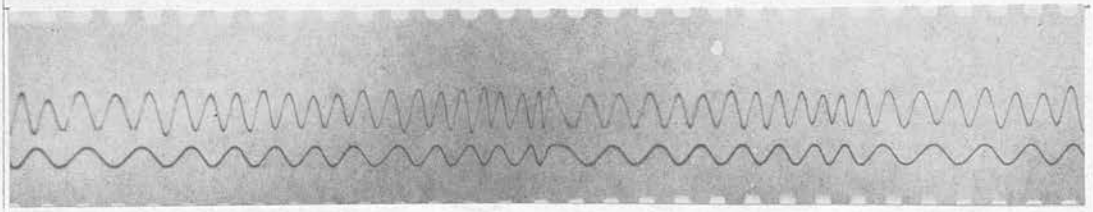

f = 80 c/sec U_o = 55 ft/sec

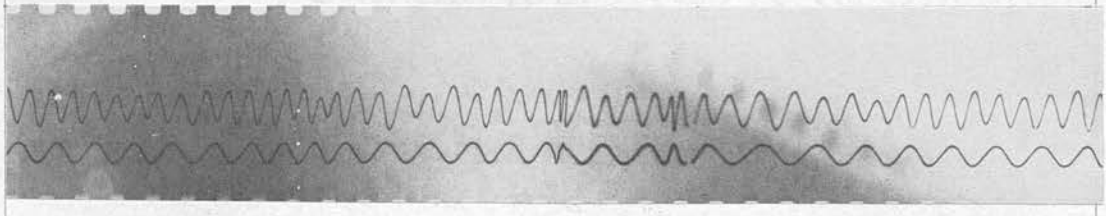

f = 90 c/sec U_o = 55 ft/sec

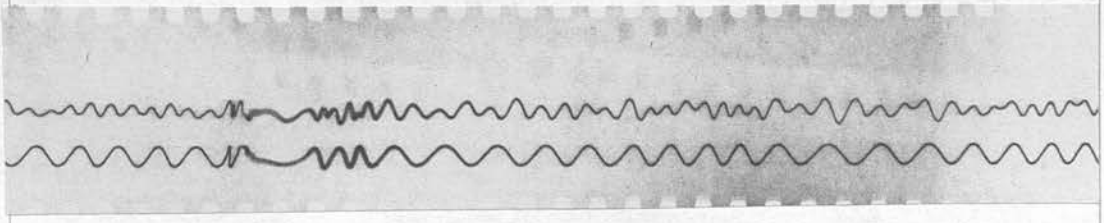

f = 100 c/sec U_o = 55 ft/sec

FIGURE 35

Vane response for constant amplitude input at varying frequencies. Lowet ttace = 50 c/sec.

Conclusions

The theoretical treatment for the vane agrees well with experimental data, obtained both for vanes in the small tunnel and for lighter vanes in the large tunnel. Considering the theory was only developed to provide a guide to and explanation of the resonant frequencies of the vane system, and that several approximations are made, notably the neglect of the effect of vane size upon the wire, the agreement is surprisingly good, and appears to improve as the vane becomes lighter.

Using the theoretical result it can be seen that it should be possible to build vanes with resonant frequencies up to 300 c/sec if we use a low density material, such as mica, and silver one surface. The wire resonant frequencies are very much higher than this, being of the order of 1 Kc/sec.

The original intention had been to use the vane as a non-resonant detector, that is, to arrange for any natural frequencies to be well above, or below, the range of interest.

The investigation has shown that it is possible to build vanes with resonant frequencies in the range required for laminar oscillations. The possibility of using the vane as a resonant detector must, therefore, be considered.

This method could have many advantages, as such a system, with a suitable sensitivity of recording, would act as a mechanical filter and remove many spurious

oscillations from view.

Consider the deflections to be expected from a vane in the boundary layer responding to the transverse component of laminar oscillations. Using Schlichtings' theoretical results, shown in figure 2, we can determine the ratio of u'/U_o to v'/U_o at any value of y/δ Schubauers' experimental results, figure 5, show us that the maximum value of u'/U_o in his case was 0.014 for branch I and 0.004 for branch II of the neutral curve, the lower figure for branch II being solely due to a lesser degree of excitation. Taking the higher value in conjunction with figure 2, we find that the ratio of v'/U_o, at $y/\delta = 0.5$, to the maximum value of u'/U_o is about 1:5. Thus we can expect, in conditions when artificial oscillations are readily observed, that v'/U_o will be of the order of 0.003, or 0.3%. If we use the local value of U at $y/\delta = 0.5$ we find $v'/U = 0.4\%$, this being the figure that should control the deflection of the vane.

In what way will the vane respond to such a velocity fluctuation? There are two extreme laws which we can choose, the truth probably lying between these. Either the vane will set itself along the local streamline, determined by v/U, or it will respond to pressure forces and set, rather, along $(v/U)^2$. Let us take the more pessimistic view and assess the sensitivity required of a recording device in this case. With $v'/U = 0.4\%$, the angular deflection, if the vane

responds to a square law, will be of the order of 2×10^{-5} o. This would require a recording system with a sensitivity 10 times as high as the optical method. The optical method could probably be improved by using a longer path length and a better lens system but was rejected as unsuitable on other grounds which are discussed later.

However, no account has been taken of the fact that the vane can be used as a resonant detector, the above supposing that it acts as a non-resonant detector. It is difficult to assess the amount by which the response is increased for the resonant case, since we were unable to measure a response curve with sufficient accuracy to determine the ratio of the peak output to the output at frequencies well off resonance. With such evidence as is available, a factor of 10 would appear a conservative estimate, and, using this, the required sensitivity is reduced to the detection of an angular deflection of 2×10^{-4} o. It is probable that we can also increase the value of v'/U to at least 1%, since Schubauer and Skramstad had a low free stream turbulence and consequently no need to use the maximum disturbance which would not affect the boundary layer too seriously. Taking this value we are left with an angular deflection of 10^{-3} o., a figure well within the sensitivity of the optical method. This figure was used when assessing whether a recording system had the required sensitivity, although it was

later found that even this value was unduly pessimistic, the reason lying either in a greater response factor than 10, or in a more favourable law than the $(v/U)^2$ case chosen.

In view of this it should be possible to use the vane as a resonant detector of laminar oscillations and we must consider the implications of this decision.

It now becomes important to control the windspeed and the exciting frequency accurately since both these parameters will affect the vane response closely. Reference to figures 33-34 shows that the windspeed should be constant to within $\pm$ 2 ft/sec if we can control the frequency accurately, this figure being for a vane with a resonant frequency of 90 c/sec. The limits will become finer as the vane frequency increases, but any deviation will be easily detected as the Q value increases rapidly.

It will also be necessary to measure the distance of the vane from the surface since this will determine the local velocity in the boundary layer.

To measure laminar oscillations in the non-resonance case, a sensitivity suitable to an angular deflection of 10^{-4} °, would be required. The detection of turbulent fluctuations with the vane would appear, at the moment, to be impracticable as the wavelength of the disturbance would be considerably less than the vane size. It might prove possible to utilize the suspension resonant frequency in some way to scan the

spectrum, as the tension is varied, though it would probably be desirable to dispense with the vane in this case and observe only the wire.

Finally we must develop a more sophisticated method of recording the vane response, as the optical method, although elegant and direct, is both time and film consuming.

Chapter 1V

Design, Construction & Calibration of Electronic Equipment.

1V. 1 Introduction

It has been seen that the essential feature of any recording device to be used with the vane is that it shall be able to detect the motion of the vane, both in amplitude and in frequency.

While the optical method described in the previous chapter has many advantages, and proved very satisfactory for the preliminary investigation it was found that when the vane was made of lighter and more flexible materials it became almost impossible to obtain an optically flat surface to use as a mirror. This disadvantage combined with a desire to inspect the motion visually before recordings were made led us to consider the development of an electronic method of recording, in which the output could be examined on an oscilloscope, and, if necessary, recorded on a moving film camera.

An electronic system must base its detection of the small movements of the vane on the changes of capacitance between the vane and some other static plate. The flat plate itself would seem the ideal choice for the static plate if it can be sufficiently isolated from tunnel vibrations. If one considers a vane of area 0.05 sq. ins at a distance of 0.05" from the surface with which it forms a capacitor, and if we consider the capacitance changes brought about by a deflection of order of $1 \times 10^{-3^{\circ}}$ corresponding to

$\frac{v}{U_o}$ = 1.0%, then we arrive at a capacitance of order 0.2 pf with a change of order 5×10^{-4} pf, or 10^{-3} pf if we consider the motion on both sides of the mean, the calculation assuming an ideal parallel plate capacitor.

Thus the electronic device must be capable of detecting changes of 5×10^{-4} pf, while the frequency characteristics, for investigation of laminar oscillations, are a flat response from 50 to 1000 c/sec a higher upper limit being necessary for investigation of turbulent spectra.

IV. 2 Design and Construction

Two possible arrangements were considered as solutions to the above requirements.

The first consisted of a high stability crystal oscillator, working at about 1 Mc/sec which would feed a constant signal into a filter circuit. The vane would be included in the filter unit which would have to satisfy the following requirements: firstly that the capacitance change due to the vane should have an appreciable effect on the resonant frequency of the filter and secondly, that the filter should have an exceptionally high Q value in order to give a detectable change of signal, the two requirements being interconnected to some extent.

If one considers the performance of a filter (or tuned) circuit, then, ideally one has

$$f = \frac{1}{\sqrt{LC}}$$

where f is the resonant frequency and L and C are the

inductance and capacitance respectively of the circuit. Consider small changes of capacitance keeping L constant.

Then $$\frac{\delta f}{\delta C} = -\frac{1}{\sqrt{LC}} \frac{1}{2C}$$

or $$\delta f = -f \, \delta C/2C$$

Thus, the smaller the value of C used, the larger will be the effect of δC. The minimum value of C is dictated to some extent by unavoidable stray capacitances and also by the difficulty of constructing a coil of sufficiently high inductance. Using values of C = 12.5pf, $\delta C = 5 \times 10^{-4}$pf and f = 1 Mc/sec then δf becomes 20 c/sec. Thus we are able to meet the first criterion demanded. The second condition, that the filter should have a high Q, is unapproachable, since the requirement of a high value for L tends to reduce the maximum Q obtainable. A value of 200 would appear to be the maximum, and using this we find that a 1 c/sec change in frequency would give a signal change of 0.4×10^{-3} Vm volts, where Vm volts is the maximum voltage developed across the filter. A crystal filter would satisfy the second requirement having a Q value of order 5×10^{3}, but proved to be far too stable to be noticeably influenced by a small change in capacity, either in series or in parallel with it. Tests performed showed that a capacitance change of 10^{-3}pf gave a frequency change of only 0.02 c/sec in a typical crystal filter. The second arrangement makes use of a crystal filter to provide a very high Q, but

obtains the required frequency change by using the vane in the oscillator circuit. Thus a frequency modulated signal is fed onto the crystal filter which converts it to an amplitude modulated signal which can then be detected and amplified by conventional methods.

The requirements for the oscillator were that it should be very stable, to within 5 parts in 10^6, but also that it should give a reasonable frequency change for a capacitance change of 5×10^{-4}pf.

A modification of a circuit due to Clapp (1956) was found to be suitable. The basic circuit is shown in figure 36, the frequency of the oscillator being dependent on the resonance of L and C. The vane, represented by δC is coupled in parallel with C so that its effect will be

$$\delta f = -f \delta C/2C$$ the value of

C being determined in relation to δC as before.

Using the same values of C and of δC, and taking a value of 5×10^3 for the Q of the crystal filter, we obtain an output from the filter of 0.01 V_m volts for a 1 c/sec change in the oscillator frequency, or an output of 0.4 V_m volts for a capacitance change of 10^{-3}pf.

The potential sensitivity of this arrangement is therefore adequate provided that the oscillator is stable enough and that the noise level is sufficiently low.

An oscillator of the above type was built and, after some trouble with the coils, which had to be

hand wound, was successfully operated. The capacitance C was specially constructed as a parallel plate air gap capacitor with a value of 20 pf downwards, control being by means of a fine screw. It was found necessary to isolate the oscillator from the succeeding stages with a buffer stage to prevent any feedback, judicious use of screening also proving necessary. The oscillator signal was then amplified and fed onto the filter stage.

The filter stage is shown in figure 36. When the input is at a frequency other than the resonant frequency, then the R.F. voltage is developed across R_1, but when the input matches the crystal frequency then the impedance becomes large compared with R_1 and almost the full R.F. voltage is developed across R_2.

It is necessary to be able to tune the oscillator to operate at any desired frequency within the range of the filter, the point of maximum sensitivity being when the input frequency is equal to the frequency of the mid-point of the steepest section of the filter response curve. In order to tune the oscillator to the desired frequency a cathode follower was included in the circuit between the filter and the detector. Then, with the aid of a valve voltmeter the frequency could be tuned to the desired operating point by observing the voltage developed across the crystal. The maximum voltage developed was between 20 and 30 volts, so that the operating point was at 10 to 15 volts the tuning being effected by varying C.

The output from the filter, which is an amplitude modulated R.F. signal is now fed through a detector, and having undergone one stage of A.F. amplification is fed into an oscilloscope, whose D.C. amplifier further increases the signal, so that the trace can be examined either visually or by means of a camera. Preliminary tests with the vane in the tunnel indicated that the sensitivity was too high and also that the capacitances introduced into the tuned circuit by the inclusion of coaxial cable to link the vane to the oscillator were considerable being of the order of 20 pf. The sensitivity was therefore reduced by tapping the tuning coil. The instrument was, however, calibrated on both ranges.

To reduce the noise level to an acceptable value it was necessary to use accumulators for the heater circuit, a power pack providing the high tension supply. This reduced the noise to about 0.05 volts, the minimum signal which we attempted to measure being approximately 20 db above this level.

The stability of the oscillator may be determined by observing the rate of drift of the valve voltmeter reading if the oscillator is tuned to one side of the response curve and allowed to drift through the peak. After the equipment has reached thermal equilibrium, a process taking about two hours, the stability is good, a given frequency being maintained for up to five minutes under optimum conditions. This allows adequate time for photographic recordings to be taken.

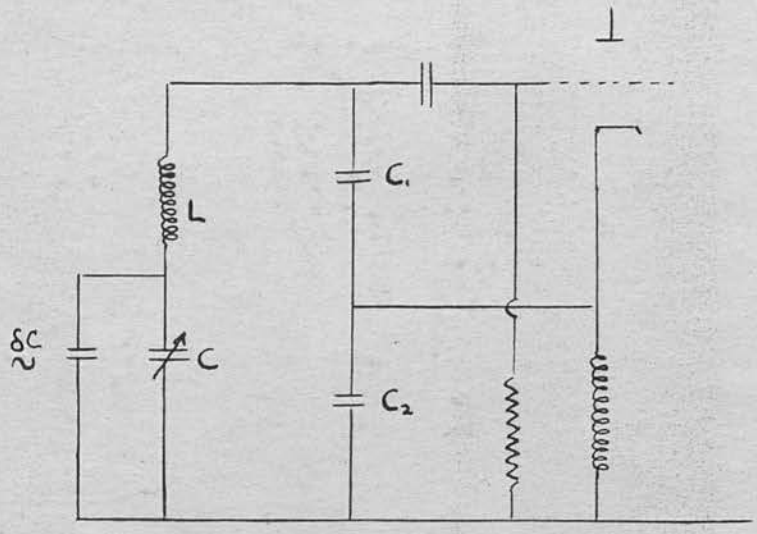

Basic Oscillator Circuit

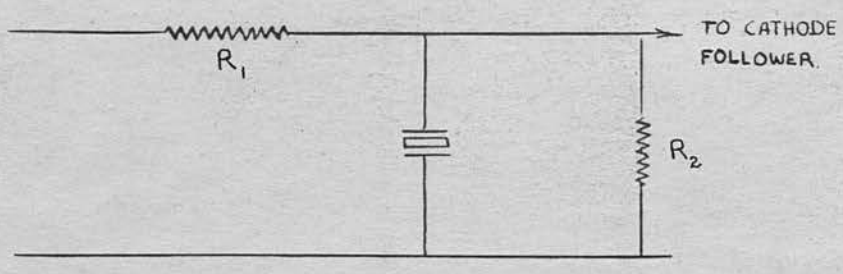

Basic Filter Circuit

FIGURE 36

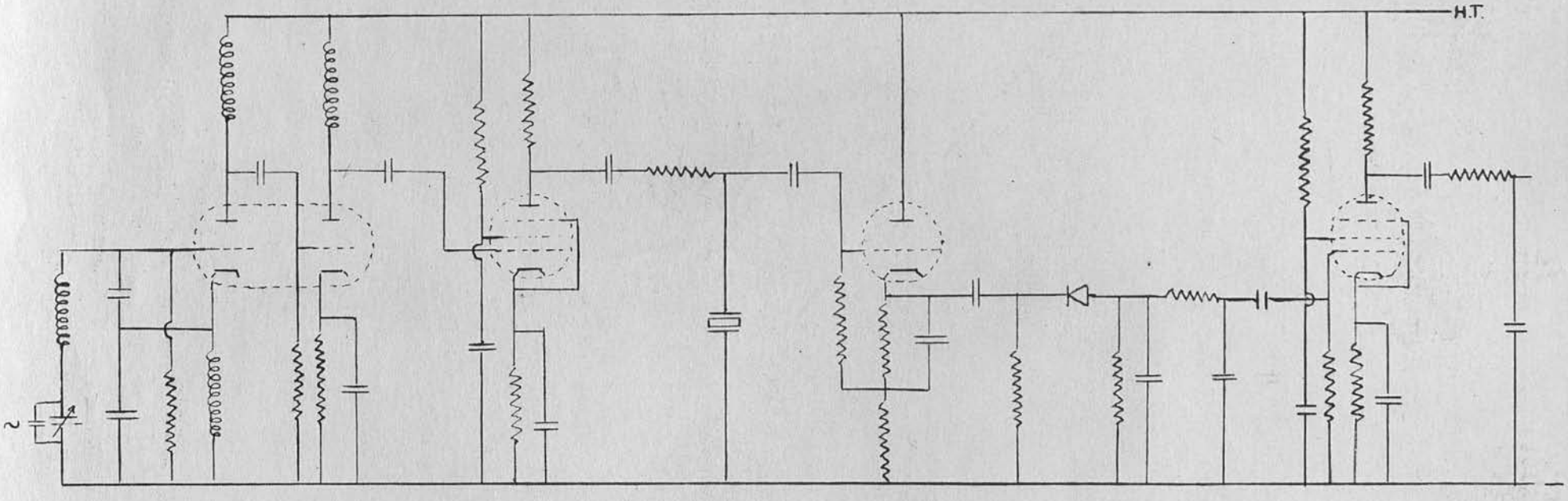

FIGURE 37

Circuit Diagram for Electronic Recording Equipment.

The output signal is interpreted as the magnitude of the modulation being a measure of the displacement of the vane, while the frequency of the modulation measures the frequency at which the vane vibrates.

We can represent the circuit by the following block diagram, the complete circuit being shown in figure 37.

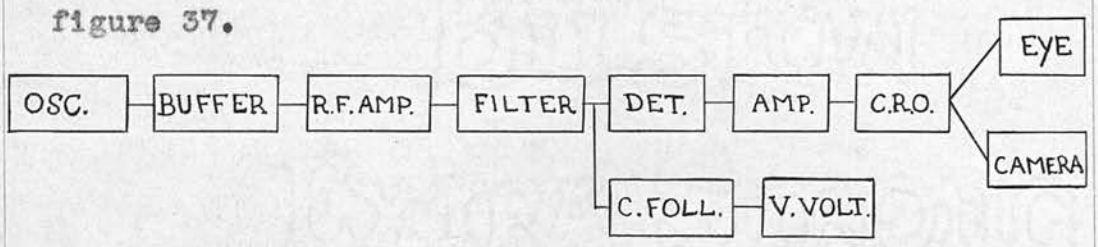

IV. 3. Calibration of Electronics

Having achieved a suitable sensitivity of response and stability of operation it was now necessary to calibrate the electronics in terms of output for a given change in capacitance.

This was effected by two distinct methods and the results were compared as a check. The first method consisted of calibrating each stage of the instrument with appropriate measuring devices and of then adding together these calibrations to obtain an overall response for the device. The second method consisted of feeding a known small change in capacitance into the system and observing the output.

(a) Calibration by Individual Stages

The final output depends, essentially, upon the voltage developed across the crystal filter since it is this which will control the voltage change for a given frequency change in the input to the filter.

It is therefore not necessary to consider the stages before the filter as they will certainly have a flat response over the frequency range of 1 Mc/sec ± 100c/sec at which they operate.

The first step is to determine the slope of the crystal filter in terms of the voltage across the crystal. The filter response curve was obtained using a signal generator and a valve voltmeter with the filter circuit, the result being shown in figure 38. The accuracy of this method is not good since the signal generator can only be set to ± 30 c/sec, the width, at half height, of the curve being about 200c/sec It is possible however to verify the general slope of the curve by observing the rate of drift of the valve voltmeter reading when the oscillator frequency is allowed to drift across the response curve. Both methods have been used in arriving at figure 38 and the accuracy should be of the order of 10% ina measurement of the slope of the curve.

The curve is not symmetrical, having a steeper slope on the high frequency side of resonance, so that we can obtain two sensitivites by tuning the oscillator to an operating point below or above the resonant frequency. From the response curve we obtain the change in output for a frequency change of 1 c/sec in the input, by measuring the slope of the curve at the midpoint of each side. This gives values of 6×10^{-3} V_m volts/c/sec for the steep side and 4.2×10^{-3} V_m

volts/c/sec for the other side, where V_m is the maximum voltage across the crystal. As the filter curve is linear about the midpoint the response to frequency changes should also be linear over a range of ± 50 c/sec for the more sensitive response, and a range of ± 90 c/sec for the latter case.

We have now to calibrate the stages beyond the crystal in order to obtain their amplification and frequency characteristics. These stages comprise of the detector, the audio amplifier and a filter, added to reduce noise above 1 Kc/sec. It proved necessary to calibrate them with an amplitude modulated radio frequency signal, the radio frequency being set at 1 Mc/sec while the modulation frequency was varied over the range 20 c/sec to 5 Kc/sec. The curves obtained are shown in figure 39, the amplification being constant in the range 50 to 700 c/sec. and having a value of 7.0.

Using this value together with the sensitivity of the crystal we obtain the voltage output for a 1 c/sec change in the oscillator frequency and can construct a set of curves, as shown in figure 40, which give the output voltage for a given frequency change in terms of the peak voltage, V_m, across the crystal. These curves are drawn for the more sensitive response, the output being reduced by a factor of 0.7 in the latter case.

To complete the calibration we need only determine

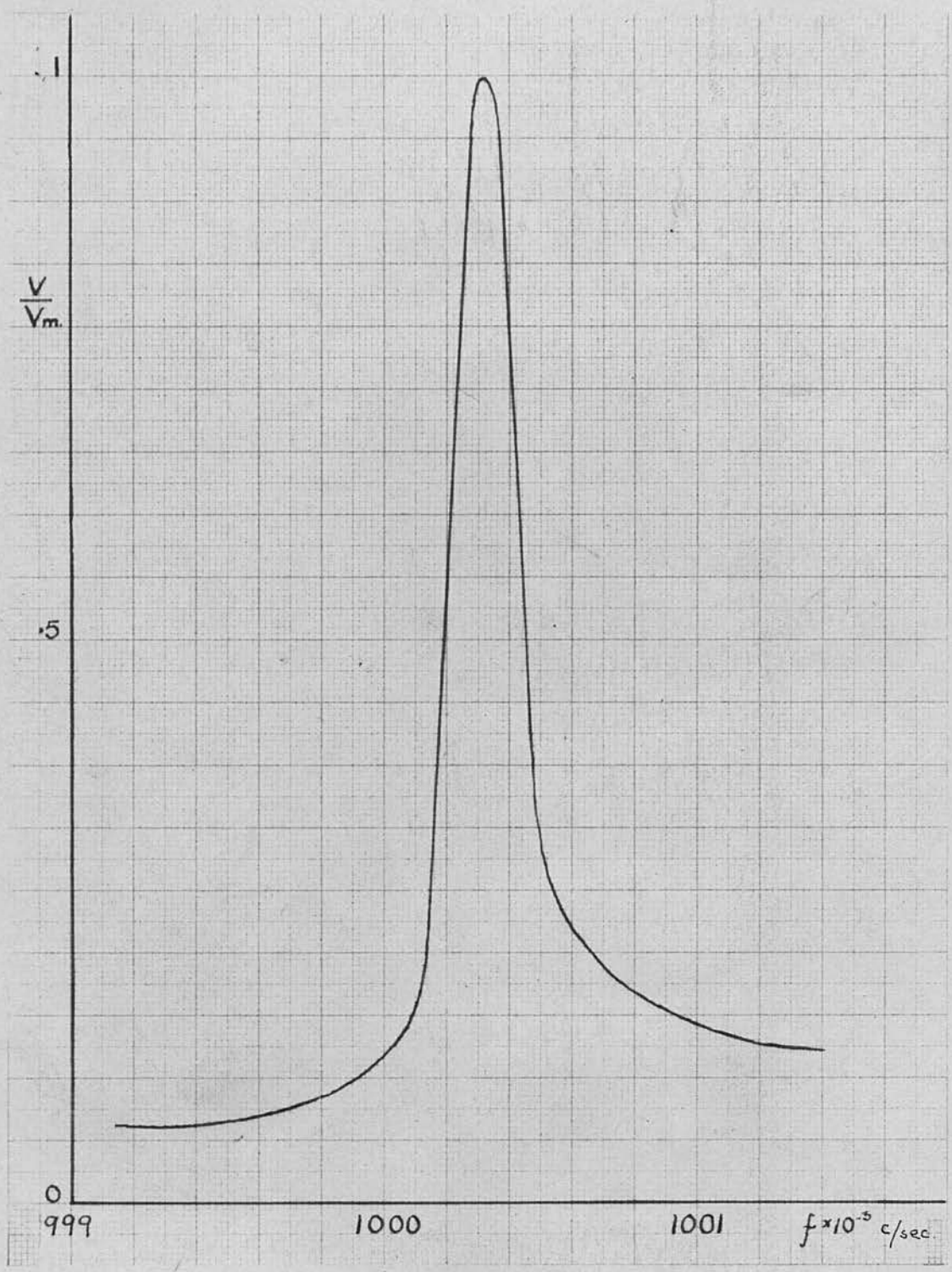

FIGURE 38

Response curve for crystal filter unit.

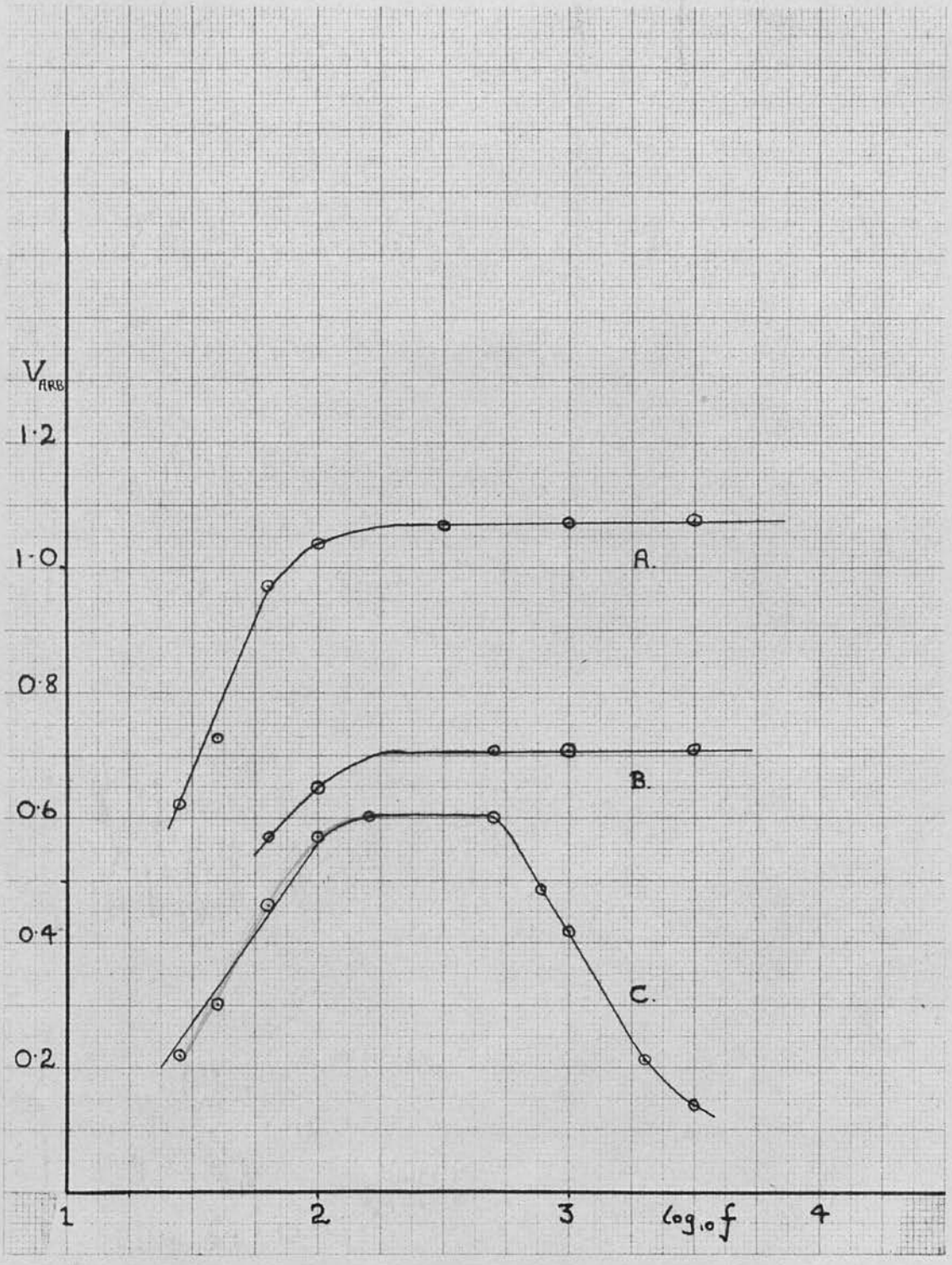

FIGURE 39

Calibration curves for Audio Amplifier and Detector stages.

A. Amplifier alone.
B. Detector and Amplifier.
C. Detector + Amplifier + Filter.

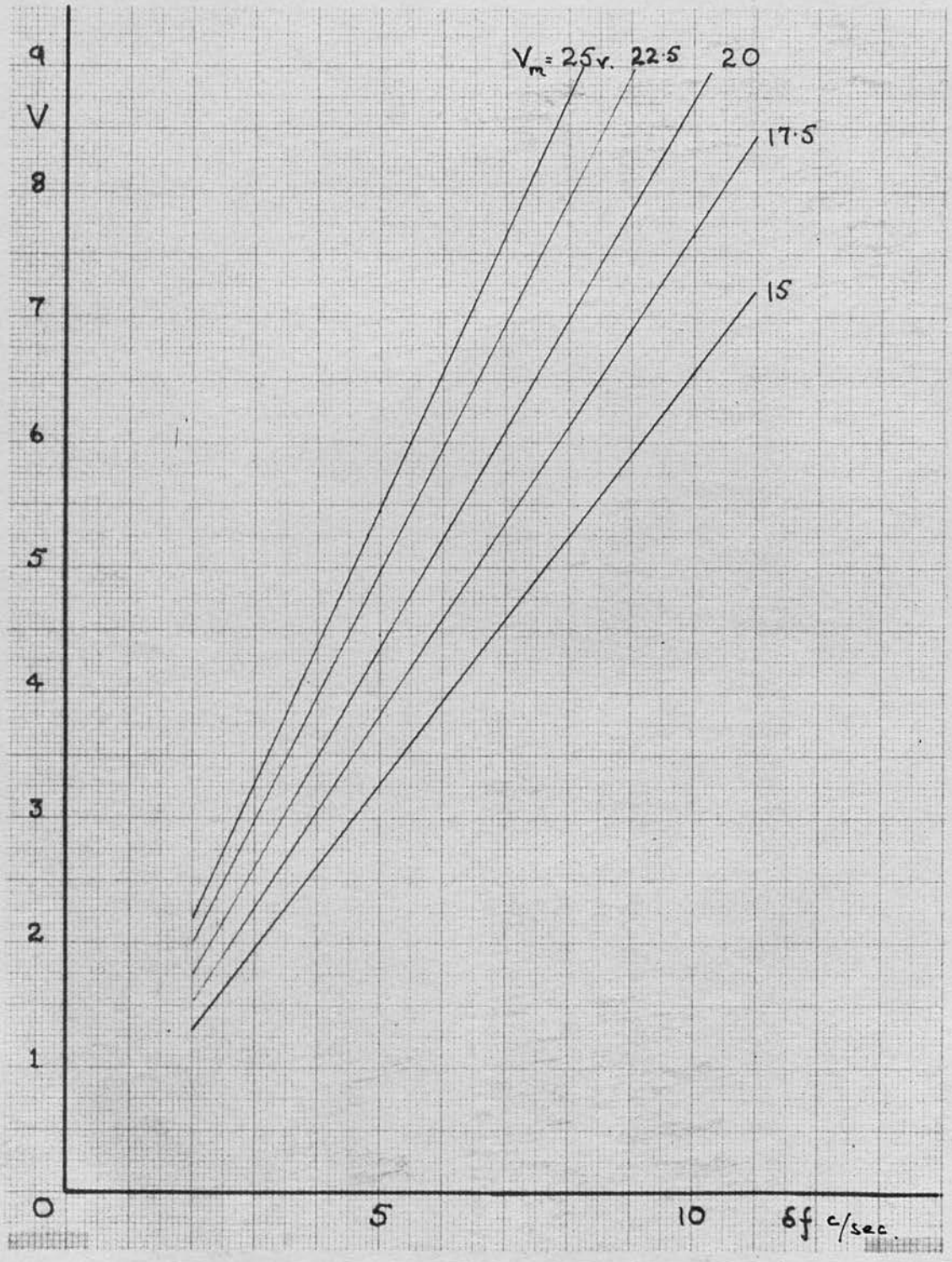

FIGURE 40

Voltage output from filter unit as a function of oscillator frequency change. Curves drawn for various values of maximum voltage across filter.

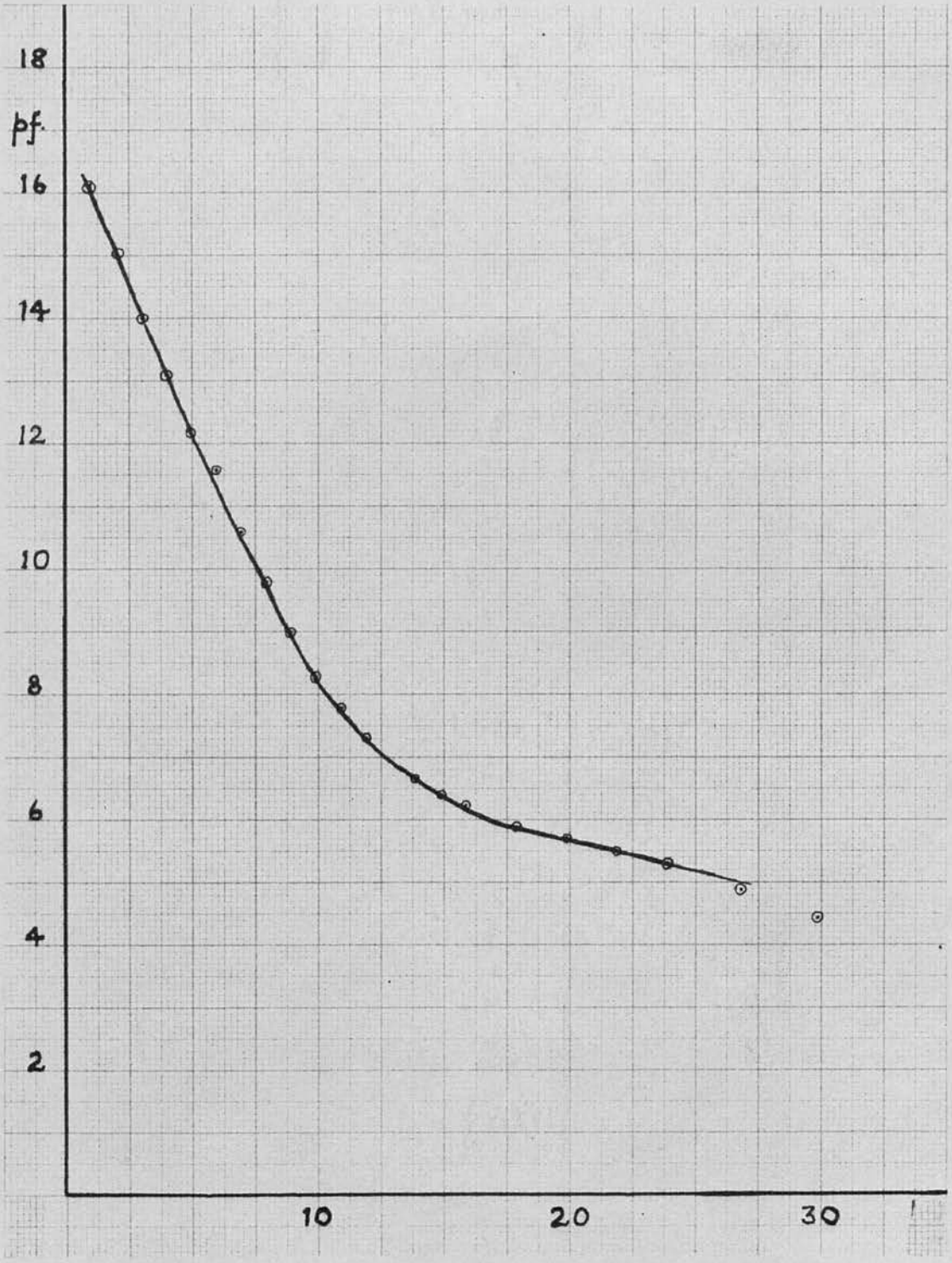

FIGURE 41

Capacitance of the oscillator tuning capacitor as a function of arbitrary plate separation.

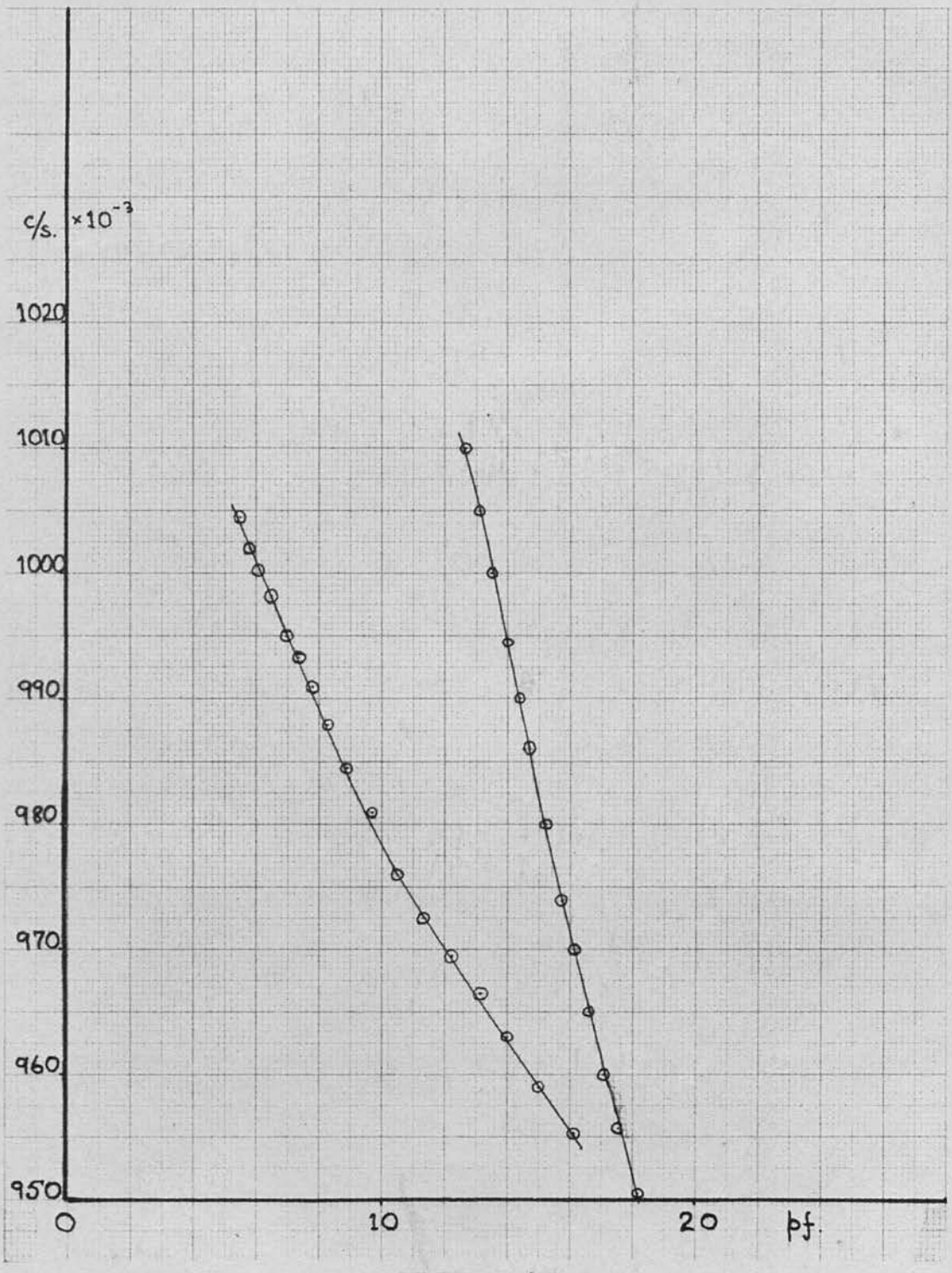

FIGURE 42

Oscillator frequency as a function of capacitance of tuning capacitor. The steeper curve is for the more sensitive coil tapping.

the frequency change in the oscillator produced by a given change in the capacitance governing the frequency. As a more detailed knowledge of the performance of the oscillator is necessary for the second method of calibration the following measurements were made.

The oscillator is controlled by a small variable capacitor, driven by a fine screw. This capacitor was calibrated on a capacitance bridge, being connected in parallel with a standard 100 pf capacitor, the sensitivity of the instrument being much greater at this value than at the 4 - 20 pf covered by the tuning capacitor. The variable capacitor was decreased by small steps and the curve shown in figure 41 constructed in which the capacitance was plotted as a function of the separation of the plates. The capacitor was now replaced in the oscillator and the frequency determined for each setting using a frequency meter, the process being repeated for the second tapping on the coil. This enabled the curves shown in figure 42 to be constructed in which the frequency of the oscillator is shown as a function of the capacitance in the tuning section. While the capacitance scale does not represent the absolute capacitance governing the oscillator, due to unavoidable and unmeasureable strays, it enables us to determine the sensitivity of the oscillator to capacitance changes. As the curves are nearly linear, over the range considered, we may take the slope at 1 Mc/sec as giving the required sensitivity.

This gives a value of 11,180 c/sec/pf for the most sensitive tapping and 4440 c/sec/pf for the second tapping, at which the instrument is used. Thus we have a reserve factor of 2.6 should it ever be needed, although it greatly increases the problems of operation.

The lower figure, gives us, for a 10^{-3} pf change in capacitance a frequency change of 4.44 c/sec., and, taking this with the earlier figures, we obtain a final sensitivity of 0.194 V_m volts/10^{-3}pf, or with V_m = 20 volts, an output of 3.9 volts for a 10^{-3} pf change, this result being for the steep side of the filter curve.

(b) Calibration by Mechanical Input

If we can arrange for a capacitor in which there is a small variation at variable frequencies to replace the vane, then, provided we know the magnitude of the variation, we can calibrate the electronics directly, without reference to the individual stages of the circuit.

To produce variations of the order of 10^{-3} pf in a capacitor of value approximately 0.2 pf we can couple a fairly large capacitor, 10 to 20 pf, with a variable section, $\pm$ 5 pf, in series with a small capacitor, of order 0.2 pf.

Consider a capacitor C_1 coupled in series with a capacitor described by $C_2 + C_3 f(\theta)$. Then the capacitance of the arrangement is given by

$$C = \frac{C_1(C_2 + C_3 f(\theta))}{C_1 + C_2 + C_3 f(\theta)}$$

Now we require the output, C, to have the form $C_4 + C_5 \sin\theta$, where C_4 is about 0.2 pf and C_5 about 5×10^{-4} pf, giving, from peak to peak a variation of 10^{-3} pf.

We then have

$$C_4 + C_5 \sin\theta - \frac{C_1(C_2 + C_3 f(\theta))}{C_1 + C_2 + C_3 f(\theta)}$$

This equation can be solved for $f(\theta)$ if we prescribe the values for C_2, C_3, C_4, and C_5. The values of C_4 and C_2 determine C_1, since we have

$$\frac{1}{C_4} = \frac{1}{C_1} + \frac{1}{C_2}$$

in the case when $\theta = 0$

Having chosen C_2, and C_4, then C_3 can be chosen to give any desired variation in $f(\theta)$, C_5 being known.

Thus with C_4 equal to 0.2 pf, and C_5 equal to 6×10^{-4} pf the function $f(\theta)$ is plotted in figure 43 as a function of θ for three cases in which C_2 and C_3 are given different values. With $C_2 = 20$ pf and $C_3 = 5$pf, $f(\theta)$ varies from + 1.3 to - 0.85, while $C_2 = 5$ pf and $C_3 = 2$ pf gives a variation from + 0.18 to - 0.17.

The equipment shown in figure 44 was built to enable the calibration to be carried out. The small capacitor C_1 was made from two Perspex blocks separated by an air gap, each block being threaded, on a common axis, to take an 8 B.A. screw, the separation of the screws varying the capacitance. The large fixed and variable capacitors were constructed as follows.

A disc of $\frac{5}{8}$" Perspex was mounted on a heavy axle which

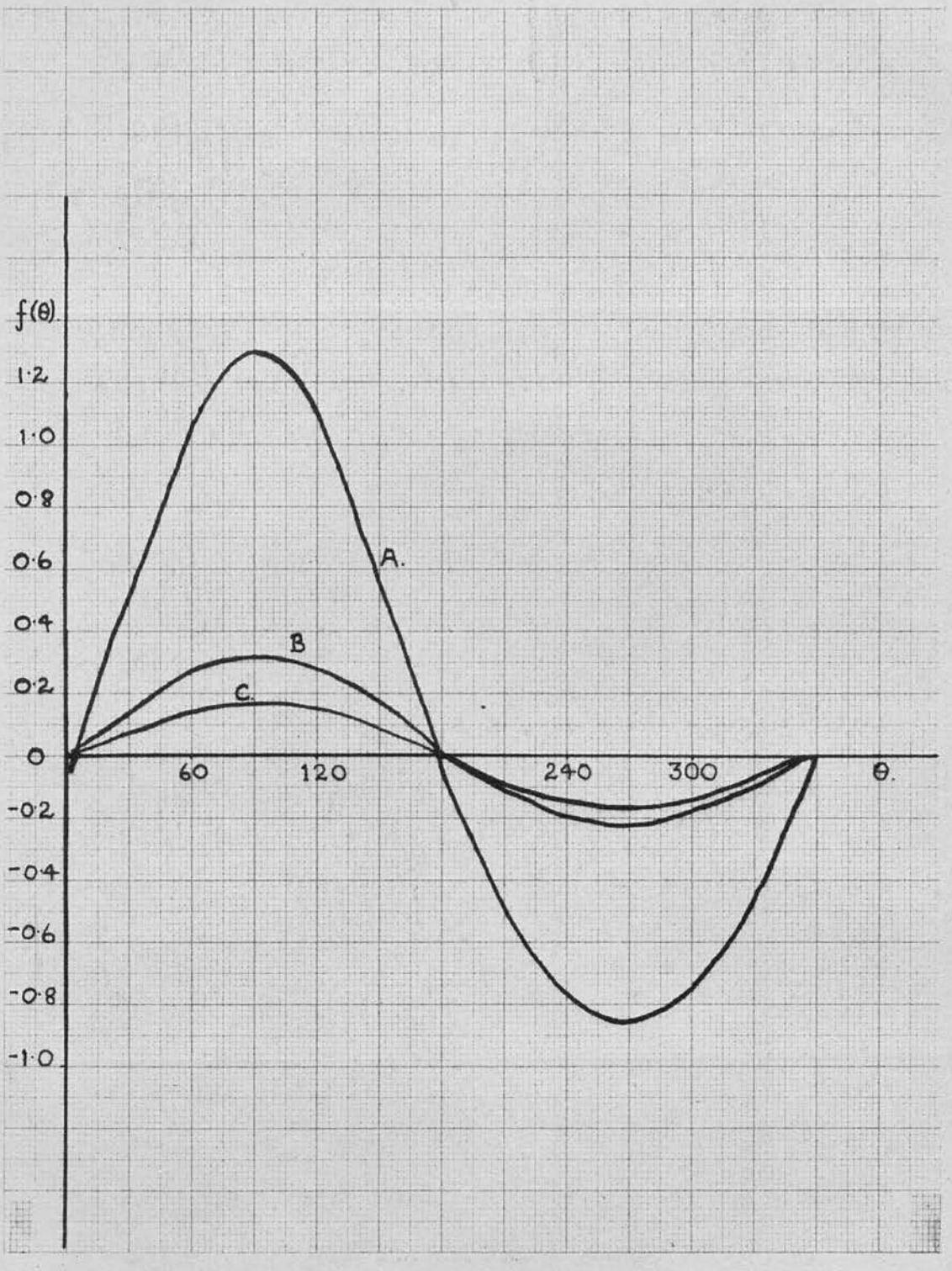

FIGURE 43

Variation of the function f(θ) with θ for

A. C_2 = 20 pf, C_3 = 5 pf.

B. C_2 = 10 pf, C_3 = 5 pf.

C. C = 5 pf, C_3 = 2 pf.

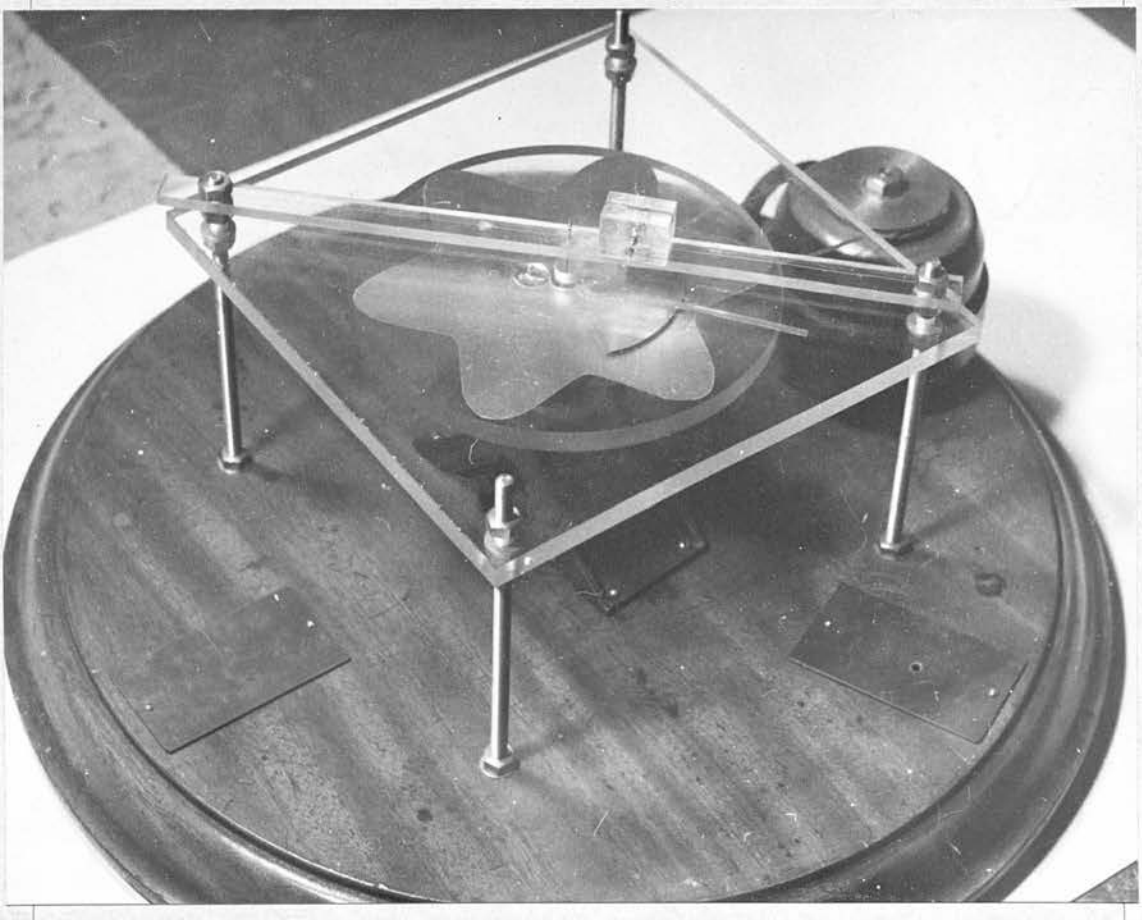

FIGURE 44

Apparatus used to provide a direct calibration of the electronics.

ran on ball races with its axis vertical. This axle was driven, through a rubber belt, at a variable speed by a small electric motor, fed from a Variac. The disc was mounted directly on the motor shaft in preliminary trials but it was found that the vibration was too great, and that the field of the motor interfered with the experiment. Cemented onto the disc was a pattern cut from metal foil, 0.0003" thick. The pattern took the form of an annulus of a circle, the outer edge being shaped in accordance with the function $f(\theta)$. A second Perspex plate was now mounted parallel to the disc and at a small, variable, separation from it. The foil glued to this disc consisted of a segment which faced the solid annulus below and a strip 0.2 cm., wide which scanned the variations in the outer section of the disc foil. C_2 consists of the capacitance formed between the plates when the scanner is in a position corresponding to $\theta = 0$, and C_3 then takes positive and negative values as the disc revolves. The foil on the disc is connected to the axle and contact is made to the rest of the circuit with a needle dipping in a mercury pool in a cup on top of the axle. A thin wire makes contact with the static foil and is connected to C_1, which is shielded from the disc by the foil on the upper plate.

The disc foil was cut to allow six complete variations in C_3, so that a rotational speed of 25 revs/sec would provide a signal of 150 c/sec.

A second disc with twelve lobes, together with gear wheels of various diameters enabled frequencies of up to 400 c/sec. to be investigated.

As the values of C_1, C_2 and C_3 were not known accurately they were determined as follows.

In the previous section the oscillator was calibrated in terms of frequency and tuning capacitance. To determine an unknown capacitance the frequency of the oscillator was measured with a frequency meter and the unknown capacitance is then included in the circuit, the change in frequency of the oscillator together with figure 42 enabling the value of the capacitor to be determined. C_1 was measured in this way, and also the maximum, minimum and mean values of the $C_2 + C_3 f(\theta)$ combination and using these values we can calculate the magnitude of the capacitance variation when C_1 and $C_2 + C_3 f(\theta)$ are connected in series.

The arrangement is then coupled into the oscillator circuit and the voltage output measured at several frequencies. The frequency is determined by measuring the rotational speed of the disc with a stroboscope. This was repeated for several different settings of the separation of the plate and the disc, varying from 0.010" to 0.1", and the results are shown in figure 45. Some difficulty was experienced in attempting to make $C_1 = 0.2$ pf, the actual value being about 0.7 pf, due to a fringing effect. It proved possible to achieve suitable values of C_5 (or δC) by

varying C_2 and C_3, so this value of C_1 was accepted. At speeds above 12 revs/sec vibration tended to set in and the frequency calibration was checked up to only 200 c/sec proving to be uniform above 50 c/sec., confirming the previous result. The amplitude calibration was extended to a variation of 15 x 10^{-3} pf and showed the response to be linear up to 10 x 10^{-3} pf the output then rising more slowly as the elbow of the filter curve came into play. The sensitivity, measured on the steep side of the filter curve, was 0.16 V_m volts/10^{-3} pf, giving 3.2 volts/10^{-3} pf for V_m = 20 volts, a figure which agrees with the 3.9 volts obtained from the first calibration to within the accuracy of the determinations.

No detailed attempt was made, at this stage, to assess the accuracy of these figures as only a guide to the performance was required. Of the two methods the second would appear the more reliable as the measurements of C_1, C_2 and C_3 can be made with about 5% accuracy with reference to figure 42. The accuracy of this curve is more difficult to estimate as it depends on the calibration on the capacitance bridge, but there is probably less than 5% error as we are concerned only with changes in capacitance.

Thus the overall accuracy of the second method is better than 10%, while the first method achieves about 20% accuracy, since it depends upon the filter response curve as well as the capacitance bridge measurements.

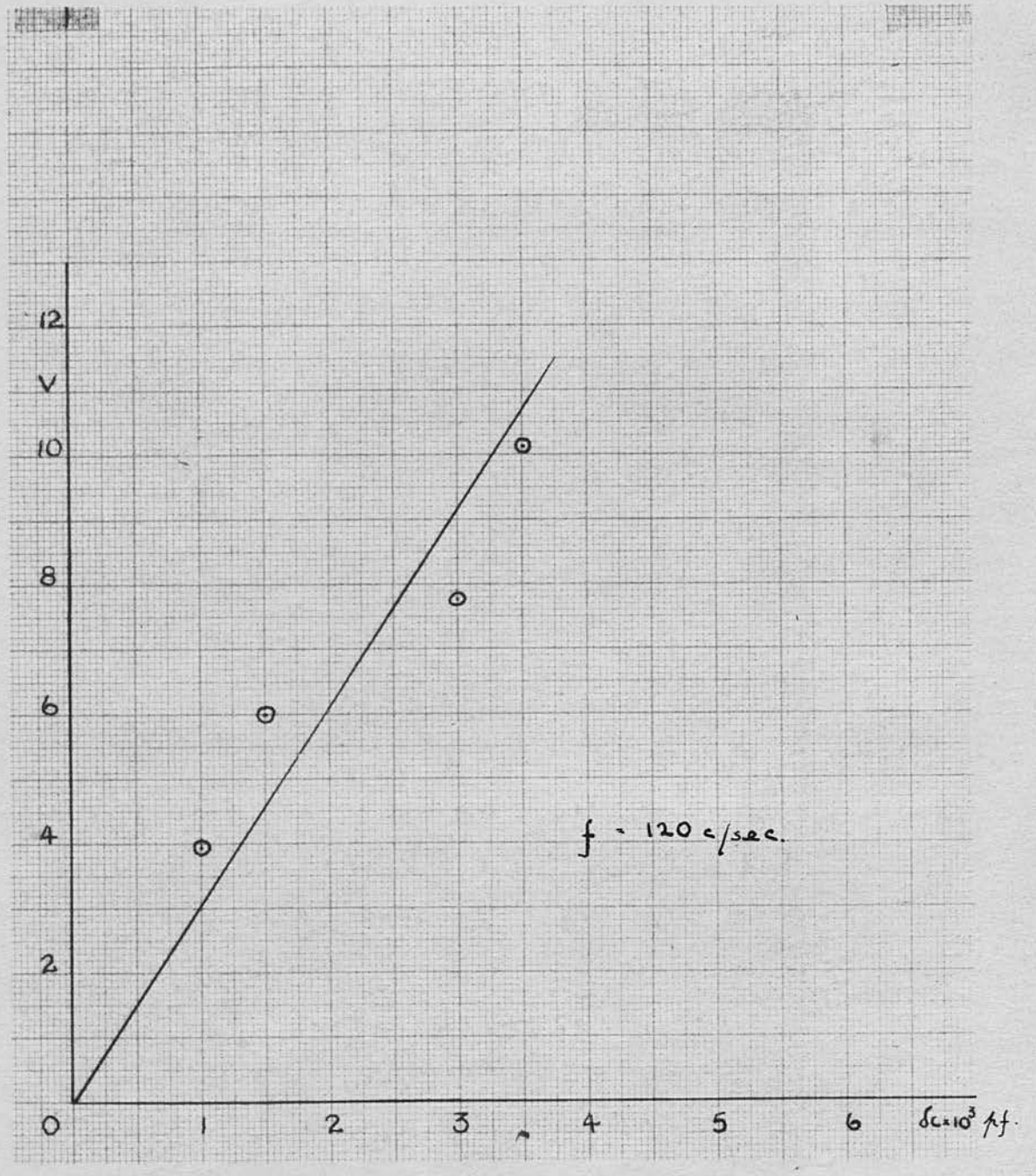

FIGURE 45

Voltage output, for V_m = 20 volts, as a function of capacitance change. Results obtained by direct calibration.

IV. 4 Conclusions

The electronic equipment is adequate for our purposes, having a reserve factor of 2.6 in a measured sensitivity of 0.16 V_m volts/10^{-3} pf. As the minimum voltage which could be measured on the oscilloscope was about 0.3 volts, a change of 10^{-4} pf can be detected, a figure which compares favourably with the required figure of 5×10^{-4} pf.

If further sensitivity were required the first step would be to increase the audio amplification since the minimum signal is 20 db above the noise level. To make use of the more sensitive tapping on the coil is more difficult as a compromise has to be accepted between the sensitivity and the distance of the vane from the electronics. The connection must be made with coaxial cable if noise and susceptibility to interference are to be kept to a minimum. With the coil used at the above tapping about 10" of cable could be included in the circuit, a greater length making it impossible to tune the oscillator to the desired frequency. This length of cable gives about 1 ft of x - movement of the vane in the boundary layer and an increase in the sensitivity would mean a rapid decrease in this figure. To utilise the maximum sensitivity it would probably be necessary to redesign the electronics to enable the oscillator to be inside the tunnel and close to the vane.

The calibration is satisfactory in that the two methods give consistent results, but we have not yet

achieved an absolute calibration.

To relate a given change in capacitance to actual movements of the vane would require further calibration;- the use of the optical method described in the previous chapter would overcome this difficulty if measurements were made on a suitable vane, but to further relate these movements to actual velocity fluctuations would require much further work and might prove insuperable when the vane is being used as a resonant detector.

Thus we have achieved a sensitivity of response suitable for a vane used as a resonant detector, and also have a potential sensitivity which would probably enable the non-resonant method to be used successfully.

Chapter V

Measurements of Boundary Layer Phenomena.

V. 1. Introduction

The situation may now be described by a synopsis of the results contained in chapters II, III, and IV.

In chapter II the free stream turbulence in the tunnel was measured at 0.3% and it was shown that transition was primarily due to a transverse contamination effect. Chapter III described the development of the vane as a detector, and indicated that its use as a resonant detector would be the most profitable line of exploration in the first instance, the development of the non-resonant case following later. The deflection of the vane was estimated for conditions which would be expected in the boundary layer and it was indicated that it would be necessary to artificially excite monofrequent oscillations in the boundary layer in order to observe clear cut laminar oscillations, since the high free stream turbulence would tend to mask any natural oscillations. Chapter IV. describes the development of a recording system of the required sensitivity, the result being, that an output 1.6 volts is achieved for a 5×10^{-4} pf change in capacity, which corresponds to a v'/U_o value of 1.0%. There is an adequate reserve of sensitivity, should it be required, as the noise level is only 0.05 volts.

The vane should, therefore, readily detect artificial laminar oscillations when it is used as a resonant detector. Consider figure 46 in which the neutral

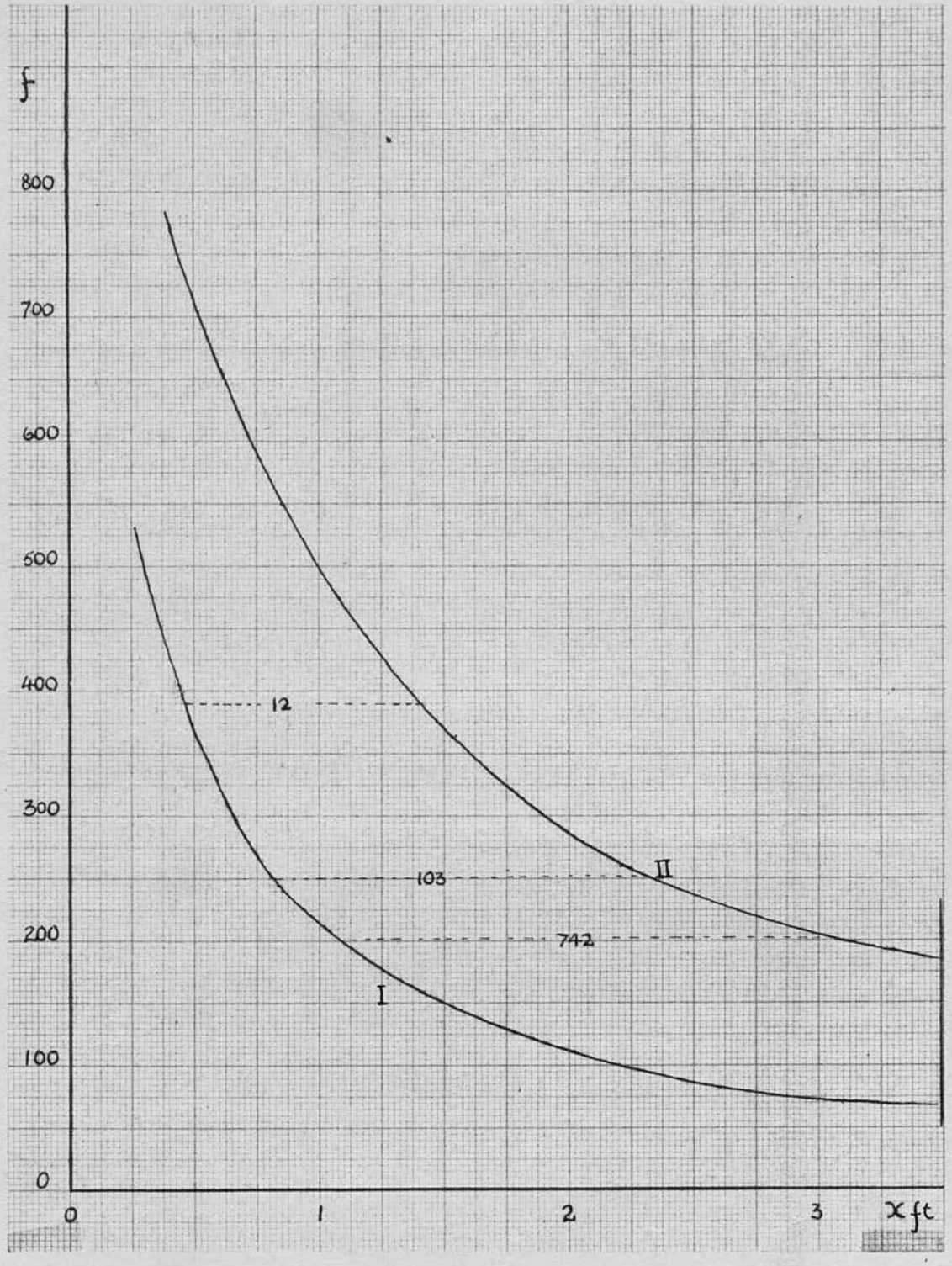

FIGURE 46

Neutral Curve drawn for U_o = 70 ft./sec., showing theoretical total amplification across zone.

curve is drawn for U_o = 70 ft/sec. The transition point due to wedge contamination is also indicated in the diagram. The maximum x value at which it will be possible to work will be somewhat less than this value since the vane has a finite extent. The limiting value at which one would expect to observe laminar oscillations is, therefore, about 3 ft., regardless of the Reynolds number. At the other end of the scale there will be a minimum x value for the position at which a ribbon, mounted to excite laminar oscillations, can be placed if it is not to disturb the general flow. This will have to be determined by experiment but should be about 1'6". Relating these values to figure 46 it can be seen that to observe points on branch II of the neutral curve it will be necessary to use vanes with frequencies of 200 c/sec upwards, while for branch I the range will be from 150 c/sec to 75 c/sec. It will be impossible to follow a given frequency right through the amplification zone. The effect of reducing the windspeed is to move the neutral curve towards the origin, so that, by working at lower windspeeds, it should be possible to obtain points on the curve at lower frequencies than those quoted above. Reduction of windspeed, however, reduces the vane resonant frequency, the two conditions of windspeed and frequency being interrelated.

Thus, although the field of exploration will be limited, it should be possible to obtain points on the neutral curve for Reynolds numbers in the range 1300 to 1800,

which will indicate whether the v oscillations follow the neutral curve.

V. 2. Preliminary Investigations

The original idea involved the use of the flat plate itself to act as the static plate of the vane capacitor. It was therefore necessary to investigate the vibration of the tunnel walls and of the flat plate itself to determine whether or not this would be possible.

In order to estimate the magnitude of the tunnel wall vibrations, a static plate, of area 0.04 sq. ins., was attached to the coaxial cable in place of the vane and the circuit completed with a small piece of foil glued to the tunnel wall. The separation of the foil and the plate was set at 0.04" with a feeler, and, since the electronics and associated equipment were isolated from the tunnel and could respond only to such vibrations as were transmitted through the floor, the output was essentially a measure of the vibration of the tunnel walls. In Figure 47 a recording is shown of the vibration when only the motor-generator set is running and a recording made with the fan running at 1830 R.P.M. The first record shows a low frequency vibration of the order of 10 c/sec which was due to panel vibrations of the wall. The higher frequency, of 175 c/sec., was eventually traced to a microphony effect in the electronics and is therefore spurious. It was eliminated by suitable insulation before the second recording was taken which shows a high frequency of 125 c/sec. This is exactly 4 x the fan frequency. As

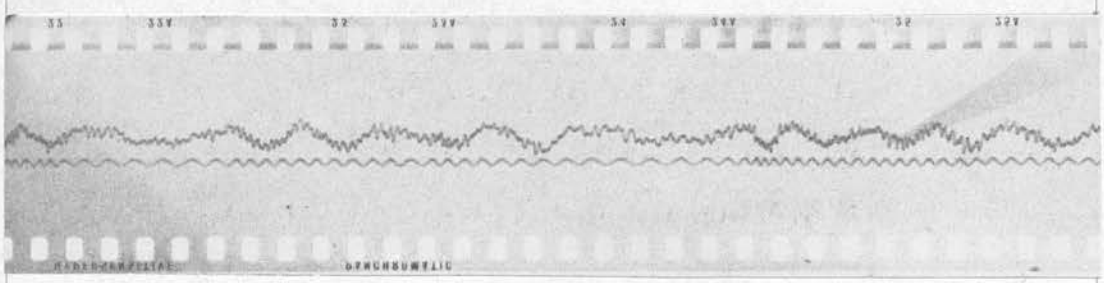

Noise from tunnel wall with motor-generator set running; low frequency panel vibration, high frequency due to microphony and eliminated from later traces.

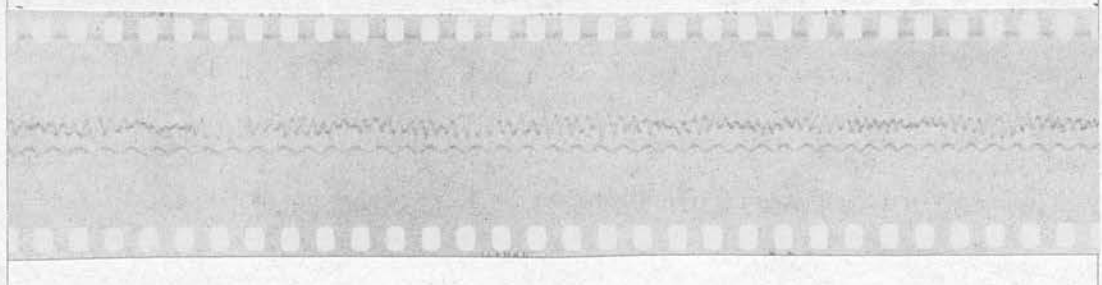

Noise from tunnel wall with fan running at 1850 R.P.M. High frequency = 125 c/sec = 4 x fan frequency.

FIGURE 47

Record of noise from tunnel wall. The amplification is 10 times that used in all other recordings. The lower trace in all recordings is a standard 50 c/sec signal.

the pick up position was varied on the wall, it was found that the amplitude decreased at the corners and also, very markedly, where the brass bars supporting the flat plate stiffened the walls.

The flat plate was next investigated by using a similar static plate moundted on the boom traverse gear, a small piece of foil being used on the flat plate. The output was fed through the coaxial cable, which left the tunnel through an oversize hole. The output would now measure the relative vibration of the flat plate and the boom. The results, similar to figure 47, showed a well marked dependence upon the fan speed. For fan speeds above 1100 R.P.M. the frequency observed was 4 x the fan speed, while below 1100 R.P.M. it became 8 x the fan speed, thus keeping the observed frequency in the range 80 to 140 c/sec. A low frequency vibration of larger amplitude, due to the boom, was also noted.

Although the amplitude of the flat plate oscillation, estimated from the output, was only 10^{-4}" and therefore unlikely to disturb the flow to any serious extent, the frequency falls in the range in which measurements are to be made. The possibility of stiffening the flat plate with transverse strakes glued to the reverse side was considered but it was decided to first investigate the possibility of a vane unit completely isolated from the tunnel and flat plate, since the boom vibrations were considerable, although of a low amplitude which could be filtered out by electronic

means.

The arrangement adopted consisted of a frame round the working section of the tunnel upon which could be mounted the vane head and any equipment required to traverse it in the boundary layer, without allowing any part of the structure to touch the tunnel.

A 2" angle iron frame was constructed around the tunnel, the legs being bedded in concrete blocks and insulated from the floor by felt pads in the same way as the tunnel. Figure 49 shows the method used to traverse the vane in the boundary layer. A set of rails was arranged to run just inside the tunnel wall, a steel shaft at each end passing through slightly oversize holes in the tunnel wall and being located in collars attached to the angle iron frame. The outer ends of these shafts were tied together with a stiff bar which carried the bodies of two micrometer heads, the probes being allowed to bear against the angle iron. The rails inside the tunnel could then be traversed parallel to themselves to an accuracy of 0.001". A simple carriage was built to run on the rails and this carried a boom at its inner end, about 1" from the flat plate. The vane heads could be screwed into this boom, the shaft of the head being curved inwards to allow the vane to approach the surface while keeping the body of the head outside the boundary layer.

Measurements of the pressure gradient were made with this arrangement in place and showed a local change of about 2%. As the semi-area of the tunnel

is only 134 sq. ins. an areal blockage of 1.5 sq. ins., provided by the vertical tie-piece at the front of the rails, would cause a local pressure change of this order. The original rails were therefore replaced by a single square rod which was tapered at its upstream end to reduce the areal blockage to only 0.12 sq. ins. This entailed a certain loss of stability as the carriage now became a box spar running on the rod with two faired strips supporting the boom mount. The boom was sufficiently heavy to reduce the natural frequency of the system below 20 c/sec and no forced oscillations were observed when the tunnel was run up. Provided that care was taken not to disturb the framework the arrangement worked well, although the x movement of the carriage proved rather stiff. An improved design is indicated if more refined work is to be attempted.

V. 3. Development of Vane Head.

The vane head unit, which was attached to the boom, is shown in figure 48. The body was made from ebonite and was about $\frac{1}{4}$" thick, being well streamlined and polished. Two diverging hypodermic tubes were mounted as indicated and were lined with fine glass tubes. The tubes projected $2\frac{1}{2}$" in front of the body having a separation of $\frac{3}{4}$" at the body and about $1\frac{1}{2}$" at their tips. A suspension wire of 0.001" diameter Nichrome wire was threaded through the glass tubes and anchored at the rear of the body, one end being soldered to a tag to which the coaxial lead to the electronics could be attached. The tension in the suspension wire

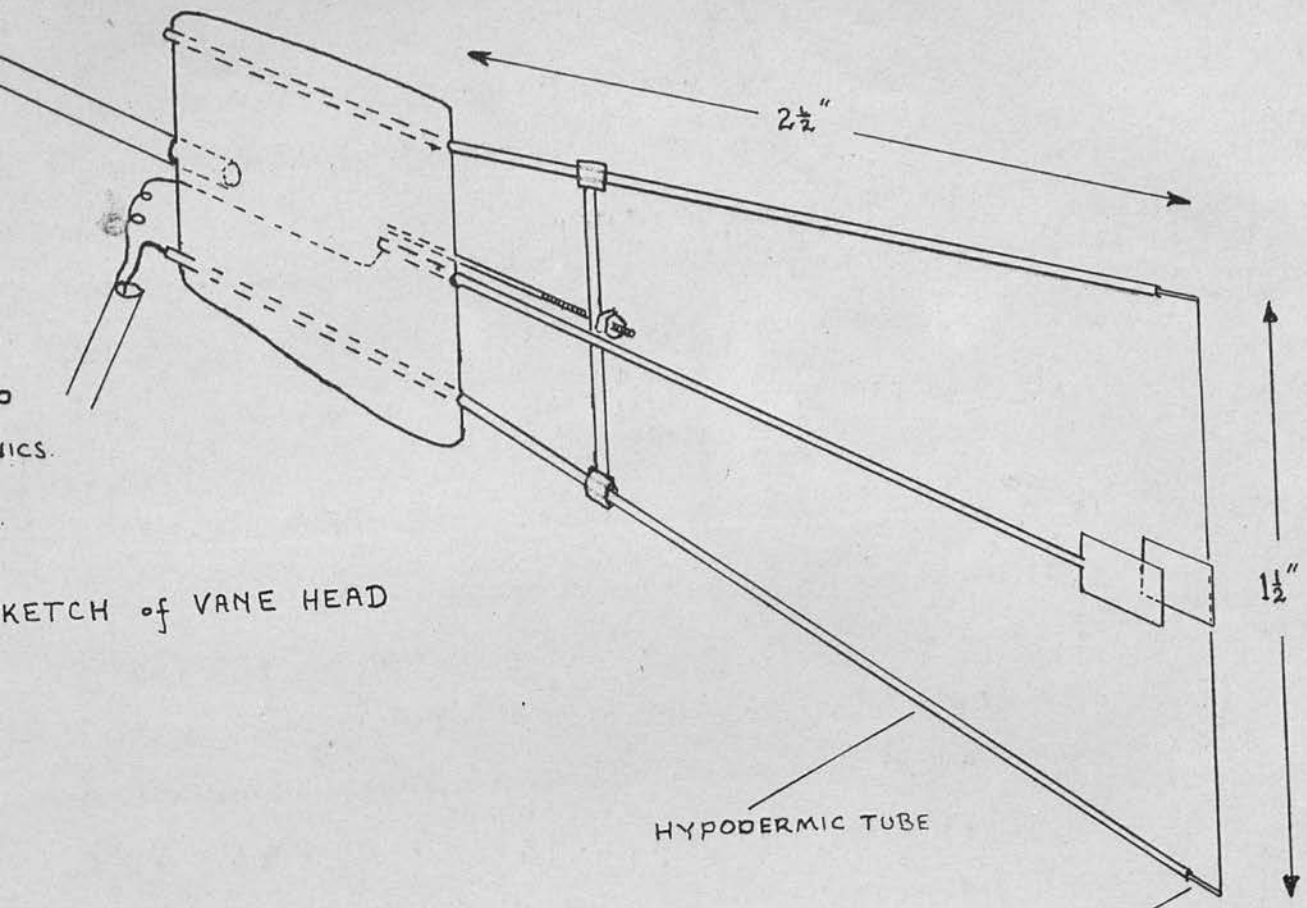

ICS.

KETCH of VANE HEAD

NE HEAD IN TUNNEL

REFLECTIONS SHOW POSITION
OF FLAT PLATE.

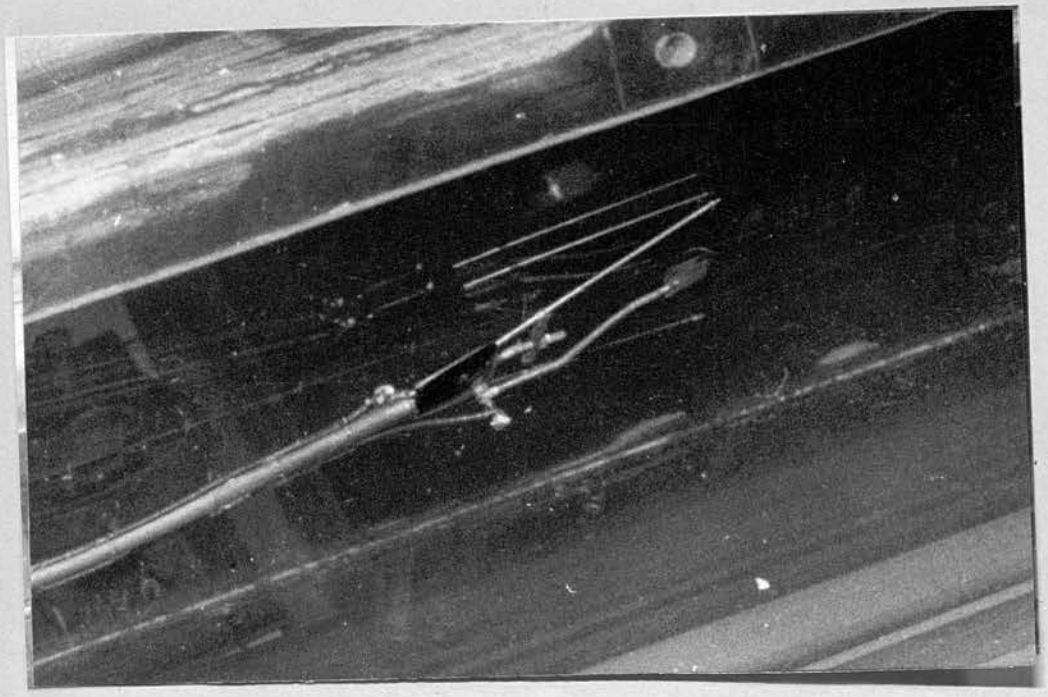

FIGURE 48.

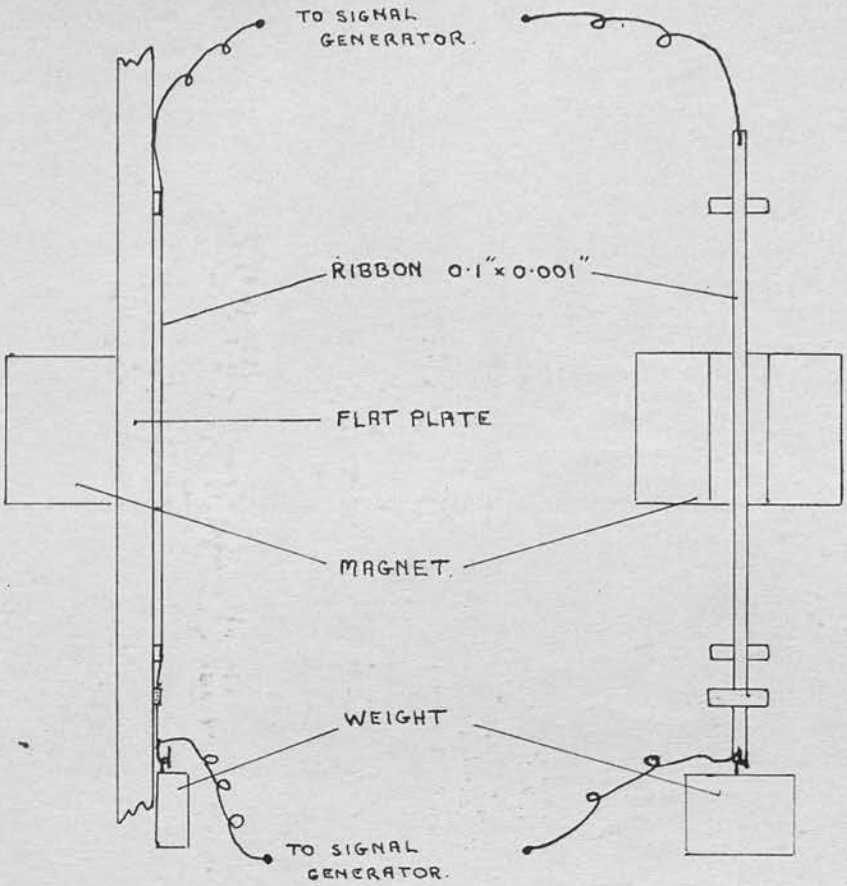

SKETCH of RIBBON LAYOUT

FIGURE 49.

SKETCH of y-TRAVERSE EQUIPMENT.

SCALE: 1cm. = 1"

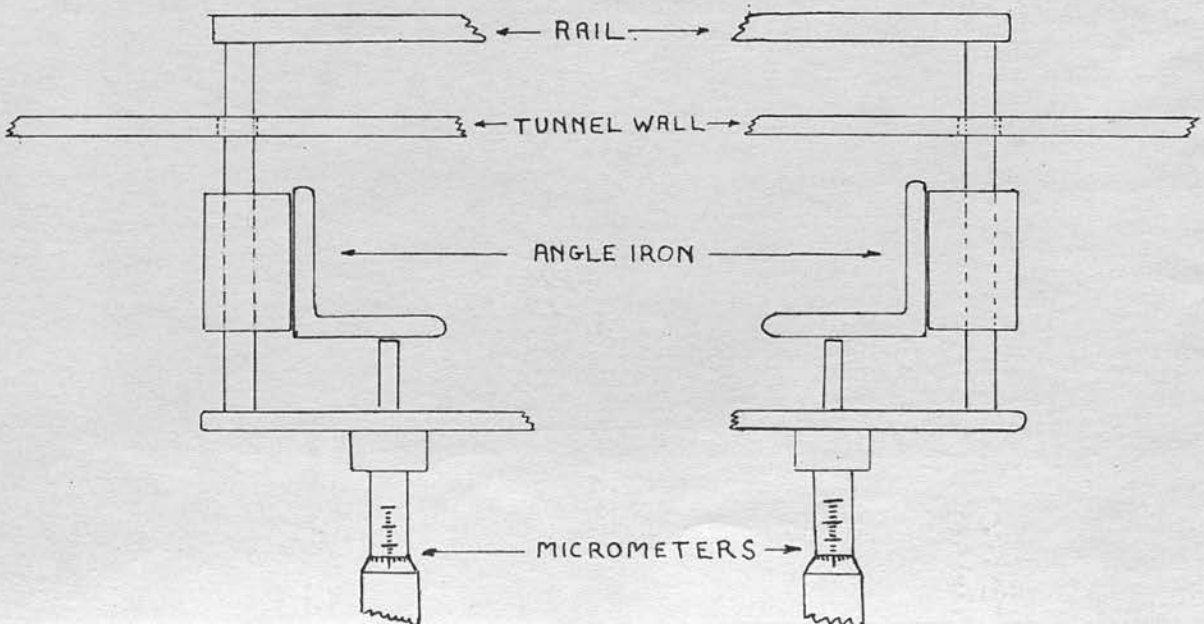

was controlled by a strut sliding on the hypodermic tubes, tension being increased by sliding the strut towards the body, a screw being provided to allow fine adjustment. A static plate was mounted on a fine boom and was placed outside the vane and with its leading edge slightly downstream of the suspension wire. It was made from 0.003" sheet, its boom being 0.05" in diameter and tapered to where it met the plate. The separation of the vane and static plate could be varied and was usually set at about 0.15", that is, with the static plate outside the boundary layer and unlikely to affect the flow over the vane. The original figures suggested that a separation of 0.04" would be necessary but, as has already been noted, these were unduly pessimistic and it was possible to use the above figure and yet still obtain a suitable output. A $\frac{1}{4}$" brass rod about 6" long connected the body of the head to the boom. This rod was bent inwards so that the hypodermic tube approached the surface at a small angle and allowed the body of the head to be outside the boundary layer. The vane, mounted on the suspension wire, could then approach the surface to a distance determined by the diameter of the tubing. This was 0.04", so that the smallest y value obtainable was 0.02". This could readily be decreased if it proved necessary. The zero of a y-measurement was determined by observing the vane head closely as it was moved outwards by means of the micrometers. When the hypodermic tube broke contact with the surface a small, but definite low frequency

oscillation of the boom took place in the plane of the flat plate. This died away fairly rapidly but gave an indication repeatable to $\pm$ 0.001".

An attempt was made to control the tension in the suspension in a quantitative way since such information would be required if it were necessary to use the suspension resonant frequency. The possibility of using the suspension itself as a strain gauge was investigated and it was found that this method would be possible, but that a delicate bridge was required to measure the small changes involved. A switching device w ould also be necessary to permit the use of the suspension in this role and trouble might be encountered with stray capacitances. A rough calibration, made by hanging weights on the upper support until the wire just became slack, showed that the tension varied from 5 g. to 20 g., giving resonant frequencies of 600 c/sec to 1200 c/sec.

It was found that the general arrangement described above was satisfactory except for the coaxial cable which ran from the body of the head to the exterior of the tunnel. The cable was substantial 0.2" in diameter and led to an appreciable drag on the vane head, and, because of its stiffness, it tended to distort the frame and alter the y value when a change in x position was made. It was impossible to use a longer, and hence more flexible, piece of cable as the 10" used just permitted the oscillator to be tuned and an increase to 12" made this impossible. Several substitutes were tried in place of the cable in an attempt to reduce the drag and capacitance of the leads. A thin Perspex strip $\frac{1}{2}$" x $\frac{1}{4}$"

½", with the leads cemented to its edges proved to have a low capacitance but was too susceptible to interference, since the vane lead was no longer shielded and the presence of a hand, to adjust the micrometers for example, was sufficient to detune the oscillator. A compromise was eventually adopted in which the leads from the vane and static plate were extended to the rear of the rod supporting the vane head, that is, about 9" behind the vane itself. The coaxial cable then took the signal to the electronics in the same way as before but the distorting tendencies were eliminated. The capacitance of the leads in this configuration was just below that required to tune the oscillator, the tuning capacitor having its plates at maximum separation which allowed very precise control of the tuning. The equipment had, in practice, to be allowed to warm up for about two hours before it would tune at all.

V. 4. Investigation of Vane Performance

Using the theory and results of chapter III, the behaviour of vanes of varying construction was next investigated. The size, in most cases, was kept of the same order of magnitude, being about 0.25" x 0.2".

In chapter III, it was indicated that vanes of silvered mica would have the desired characteristics and these were the first to be subjected to trial. Vanes made from varying thicknesses of mica were attached to the suspension by hinges made from 0.0007" diameter wire twisted round the suspension and glued to the vane. If the vanes were now silvered it proved

difficult to ensure that the vane surface made good contact with the hinge and hence with the suspension. A further difficulty was that the vane slipped down the suspension wire and an effective stop which would not impede the movement proved difficult to make; a fine wire tied round the suspension proving the most satisfactory. Such vanes as were made proved fairly successful, it being possible to excite their resonant frequencies in the free stream if the suspension was kept at a fairly low tension. Resonant frequencies in the range 70 c/sec to 350 c/sec were readily achieved with mica of a minimum thickness of 0.0005". The hinge system, however, was not satisfactory amd allowed vanes to be blown away very easily and in view of this the possibility of making a vane of thin metal foil was investigated.

Vanes were made from foil 0.0003" thick by simply folding the foil over the suspension wire and gluing the two leaves together. This could be done so that the vane was of double thickness over its entire surface or in such a way that the double section was restricted to a small region near the hinge. These vanes eliminated the difficulties of contact with, and of sliding down, the suspension wire but were found to vibrate in a different manner. While the mica vanes were sufficiently rigid to maintain their shape in the air stream the foil vanes flexed and bent, oscillating in such a way that the displacement was not proportional to the distance from the hinge but increased very rapidly at

the rear of the vane. These effects were detectable by visual inspection in suitable lighting. Vanes made with part of their area of single foil appeared to vibrate only over the single area, the tail of the vane responding to fluctuations.

While this performance made it impossible to use the theory to predict the behaviour it was found that such vanes possessed a resonant frequency which did not depend upon windspeed to a marked extent. Frequencies in the same range as for the mica vanes were obtained but, once excited, the amplitude tended to be rather uncontrolled and the vanes were easily damaged by this behaviour. If a vane of this type could be controlled, it would prove useful as the criterion of accurate y-positioning would then become relaxed, as the frequency being no longer dependent on the windspeed.

A compromise between the silvered mica and the foil vane was therefore adopted and a vane made from foil stiffened with a mica leaf. In a typical case the mica leaf was 0.0002" thick and was covered on both sides with foil making the total thickness 0.0008". These vanes proved very successful and results obtained with one have already been quoted in chapter III. They could be built to respond to frequencies from 60 to 300 c/sec and their resonant frequency varied linearly with windspeed as predicted by the theory.

The amplitude of the oscillation could be controlled by adjusting the tension in the suspension and the results in chapter III were obtained by placing the

vane in the free stream with a low tension on the suspension. The amplitude further depended upon the stiffness of the hinge, which had to be wrapped round the suspension sufficiently tightly to prevent the vane sliding down the wire.

Thus adequate control over the response amplitude to a given signal could be achieved and vanes of this type were adopted for the investigation of laminar oscillations by means of a resonant detector.

V. 5. Observation of Laminar Oscillations

(a) Natural Oscillations

Using the foil and mica vanes a search was made for natural oscillations in the boundary layer. Inspection of the neutral curve shows that we could expect to observe points on Branch II at frequencies of 200 to 300 c/sec at x values varying from 2 to 3 ft., if the windspeed is in the range 50 to 70 ft/sec. On observing a given frequency we should expect the energy at that frequency to increase with increasing x until a turning point was reached. The x value of the turning point, taken with the frequency and windspeed, would enable a neutral point to be plotted on the diagram.

Vanes of these frequencies were constructed and moved down the flat plate in the boundary layer. The results were not convincing in that they were not readily repeatable although, at times, they appeared to show the desired effect. It seemed that a vane required a certain minimum energy level to excite it, but

FIGURE 50

General view of working section during observation of laminar oscillations.

would continue to oscillate at lower energies once the motion had been established.

The investigation was not pursued at this stage as the high free stream turbulence, together with the band width of the vane response, combine in an unfavourable manner to mask the desired effect. This situation is discussed in detail in section 6.

(b) Artificial Oscillations.

The method used to excite artificial oscillations is due to Schubauer and Skramstad. A thin ribbon is held close to the surface of the flat plate and is caused to vibrate by passing an alternating current in the presence of a magnetic field.

Such a system was set up in the tunnel and is indicated in figure 49. The ribbon, a phosphor bronze strip 0.001" thick, was held 0.007" from the surface by small metal bridges, the separation of which can be varied. A signal generator was used to pass a current at variable frequency through the ribbon and a powerful permanent magnet was placed on the reverse side of the flat plate, so that the ribbon vibrates normal to the plate and to the airstream.

A ribbon 0.01" x 0.001" was first tried but did not appear to excite laminar oscillations, probably due to the width being too small compared with the wavelength of the oscillations. Schubauer had used ribbons up to 0.25" wide and we therefore obtained a 0.1" x 0.001" ribbon and repeated the experiment.

The vane immediately picked up the oscillations

set up by the ribbon and traced them down the plate. We had succeeded in detecting artificial laminar oscillations. It was therefore decided to calibrate the amplitude of vibration of the ribbon in terms of its resonant frequency and the current passed through it. The effect of the ribbon on the boundary layer was also investigated to determine at what position the ribbon could be mounted without unduly disturbing the boundary layer.

Unfortunately the most powerful signal generator available had a maximum output of $\frac{1}{2}$ watt and with this power we were unable to force the ribbon to vibrate at appreciable amplitudes at frequencies far removed from resonance. The following experiments were carried out to enable us to predict the amplitude under given conditions.

A ribbon was set up on a Perspex plate in an identical fashion to the ribbon in the tunnel. The mode and amplitude of the oscillation were studied with a microscope fitted with a graduated eyepiece. Under suitable conditions of illumination the ribbon appeared as a fine gold line against a dark background, broadening to a band as the amplitude increased. The output control of the signal generator was calibrated in volts and this reading, which is directly related to the current in the ribbon, is taken as the measure of the exciting force in the remainder of this chapter. It was observed that, provided the frequency was below the first resonant frequency, the ribbon vibrated in

a single loop and, as its behaviour above the resonant frequency was erratic, it was decided to restrict the operating frequency to below the resonant frequency. It was however, necessary to work fairly close to resonance to obtain suitable amplitudes of oscillation.

The resonant frequency was first determined as a function of ribbon length and of the tension. Special weights of 50, 100 and 150 g., were cast in a streamline shape for use in the tunnel and the curves in figure 51 show the resonant frequency as a function of length, determined by the separation of the bridges, for these three tensions. Using these curves we could determine the tension and bridge separation for any desired resonant frequency. The actual resonant frequency was readily determined by ear after the ribbon had been set up. Figure 52 shows typical curves for the variation in the voltage across the ribbon to maintain a constant amplitude as the frequency is varied. These curves were obtained with a narrower ribbon, the curves for the 0.1" ribbon being similar, but steeper. Using a set of these curves it was possible to construct curves of the type shown in figure 53. These show the voltage necessary to maintain a constant arbitrary amplitude of oscillation when the frequency is 10, 20 and 30 c/sec below the resonant frequency. The curves are constructed for constant tension and show the variation of voltage with length, from which the resonant frequency can be determined. Three such sets of curves were constructed for the three tensions used. The arbitrary

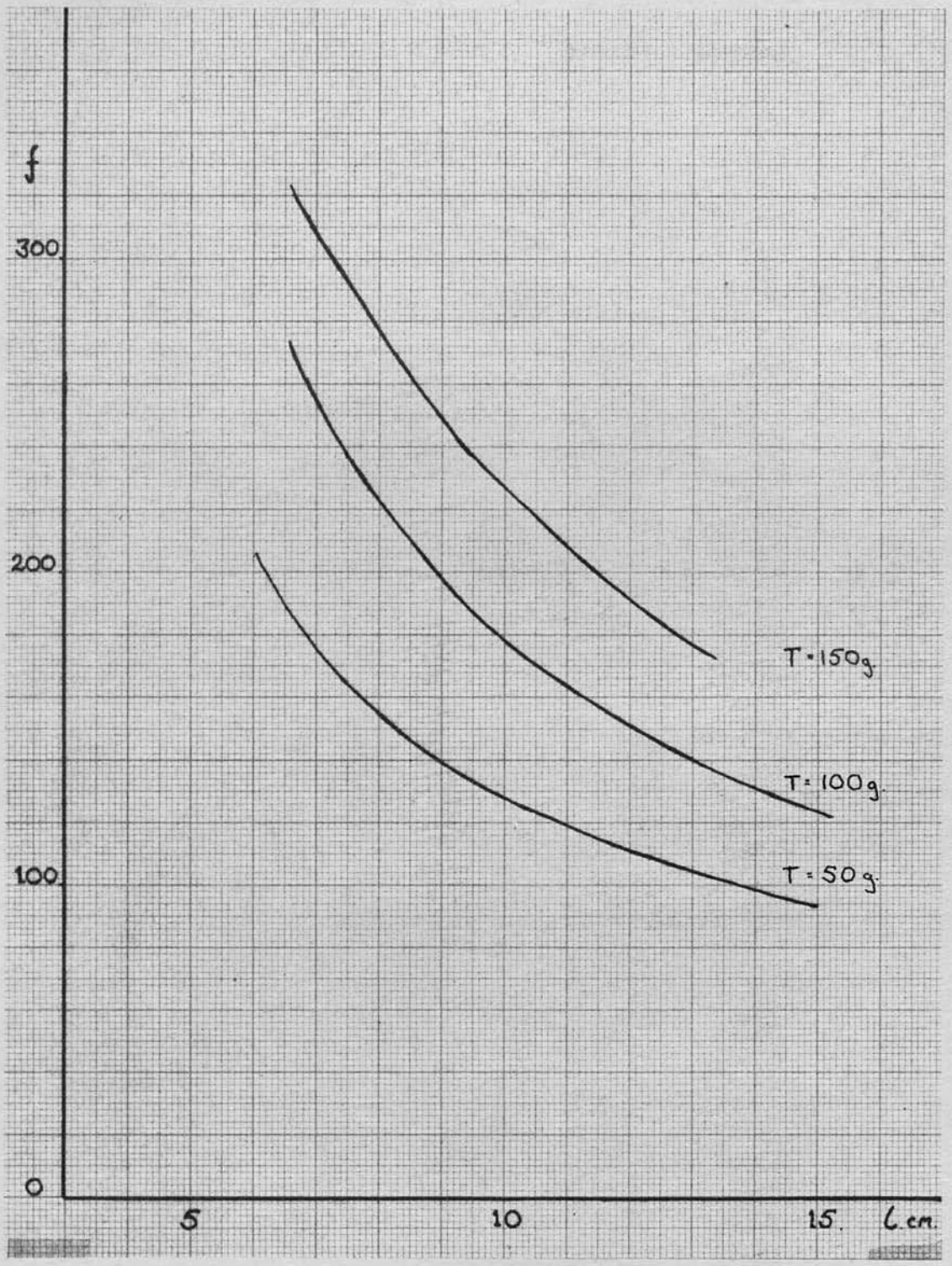

FIGURE 51

Resonant frequency of ribbon as a function of length for various tensions.

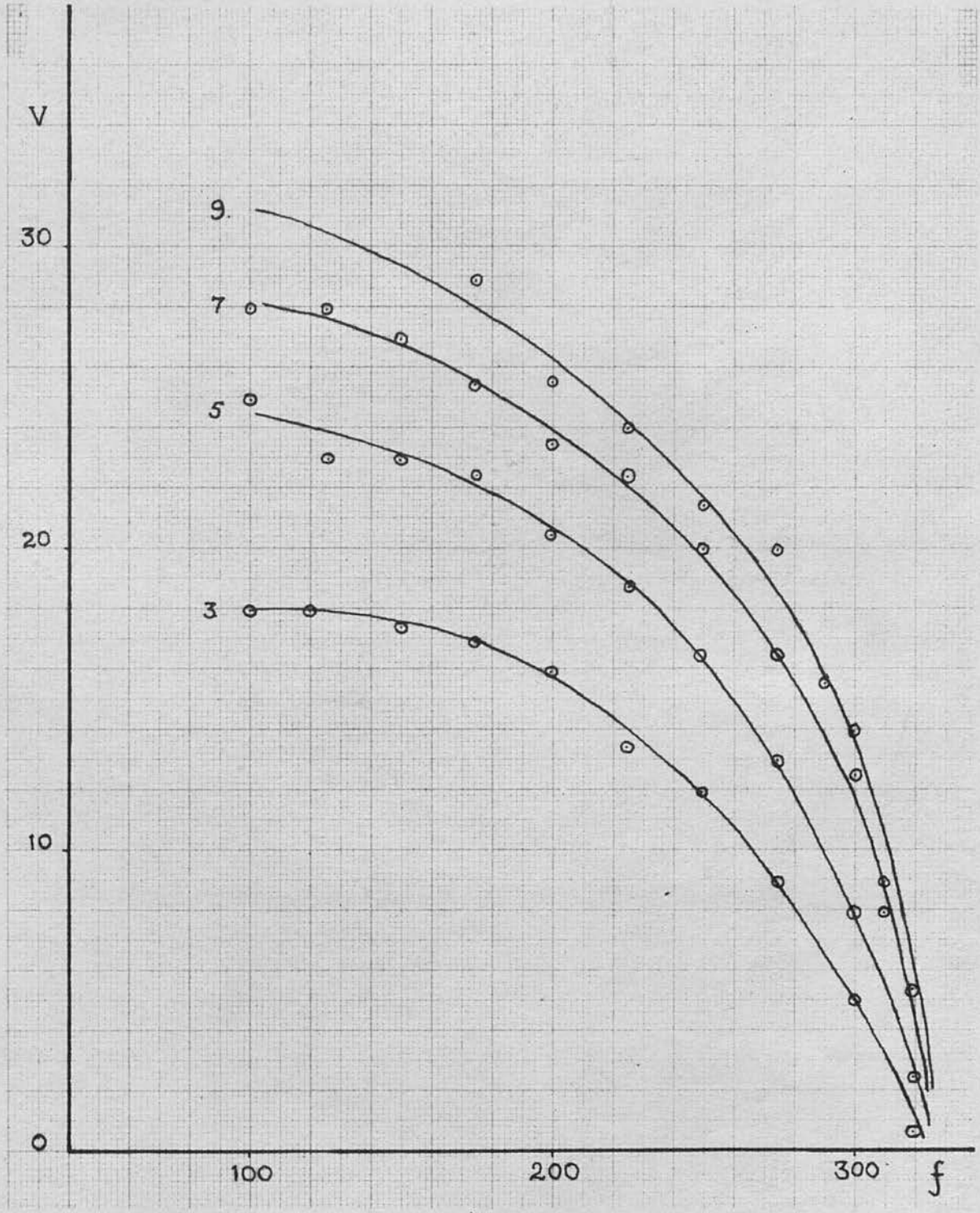

FIGURE 52.

Voltage across ribbon necessary to maintain a constant arbitrary amplitude with varying frequency. Curves obtained with 0.01 x 0.001" ribbon.

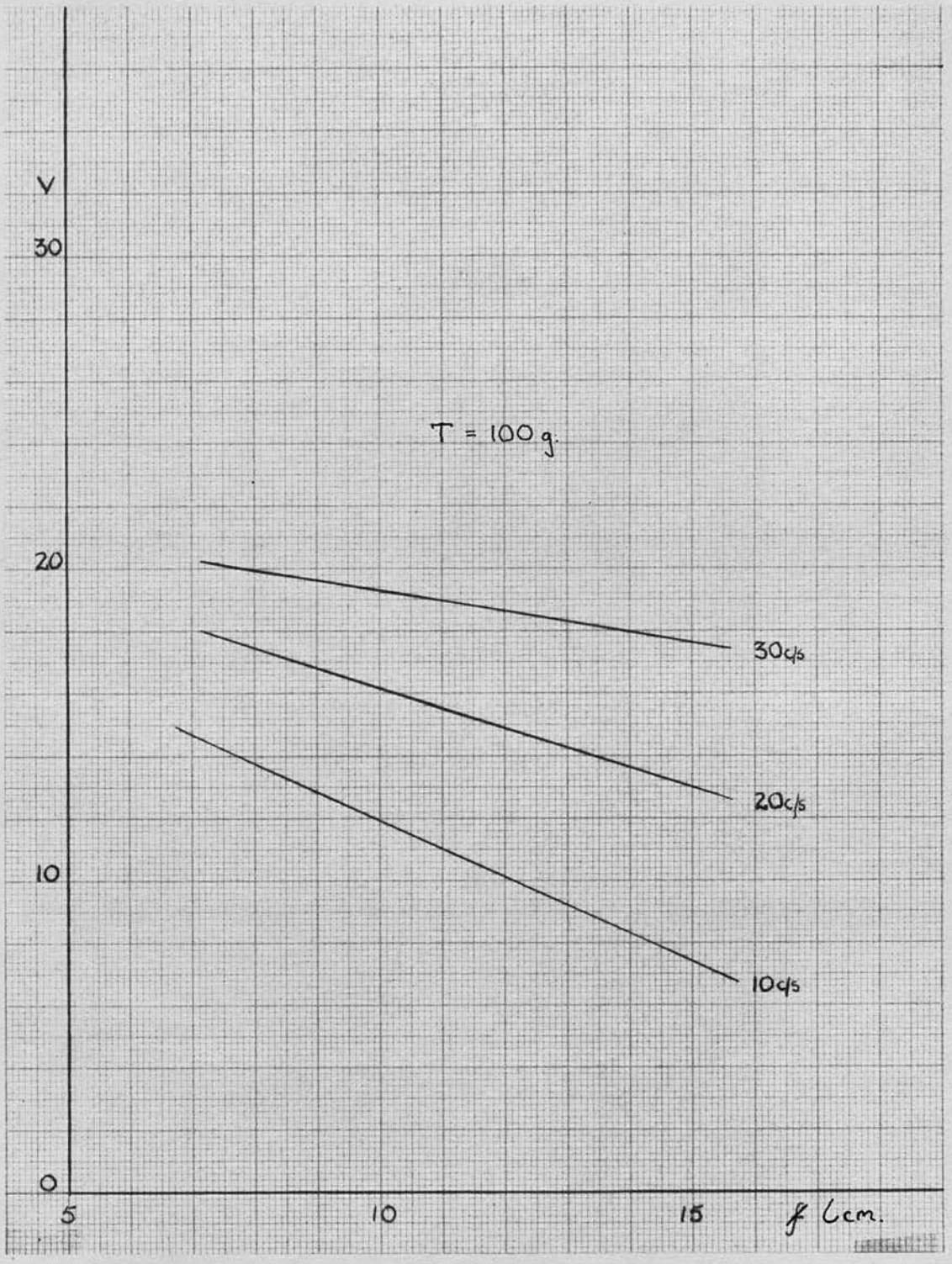

FIGURE 53

Voltage across ribbon to maintain a constant amplitude of 0.008" for frequencies 10c/sec, 20c/sec. and 30c/sec. below the resonant frequency.

amplitude was measured in the units of the eyepiece scale, and calibration of this gave the actual amplitude, for figure 53, as 0.0083".

By plotting amplitude against voltage for constant length and tension we found that the amplitude varied linearly with the voltage up to an amplitude of 0.012", provided that the frequency was near the resonant frequency. Indeed, except for cases of low resonant frequency it was difficult to exceed this amplitude at more than 20 c/sec from the resonance. Thus the ribbon never actually touched the surface of the flat plate, approaching to 0.001" at the maximum amplitude.

The ribbon in the tunnel was now used to investigate the effect of ribbon amplitude, frequency and position upon transition. The tests were not exhaustive, but established that with the ribbon at 1'2" from the leading edge amplitudes greater than 0.006" brought the transition front forward, but that, with the ribbon at 1'6" the maximum amplitude of 0.012" had no effect on the transition. The ribbon was therefore placed at 1'6" during the following investigations except for a few cases when it was used at 1'2".

We could now describe the motion of the ribbon in both amplitude and frequency and an attempt was made to use this information to obtain a minimum signal level to which the vane would respond.

A vane with a resonant frequency of 120 c/sec was placed 6" downstream of the ribbon which was at 1'6". The windspeed was adjusted to 70 ft/sec so that the signal from the ribbon would receive a nett amplification

of zero on arrival at the vane. The minimum voltage required to excite a well defined oscillation of the vane was then determined. Knowing the amplitude and frequency of the ribbon, its mean velocity could be calculated, assuming it executed S.H.M. Thus a value of v' could be obtained for the input signal. Assuming that this value is maintained to the position of the vane, then the signal at the vane is v'/U, where U is the local velocity at the vane. A value of $v'/U = 0.5\%$ was obtained which agrees with our estimate, in chapter III, of 1% as being a readily detectable signal. The response is actually greater than predicted since the sensitivity was reduced by a factor of 3 when it was found that the static plate could be used at 0.15" from the vane. The amplitude of the output could be controlled to some extent by varying the tension in the suspension, but the same exciting voltage was required to establish a well defined signal.

A figure of order 0.5% may also be predicted from our knowledge of the free stream turbulence level as 0.3% since we would expect a detectable signal to be of greater magnitude than this value.

In fact the minimum level varied from vane to vane, depending on the resonant frequency of the vane and the stiffness of the hinge. The result above is for a typical vane.

Using the ribbon and vane we now proceeded to trace the progress of laminar oscillations downthe flat plate. It was found more reliable to determine the minimum

voltage which would excite a well defined signal in the vane at each x position than to measure the amplitude of the vane response at each station for a constant signal. The well defined signal respresents an arbitrary level, depending on frequency, when the oscillations become predominant over the background noise. For the purposes of photographic records the second method, that of using a constant input, was also used, and, while less repeatable, gave results in agreement with the first method.

The procedure was then as follows: A vane was constructed and placed in the tunnel about 4" downstream of the ribbon where its resonant frequency was first measured by using the ribbon at maximum amplitude and varying the frequency until the resonance was found. The vane was then traversed downstream and, at each x position, the voltage to excite the arbitrary response was determined, the frequency being maintained at the vane resonance frequency. The voltage was then plotted as a function of x and figures 54 and 55 show typical results obtained in passing through branch I of the neutral curve, while figures 56 and 57 represent traverses through branch II.

During these runs the vane was kept at a constant distance from the surface of the flat plate if its resonant frequency was below 100 c/sec, and, for vanes of 200 to 300 c/sec the y distance was adjusted to maintain a constant resonant frequency. As the x value is increased the local U value, for constant y,

will decrease due to the thickening of the boundary layer. For a change of x from 1.75 to 2.25 ft, which is a typical case, the local U value decreases by 10%. Using figure 33 it can be seen that, for a vane with a resonant frequency of about 80 c/sec., the resonant frequency will change by about 5 c/sec. Reference to figure 34 shows that this will not reduce the response of the vane to a marked extent. Accordingly no compensation was attempted in this case. For high frequency vanes the response curve is narrower and the frequency change larger and the fall in response was noticeable. To compensate for this y was increased as x was increased, to maintain constant y/δ, or, alternatively, the signal generator was retuned to the vane resonant frequency at each x position.

Recordings were also obtained by photographing the vane response at various x stations, the exciting voltage being kept constant. Figures 58 and 59 show the variation in amplitude as the vane is traversed through branch I of the neutral curve. Figure 60, in which small frequency variations due to varying y/δ can be detected, shows the results of a traverse through branch II of the neutral curve. These results shownin figures 58 to 60 are especially favourable cases, and, in general, the amplifiaction and decay were not so well defined when using this method. The camera used was designed to run at higher speeds and the uneven film speed is caused by running it at a reduced voltage. The lower trace in these recordings is 50 c/sec.

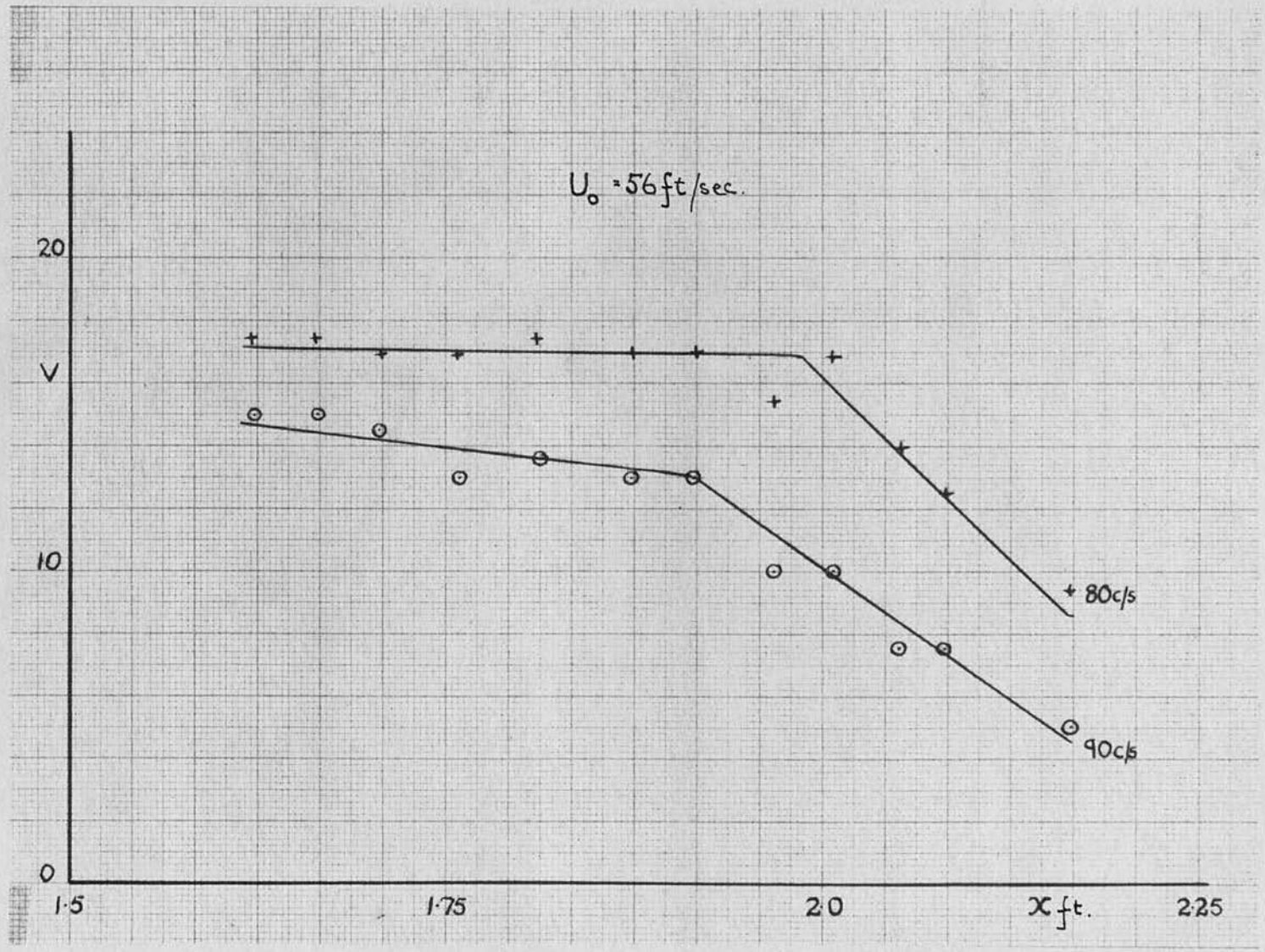

FIGURE 54

Voltage on ribbon to maintain a constant signal as the vane is traversed down the boundary layer.

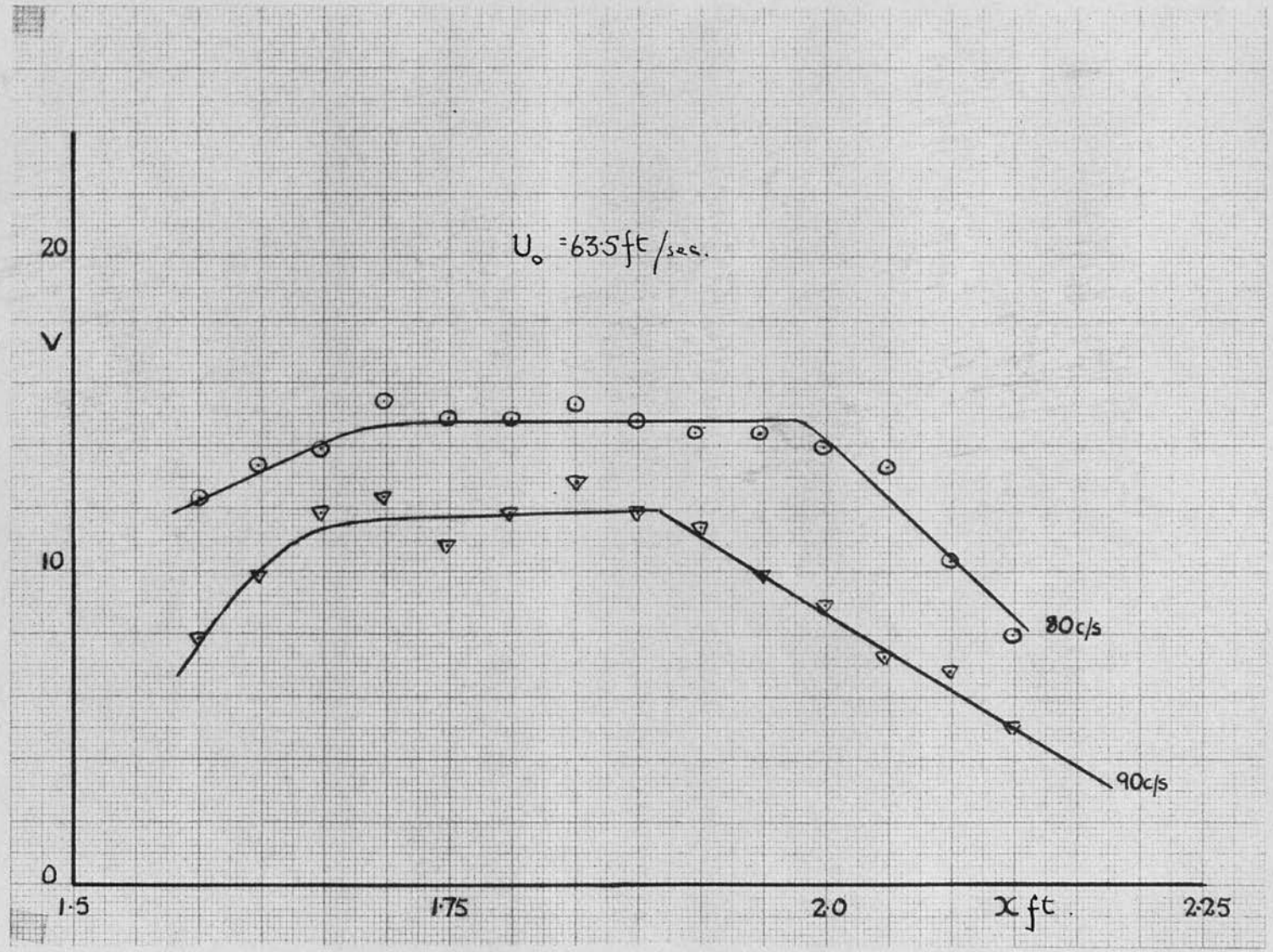

FIGURE 55

Voltage on ribbon required to maintain constant signal as the vane is traversed down the boundary layer
Ribbon at x = 1.5 ft.

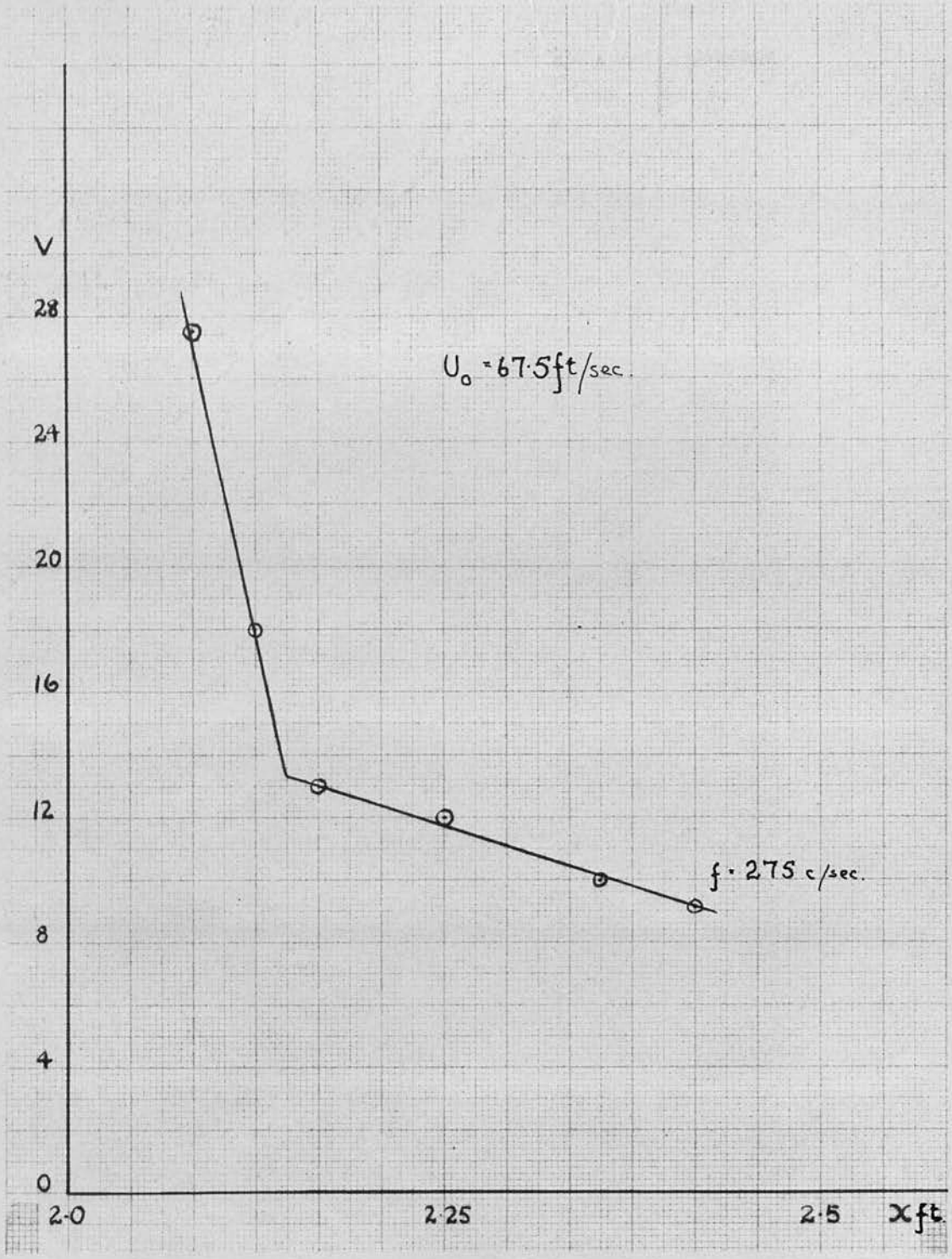

FIGURE 56

Voltage on ribbon to maintain constant signal as vane is traversed through branch II of the neutral curve. Ribbon at x = 1.5 ft.

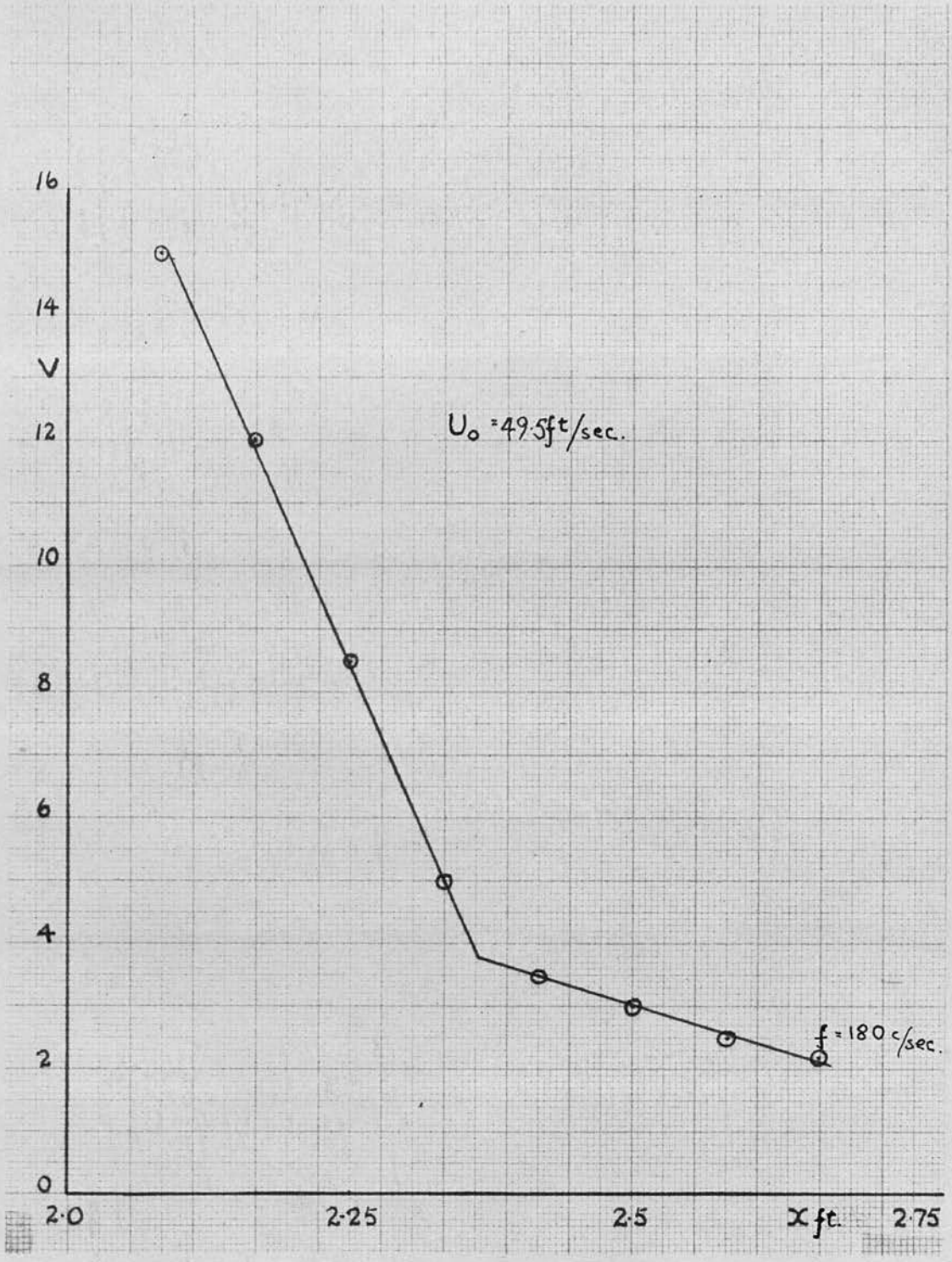

FIGURE 57

Voltage on ribbon to maintain constant signal as vane is traversed down boundary layer.

V. 6. Interpretation of Results

The results obtained from these experiments were interpreted as follows: In figures of the type shown (54 to 57) the general slope of the first few points was taken and a line drawn through them, the same being done for the points at higher x values. The x value of the intersection of these lines was taken as the point of crossing the neutral curve, when the amplification is zero, and using this value, together with the wind-speed and the frequency at which the record was taken, the parameters $\frac{2\pi f\nu}{U_0^2}$ and R were calculated and plotted as neutral points on figure 61. The solid curve, in figure 61, is the neutral curve due to Schlichting, while the chain curve is due to Lin. The results are seen to agree well with the theoretical curves over the limited range of Reynolds numbers which could be investigated.

Interpreting a decrease in ribbon voltage as indicating amplification of the signal, and vice versa, it can be seen that figures 54 and 55 appear to show a constant, or neutral, signal followed by an amplification zone, while figures 56 and 57 show amplification followed by amplification at a decreased rate. As the free stream turbulence is comparable in magnitude, though differing in frequency characteristics, with the artificial input we must consider its effect upon the observations.

Over the range of Reynolds numbers which were investigated the slope of the neutral curve, with refer-

ence to the x (or R) axis is small and if we consider, not a single frequency, but a band of frequencies, approaching the curve there will be a considerable change in Reynolds number between the value at which the highest crosses the neutral curve and the value when the whole band has entered the amplifiaction zone.

Consider now a vane of resonant frequency f_o which is being fed an artificial signal, also at frequency f_o The vane can receive energy over a range of frequencies $f_o \pm \delta f$, where δf is the half width of the vane response, and, while the artificial signal should exhibit first decay and then amplification we must add to this the energy fed to the vane from natural inputs in the range $f_o \pm \delta f$. Those in the range f_o to $f_o + \delta f$ will receive amplification before f_o does and will cause an apparent decrease in the damping of the artificial signal. If δf is appreciable a signal at $f_o + \delta f$ will have penetrated well into the amplification zone and, as the rate of amplification increases to a maximum at the centre of the zone, while the rate of damping falls to zero at the neutral curve, we may even observe an apparent amplification in the damping zone which would displace the observed neutral point to the left of its true position. Figures 54 and 55 display these effects as the signal first decays, before energy at $f_o + \delta f$ is fed to the vane, then displays a constant level as the increasing natural energy compensates for the decaying artificial signal, and finally shows an amplification when, or slightly before, f_o reaches the neutral curve. The

experimental points for branch I in figure 61 are seen to lie slightly outside the neutral curve. The value of δf for vanes used in this region is approximately 10 c/sec and, refering to figure 46, it can be seen that natural energy will be fed to the vane for 3" before f_o reaches the neutral curve.

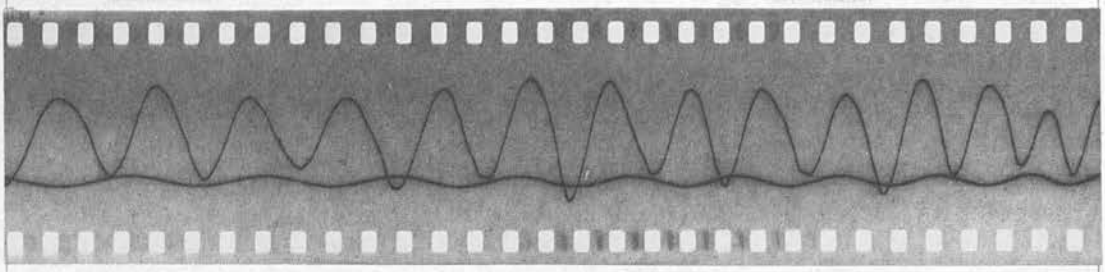

f = 70 c/sec R_x = 0.651 x 10^6

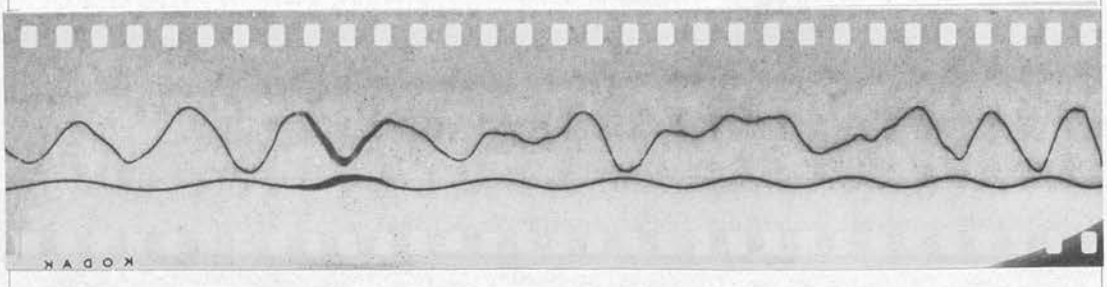

f = 70 c/sec R_x = 0.71 x 10^6

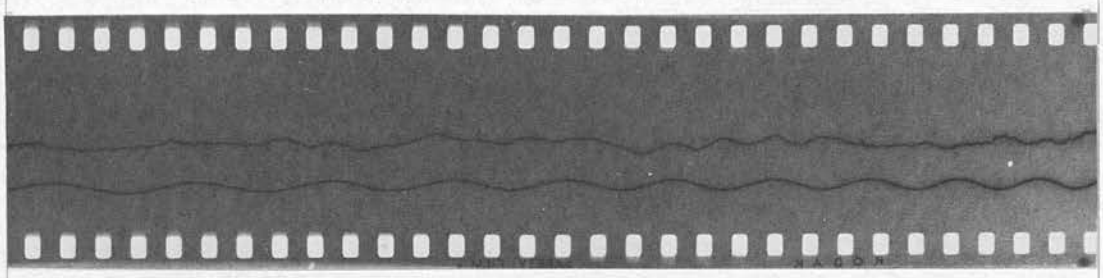

f = 70 c/sec R_x = 0.77 x 10^6

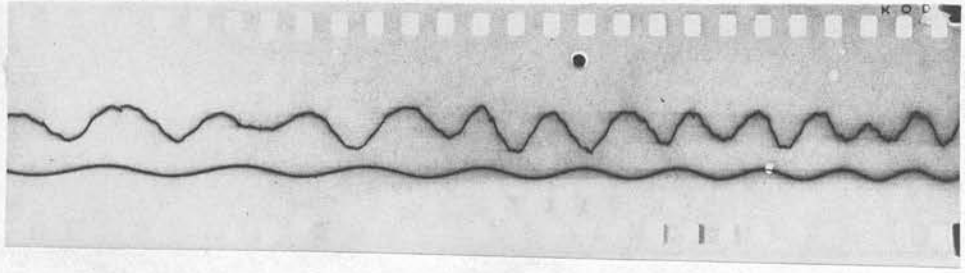

f = 70 c/sec R_x = 0.798 x 10^6

FIGURE 58
Response of vane to constant signal applied to ribbon
U_o = 55 ft/sec.

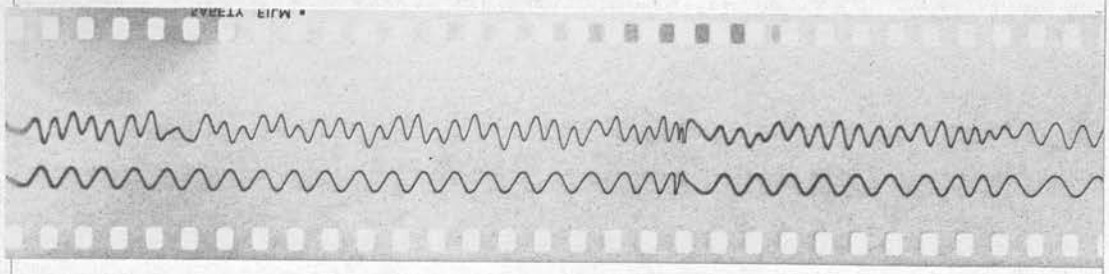

$f = 85$ c/sec $R_x = 0.592 \times 10^6$

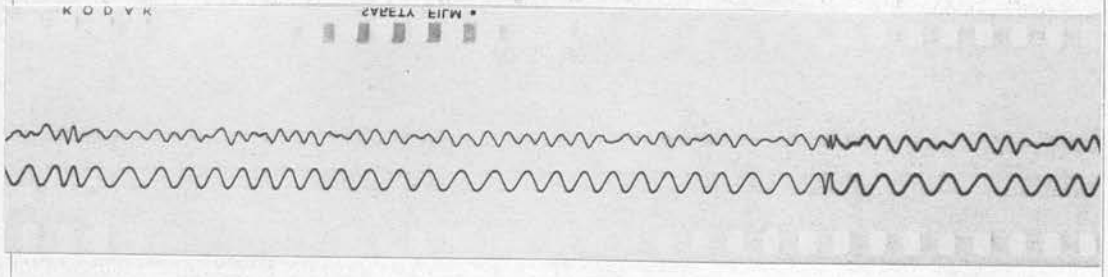

$f = 85$ c/sec $R_x = 0.651 \times 10^6$

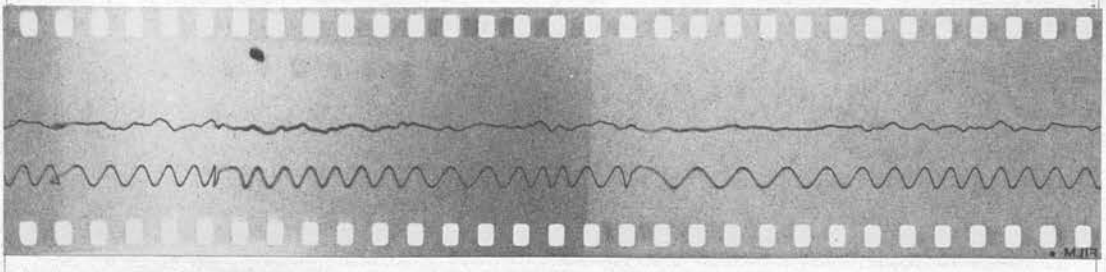

$f = 85$ c/sec $R_x = 0.680 \times 10^6$

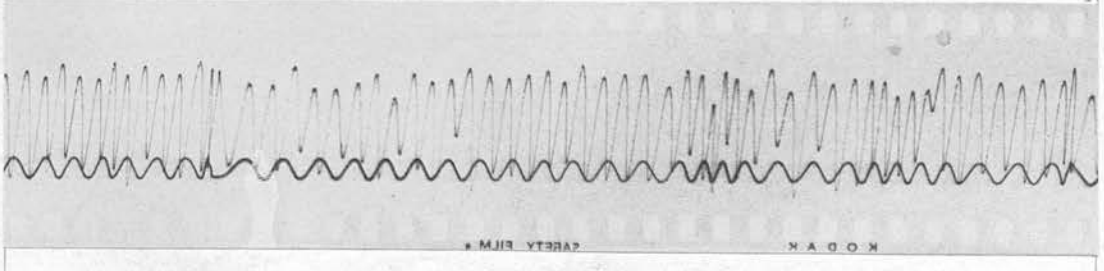

$f = 85$ c/sec $R_x = 0.740 \times 10^6$

FIGURE 59

Response of vane to constant signal applied to ribbon

$U_o = 55$ ft/sec.

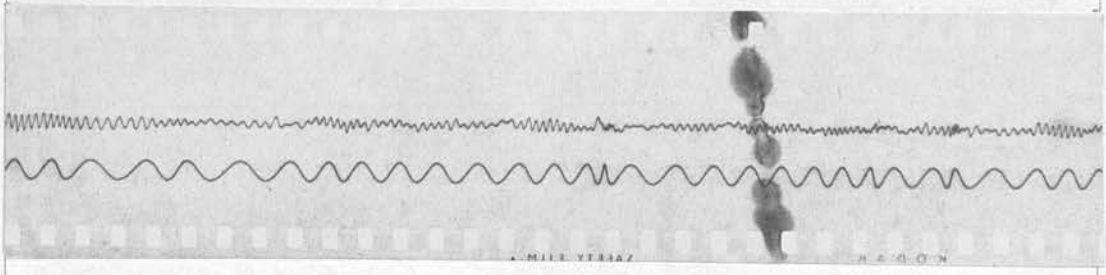

f = 267 c/sec R_x = 0.723 x 10^6

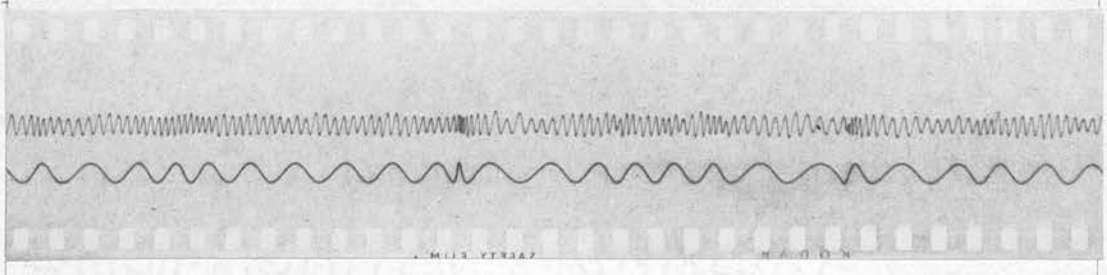

f = 267 c/sec R_x = 0.774 x 10^6

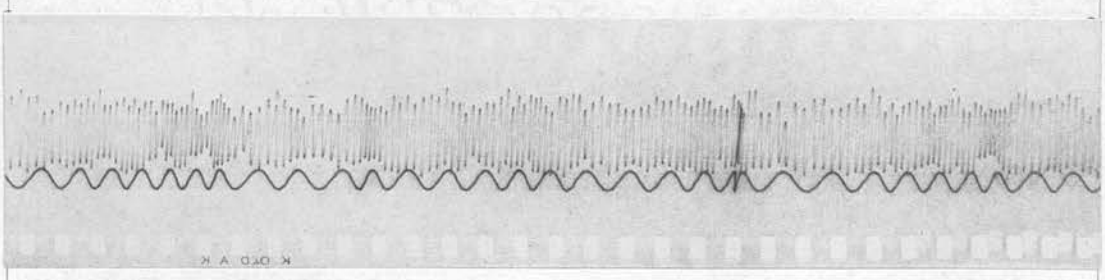

f = 267 c/sec R_x = 0.826 x 10^6

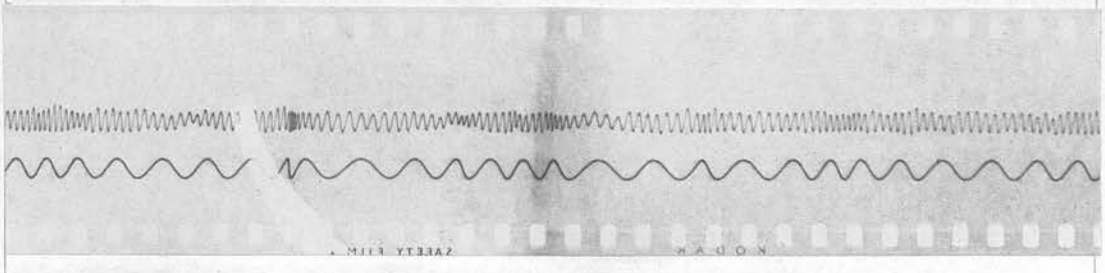

f = 267 c/sec R_x = 0.895 x 10^6

FIGURE 60

Response of vane to constant signal applied to ribbon
U_o = 64 ft/sec.

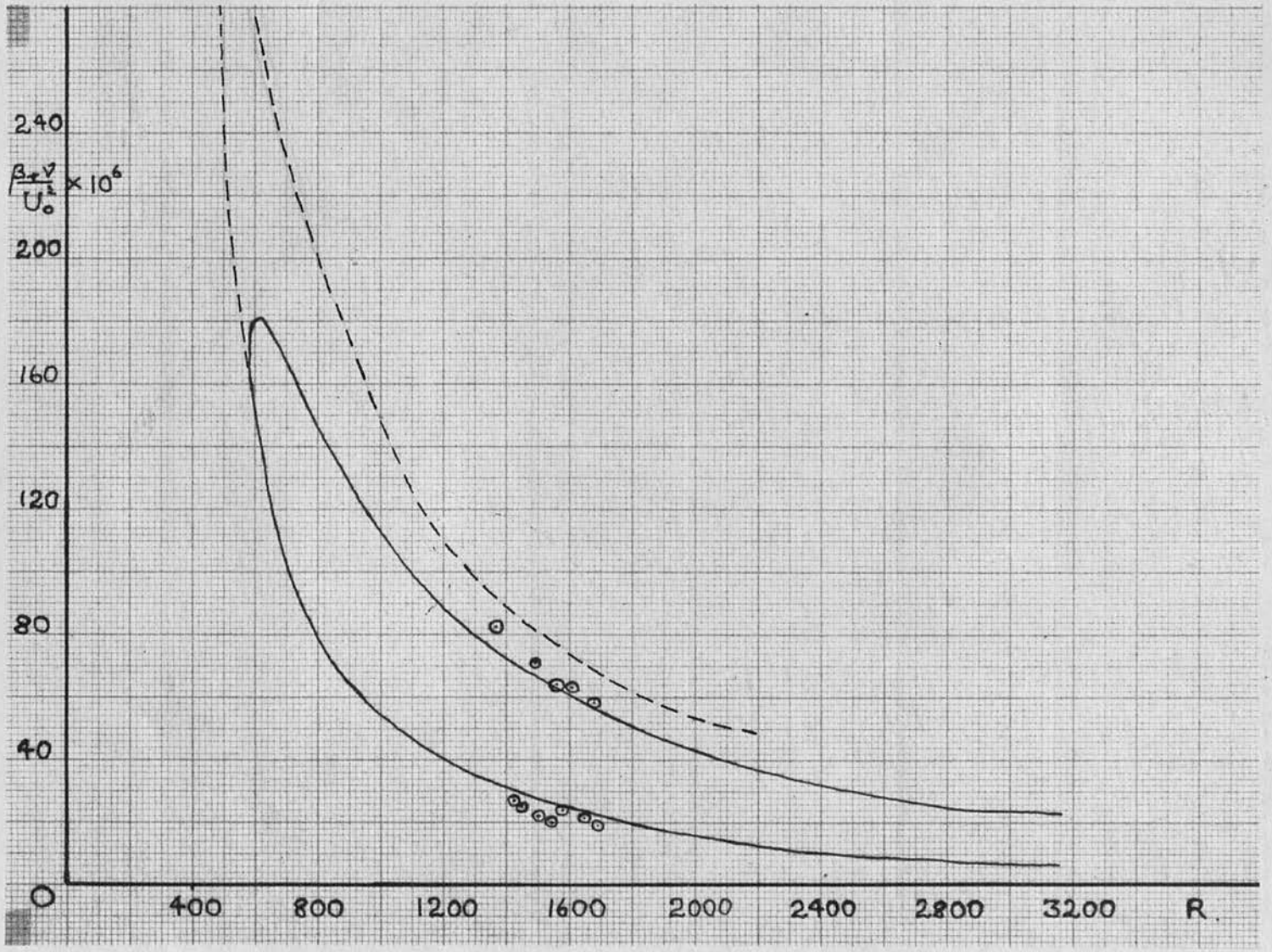

FIGURE 61

Experimental points compared with neutral curves due to Schlichting, solid curve, and Lin, chain curve.

This figure agrees with the results shown in figure 55.

The same effects will be noted as a vane is traversed from the amplification zone through branch II and into the damping zone. Frequencies in the range f_o to $f_o - \delta f$ will now contribute to apparently prevent the decay of f_o. Figures 56 and 57 show this effect to the extent that no decay is actually observed, but only a decrease in the rate of amplification. The decrease is, however, sufficiently well marked to permit of the interpretation that branch II has been crossed.

The effect of the finite width of the vane response and of the free stream turbulence may, therefore, be represented by a rotation of the axis of figures 54 to 57 in an ~~anti~~clockwise direction together with a small displacement of the origin to the left along the x axis.

It should also be noted that the lines drawn in figures 54 to 57 are not intended to be smooth curves but are drawn to arrive at the x position of the neutral point as indicated at the beginning of this section. The reasoning in the preceding paragraphs may also be applied to the observation of natural oscillations. The conclusion must be that, as there is no definite frequency at which the energy is preferentially concentrated, any observations will reveal only general tendencies rather than a definite point at which amplification supercedes decay.

Our observations described in section 5(a) support this conclusion, and any definite data on natural oscillations will probably have to be obtained either

at lower Reynolds numbers or by reducing the free stream turbulence.

V. 7. Conclusions and Suggestions for Further Work.

A new method of observing velocity fluctuations perpendicular to the main flow has been developed together with a suitable recording system. The device has been used as a resonant detector to measure laminar oscillations, the results verifying the theory for v oscillations.

The range of Reynolds numbers over which results have been obtained was limited by the nature of the tunnel used and, before a further exploration of the flow is attempted, it would be desirable to extend this range. To obtain points at greater Reynolds numbers on branch I it would be necessary to use a vane of low frequency and hence a large band width, which, combined with the small slope of the neutral curve in this region, would make any observations very ill defined. To work at lower Reynolds numbers, where the increasing slope of the neutral curve makes circumstances more favourable, we must either move the ribbon further forward or reduce the windspeed. Reduction of the windspeed below 50 ft/sec increases the free stream turbulence in the tunnel so that an improvement of this is indicated. The screens used at present reduce the turbulence level by 20% and the addition of further screens would not improve matters to any marked degree, a further 5% being a probable maximum. A more efficient honeycomb straightener could, however, improve matters

considerably, reducing the level by some 30% and improving the efficiency at lower windspeeds.

A more detailed investigation of the effect of the ribbon upon the flow is necessary to determine the minimum x position at which it can be placed in various circumstances. Taken together, these should permit lower Reynolds numbers to be investigated and might also enable vanes to be traversed completely across the amplification zone. Similar remarks apply to branch II of the neutral curve.

The original intention to proceed to an investigation of the transition region has been hampered, to some extent, by the wedge contamination preventing the development of a natural transition front and to investigate this region an artificial means of causing transition must be developed. The most promising approach lies in a further extension of the ribbon technique to cause transition due to artificial oscillations. The extension of the region over which the magnetic field operates together with the use of a more powerful signal generator would enable a better approximation to a two dimensional disturbance to be achieved and, using this, the phenomena involved in transition due to a monofrequent laminar oscillation could be studied, a simplification of the natural process which might throw light on hitherto unrevealed aspects of the problem.

The sensitivity of the vane and recording system is adequate for recording fluctuations when it is used as a resonant detector and an investigation of transit-

ion by monofrequent oscillations would be best studied, in the first instance, by this method. It would enable the way in which the energy concentrated at the preferred frequency was distributed to the rest of the spectrum to be investigated from a special viewpoint. The use of the vane as a non-resonant detector would be desirable, however, at a later stage of the investigation and the appropriate steps to increase the sensitivity of the recording system have already been indicated in chapter IV. Records obtained in this role would be more difficult to interpret and an examination of the output with a frequency analyser is suggested as a first step to determine whether any interesting effects are present.

Should the results of such an investigation prove promising in their indications it would be desirable to work in a more suitable tunnel, and unless the present tunnel is rebuilt, this would involve transferring the equipment to another site.

Quite apart from its role as a detector of velocity fluctuations the equipment provides a comparatively simple and robust device for measuring small vibrations both in amplitude and frequency, under conditions which require a minimum of disturbance to the object under investigation.

The results of the investigations described in this resport, while satisfactory in themselves, open interesting avenues of exploration which should throw further light upon transition phenomena.

REFERENCES.

1. Batchelor G.K. (1945), Australian Council of Aeronautics (Reports).13

2. Blasius H. (1908), Z. Math. u. Physik., 56 1.
also N.A.C.A. Tech. Memo. 1256.

3. Clapp, see Electronics, September 1956.

4. Dryden H.L. (1955) Science 121, 375 -380.

5. Emmons H.W. (1951) Journ. Aero. Sci. 18, 490

6. Howarth L. (1938) Proc. Roy. Soc. (A) 164, 547.

7. Lin C.C. (1952) 'The Theory of Hydrodynamic Stability' C.U.P.

see also Shen S.F. (1954) Journ. Aero Sci. 21, 62.

8. Macphail D.C. (1944) R & M of A.R.C. 2437.

~~9. Miles (1950) Aeronautical Quaterly Vol. II Part 3.~~

10. Nikuradse (1942) Monograph, Zentrale f. wiss Berichtaresen, Berlin.

see also 'Boundary Layer Theory' Schlichting.

11. Prandtl L. (1904) Proc. 3rd. International Math. Congress.
also N.A.C.A. Tech. Memo. 452.

12. Prandtl L. (1914) Gottinger Nachr. Math. Phys. Klasse, 177.

13. Prandtl L. (1925) Proc. of 2nd Intern. Cong. of App. Mech. Zurich (1936)

see also 'Aerodynamic Theory' Part III 'The Mechanics of Viscous Fluids', 34-208

14. Rayleigh, Lord (1887) Proc. London Math. Soc., 19 67.
also Proc. London Math. Soc.11, 57, (1880).

15. Reynolds O. (1883) Phil. Trans. Roy. Soc. 174, 435.

16. Schlichting H. (1933) Z. a. Math. Mech. 13, 171.

17. Schlichting H. (1935) Z. a. Math. Mech. 15, 313

see also ' Boundary Layer Theory', Schlichting,

REFERENCES. (Contd).

17. Schlichting H. (1935) Pergamon Press, London 1955.

18. Schubauer and Skramstad (1947) Journ. of Res. of Nat. Bureau of Standards, Vol. 38, R.P. 1722.

19. Schubauer and Klebanoff (1955) Symposium on Boundary Layer Effects in Aerodynamics, N.P.L.

20 Taylor G.I. (1935) Proc. Roy. Soc. (A) 151 451.

21. Taylor G.I. (1936) Proc. Roy. Soc. (A) 156, 307.

22. Tietjens (1925) Z. a. Math. Mech. 5 , 200.

23. Tollmien W. (1931) N.A.C.A. Tech. Memo. 609.

24. Tollmien W. (1936) N.A.C.A. Tech. Memo. 792.

25. Tani I. and Sato H. (1956) Paper presented at 9th Intern. Congr. for App. Mech.

26. von Karman T. (1921) N.A.C.A. Tech. Memo. 1902.

27. Willis J.B. (1945) Australian Council for Aeronautics(Reports) 19.

ACKNOWLEDGEMENTS.

I should like to thank Dr. M.A.S.Ross for suggesting the topics of this thesis and for her continued suggestions and encouragement during the work, Professor W.H.J. Childs for providing the laboratory accomodation and workshop facilities and for encouraging the project in every way. I am also indebted to Professor N. Feather F.R.S. for his constant and active support of the work.

My thanks are also due to Dr. W.S. Peat, who read the manuscript and corrected many errors, and to my wife for her continued help in the final preparation of this thesis.